HUNGARIAN UNIVERSITY OF
AGRICULTURE AND LIFE SCIENCES

DOCTORAL THESIS

A thesis submitted for the degree of Doctor of Philosophy

At the Doctoral School of Environmental Sciences

Hungarian University of Agriculture and Life Sciences

By

Sahar Saeidi

Gödöllő, Hungary

July 2025

Integrated Assessment of Land Use Impacts on Surface Water Quality in the Rákos Stream Catchment Using QUAL2K Modeling

Discipline: Environmental Sciences

Name of Doctoral School: Environmental Sciences

Head: Dr. Erika Michéli

Professor, DSc

MATE, Faculty of Environmental Sciences

Supervisor (s): Dr. István Waltner

Associate professor, Ph.D.

MATE, Department of Water Management and Climate Adaptation

Dr. Csaba Centeri

Associate professor, Ph.D.

MATE, Institute for Natural Resources Conservation

Department of Nature Conservation and Landscape Management

Approval of supervisors:

Signed by: Dr. István Waltner Dr. Csaba Centeri

Table of Contents

List of figures

List of tables

1 INTRODUCTION

Land use and land cover (LULC) patterns play a significant role in shaping water quality across various landscapes. The relationship between LULC and water quality is inherently complex, governed by multiple interacting factors such as spatial and temporal variability, watershed characteristics, landscape configuration, land use intensity, and seasonal hydrological dynamics (Uriarte et al., 2011; Xiao et al., 2018). Understanding these interactions is essential for developing effective watershed management strategies and land use planning practices aimed at protecting surface water resources.

Among various LULC types, urban and agricultural areas are widely recognized as major contributors to water quality degradation. These land uses often increase pollutant loading through stormwater runoff, fertilizer and pesticide application, and soil erosion (de Oliveira et al., 2017; de Mello et al., 2018; Ferreira & Féres, 2020). The interactions between human activities, climate, soil, and vegetation produce site-specific impacts that vary across regions and seasons, further complicating the assessment of LULC effects on water quality.

Land use refers to the human utilization of the Earth's surface for purposes such as agriculture, urban development, forestry, and industry. Changes in land use — whether gradual or abrupt — can significantly alter the physical, chemical, and biological characteristics of water bodies. These alterations often manifest as increased sedimentation, nutrient enrichment, pollution, and disruption of hydrological pathways such as infiltration, runoff, and evapotranspiration (Foley et al., 2005; Chhabra et al., 2006; Metzger et al., 2006; Feng & Huang, 2008; Tang et al., 2008; Vörösmarty et al., 2010; Burkhard et al., 2012; Zang et al., 2012; Kindu et al., 2016).

In recent decades, accelerating population growth, climate change, and rising water demand have led to widespread land use transformations, especially in rapidly urbanizing areas. These pressures have raised serious concerns about water availability and quality (Azevedo-Santos et al., 2023; Kundu et al., 2017). Unplanned urban expansion, intensive agriculture, and deforestation continue to challenge the resilience of aquatic ecosystems. LULC change can alter watershed hydrology by increasing impervious surface coverage, reducing groundwater recharge, and increasing surface runoff — all of which contribute to pollutant transport into rivers and streams (Shrestha & Acharya, 2021).

Numerous studies have demonstrated that land use change impacts extend beyond immediate areas, affecting downstream water users and ecosystems through interconnected watershed processes (Liu et al., 2018). For example, conversion of forests to agricultural land increases erosion and sediment loads in streams, which can degrade aquatic habitats and reduce water clarity (Cuo et al., 2013). Sediments often carry contaminants such as nutrients, heavy metals, and pesticides, further impairing water quality (Harris, 2007).

Nutrient enrichment, particularly from nitrogen and phosphorus, is another major consequence of land use change. Excessive fertilizer use and poor waste management can lead to nutrient loading in rivers and lakes, causing algal blooms, oxygen depletion, and long-term ecosystem degradation (Shrestha & Acharya, 2021). Similarly, impervious surfaces in urban areas prevent infiltration and increase the volume and velocity of stormwater runoff, which transports pollutants such as oil, metals, and organic waste into nearby water bodies (Feng & Huang, 2008; Zang et al., 2012).

Although various policies and planning frameworks have been developed to regulate land use and reduce its environmental impacts, accurately forecasting future LULC dynamics remains a challenge due to uncertainties in socioeconomic development, climate variability, and policy implementation (Gashaw et al., 2018; Lagakos, 2020; Liu et al., 2018).

As a result, integrated watershed management approaches and adaptive planning tools are increasingly important for ensuring sustainable water resources.

Given these challenges, this study investigates the impacts of LULC on water quality in the Rákos stream catchment in Hungary. It aims to examine how different land use types and their spatial and temporal characteristics influence water quality patterns. The findings from this research can support evidence-based watershed management and inform future land use policies to enhance water resource protection.

1.1 Background of the Rákos Catchment

Hungary has abundant freshwater resources, mainly sourced from surface water bodies and groundwater systems. Approximately 95% of the country's drinking water comes from riverbank filtration and aquifers, including both shallow, pollution-prone sources and deeper, less contaminated reserves. However, the distribution and availability of these resources vary across regions and seasons.

Nearly two-thirds of Hungary's water resources are considered vulnerable to pollution. River water quality is strongly influenced by transboundary inflows, which carry various contaminants through interconnected watercourses. This has led to adverse impacts on surrounding ecosystems.

Most of Hungary's water bodies are located within small watershed areas, but there is a lack of well-organized data to comprehensively describe their characteristics (Halász et al., 2007). The Rákos stream, the focus of this study, is one of the smallest streams situated in the central part of Hungary. It originates in the Gödöllő Hills and flows through the towns of Isaszeg and Pécel before joining the Danube River north of Budapest. It also receives treated municipal effluents from nearby urban settlements.

Due to its proximity to the capital, the Rákos stream is a popular location for recreational activities, such as running, cycling, and walking. However, as it flows through diverse land use zones, including residential, industrial, agricultural and forested areas, it is exposed to multiple pollution sources. Consequently, this study evaluates the spatial and temporal distribution of pollutants across different sampling locations and years, and determines the influence of surrounding land use on the water quality of the Rákos Stream.

1.2 Scope of the Study

This study assesses how land use affects water quality in the Rákos Stream catchment in Hungary. To achieve this objective, two years of water quality data collected from November 2019 to November 2021 was analyzed. The measured water quality parameters included chemical, physical, and biological characteristics, which helped identify the level of pollutants and their impact on the overall water quality.

In addition to the water quality assessment, this study also examined land use and land cover (LULC) in the Rákos catchment. The CORINE land cover dataset was used to identify LULC patterns and trends in the area. This spatial analysis provided insights into how land use surrounding the Rákos Stream influenced water quality during the study period.

By integrating field-based water quality data with spatial LULC analysis, this study provided a comprehensive assessment of the effects of the surrounding LULC on the water quality of the Rákos Stream.

1.3 Objectives

1.3.1 Main objective

The main objective of this study was to investigate the effects of surrounding land use on water quality in the Rákos catchment and analyze the relationships between different land use types and water quality parameters.

1.3.2 Specific Objectives

To achieve the main objective, the study had the following specific objectives:

- To monitor and assess the physical and chemical water quality parameters of the Rákos Stream through field sampling.
- To evaluate the spatial distribution and extent of land use and land cover (LULC) types in the Rákos catchment using GIS-based analysis.
- To simulate the hydrodynamics and water quality processes of the Rákos Stream using the QUAL2K model, incorporating both field data and land use-derived pollutant loads.

2 LITERATURE REVIEW

2.1 Overview of the Land Use–Water Quality Relationship

Surface water quality is widely regarded as a key indicator of the environmental condition of a watershed because it reflects the combined influence of natural processes and anthropogenic activities. Among the drivers of water quality degradation, land use and land cover (LULC) change is of particular concern due to its direct impact on runoff generation, pollutant loading, and the ecological integrity of streams (Locke, 2024a; Zhang et al., 2020).

Changes such as urban expansion, deforestation, and intensive agriculture alter fundamental hydrological processes, including infiltration, evapotranspiration, and overland flow. These modifications influence the mobilization and transport of pollutants to water bodies in ways that vary across spatial and temporal scales. Urbanization typically increases impervious surface coverage, leading to greater stormwater runoff volumes and velocities, which mobilize a wide range of contaminants such as nutrients, heavy metals, hydrocarbons, and microbial pathogens. In agricultural catchments, excessive fertilizer application and poor land management practices contribute to elevated nitrogen and phosphorus levels, promoting eutrophication and oxygen depletion (Hughes & Quinn, 2019; Malmqvist & Rundle, 2002). However, the relative dominance of agricultural versus urban sources remains contested in the literature: some studies identify agriculture as the principal driver of nutrient loading (Welde & Gebremariam, 2017), while others report that urban non-point and point sources can dominate in peri-urban catchments (Halász et al., 2007). Such discrepancies often arise from differences in study scale, land management intensity, climate, and the timing of sampling, highlighting the need for site-specific assessments.

Peri-urban and mixed-use watersheds such as the Rákos Stream catchment in Hungary present additional complexity due to the mosaic of interacting land use types. Numerous studies have demonstrated that localized variables — including slope, soil type, vegetation cover, and riparian buffer width — can strongly mediate the impact of LULC on water (Masood et al., 2022; Mello et al., 2018b; Taniwaki et al., 2017; Woldesenbet et al., 2017). Land use within riparian buffer zones, typically within 100–300 m of a stream, often exhibits stronger correlations with water quality than land use patterns measured at the entire watershed scale (Zhang et al., 2020). Furthermore, recent findings indicate that spatial configuration and fragmentation of land cover can be as influential as the overall composition. For example, Zhang et al. (2020) in the Daning River Basin, China, found that

metrics such as Shannon's Diversity Index (SHDI) and Landscape Shape Index (LSI) significantly affected nutrient concentrations. Similarly, Locke (2024b) emphasized that preserving unfragmented natural vegetation across entire catchments — rather than focusing solely on riparian zones — is critical for reducing diffuse pollution.

Advances in environmental modelling have made it possible to quantify and predict the impacts of LULC change under various management scenarios. Process-based models such as QUAL2K, SWAT, WASP, and HSPF are widely used to link terrestrial processes with in-stream water quality dynamics. SWAT, for example, is well-suited for large, data-rich catchments to simulate long-term hydrology and pollutant export, whereas WASP offers greater flexibility for multi-dimensional water quality simulations in lakes and estuaries. HSPF provides integrated hydrological and water quality modelling for mixed-use catchments. In contrast, QUAL2K is particularly appropriate for small to medium-sized rivers where steady-flow conditions and detailed longitudinal water quality dynamics are the focus (Chapra et al., 2013). In the present study, QUAL2K was selected due to its ability to simulate spatially explicit pollutant transport along the Rákos Stream, the availability of required input data, and the need to integrate field monitoring results with modelled scenarios. Moreover, Hungary-focused studies strengthen the regional relevance of the present research. For example, Saeed et al. (2024) applied GIS-supported geochemical modelling, multivariate statistics, and Monte Carlo simulation to assess surface water quality in the Hungarian sector of the Danube Basin, providing valuable insight into pollutant sources and variability under different environmental conditions. Similarly, Horvat et al. (2024) conducted hydrological modelling of the Magyaregregy experimental catchment in Hungary using HEC-HMS 4.3, highlighting challenges in model validation, particularly in estimating initial conditions. Although neither study applied QUAL2K, both illustrate the breadth of modelling approaches implemented in Hungarian watersheds and offer methodological and regional insights that complement the present study's application of QUAL2K in the Rákos Stream catchment.

This review therefore establishes the conceptual basis for the integrated assessment undertaken in this research, with emphasis on the influence of agricultural, urban, and forested land covers, as well as the spatial configuration of land use and its seasonal variability, in determining pollutant delivery to the Rákos Stream.

2.2 Impacts of Land Use and Land Cover on Surface Water Quality

Different land use types exert distinct influences on water quality through their effects on runoff volume, erosion, nutrient input, and pollutant generation. Agricultural land use is consistently associated with elevated concentrations of nutrients, particularly nitrate (NO_3^-), ammonium (NH_4^+), and phosphate (PO_4^{3-}), due to fertilizer use, manure application, and soil disturbance. These nutrient inputs can trigger eutrophication, algal blooms, and oxygen depletion, especially during the rainy season when runoff intensifies. The impact of land use on water quality also varies depending on land management practices, the intensity of land use, and seasonal patterns. For example, studies have reported higher pollutant loads during the wet season in agriculturally dominated catchments, linked to increased surface runoff and fertilizer application (K. L. de Oliveira et al., 2021; S M et al., 2017). For instance, studies in Brazil and Ethiopia have reported higher nutrient loads in catchments dominated by agricultural activities, with seasonal variation corresponding to rainfall and fertilizer cycles (Mello et al., 2018a; Welde & Gebremariam, 2017).

Urban areas contribute a diverse range of pollutants, including heavy metals, hydrocarbons, and pathogens, primarily through stormwater runoff from impervious surfaces such as roads and rooftops (Li et al., 2012; Zheng & Hu, 2018). Rapid runoff in these environments not only transports pollutants but also reduces infiltration and natural filtering. Research in Hungary and elsewhere has shown that urban streams often exhibit higher levels of nitrogen, phosphorus, and chemical oxygen demand (COD), indicating the influence of both point and diffuse sources (Halász et al., 2007; Zhang et al., 2020). Despite extensive research, there is still debate over whether urban or agricultural land use exerts a stronger influence on stream water quality, as findings vary by region and scale (Donohue et al., 2006).

In contrast, forested and semi-natural areas generally act as buffers that enhance water quality by promoting infiltration, reducing surface runoff, and facilitating nutrient uptake through vegetation and soils. Numerous studies have found inverse relationships between forest cover and nutrient concentrations in stream water (Hughes & Quinn, 2019; Locke, 2024a). In the Hungarian context, forested headwaters of the Rákos Stream have been associated with improved water quality, consistent with similar observations across European catchments (Angyal et al., 2016).

Spatial configuration also plays a critical role in shaping water quality outcomes. Land use patterns within riparian buffer zones, typically within 100 to 300 meters of streams, have been shown to exert stronger influences on pollutant transport than overall catchment-level statistics (Zhang et al., 2020).

Consequently, land use analyses that focus on proximity to streams offer more accurate predictions of water quality impacts. In the present study, this approach was adopted through the use of CORINE 2018 data and buffer-based extraction upstream of each sampling site, following recent methodological advances (Locke, 2024b; Taniwaki et al., 2017).

The effects of land use are further modulated by seasonal variations in rainfall, temperature, and streamflow. During wet periods, increased runoff amplifies pollutant transport from both agricultural and urban landscapes. In contrast, dry seasons are characterized by reduced dilution and potential accumulation of organic pollutants. Studies have shown that the timing of peak pollutant loads often coincides with seasonal patterns in land management and precipitation (Mello et al., 2018b; Welde & Gebremariam, 2017), reinforcing the importance of capturing temporal dynamics in LULC–water quality analyses.

In summary, the literature strongly supports that:

- Agricultural lands are key sources of nutrient loading, particularly nitrogen and phosphorus compounds.
- Urban areas contribute a wide array of pollutants through rapid stormwater runoff.
- Forested and natural areas provide a mitigating effect through physical and biogeochemical processes.
- Spatial arrangement, especially in riparian zones, significantly influences pollutant pathways.
- Seasonal variations are essential for understanding land use–water quality interactions.

These insights provide a robust scientific foundation for the current study's focus on buffer-scale LULC analysis, seasonal data collection, and the application of process-based modeling to assess pollutant dynamics in the Rákos Stream watershed.

Understanding water quality and its determinants is essential for assessing the environmental impacts of land use and planning effective monitoring strategies. Surface water quality is typically evaluated based on physical, chemical, and biological parameters in relation to ecological thresholds (Obilonu et al., 2013). Degradation of water quality can result from a combination of natural processes and anthropogenic pressures, including runoff, wastewater discharge, and landscape modification (Plessis et al., 2014).

In catchment-scale studies, a crucial conceptual distinction is made between point sources and non-point sources of pollution. Point sources refer to localized and identifiable discharges such as municipal and industrial effluents, which can be measured and regulated directly (Puri et al., 2011). In contrast, non-point sources are diffuse and difficult to trace, arising from urban and agricultural runoff, atmospheric deposition, and surface erosion (Amlor & Alidza, 2016; Liang et al., 2013).

The Rákos Stream catchment presents both types of pollution due to its mixed land use pattern, making this distinction particularly relevant for interpreting water quality dynamics in the study area.

2.3 Monitoring and Sampling Strategies

Effective assessment of land use impacts on water quality requires a robust monitoring framework that captures spatial heterogeneity and seasonal dynamics (Chang et al., 2008; Halász et al., 2007) Poorly designed monitoring may fail to identify pollution sources or misrepresent the extent of land use–water quality relationships.

2.3.1 Spatial Design

Monitoring stations should reflect the dominant upstream land use types and major hydrological transitions. Several studies (Romano et al., 2018; Schauer et al., 2025) have emphasized placing sampling points in zones representing agricultural, urban, and forested areas. In the Rákos and Galga catchments, Halász et al. (2007) implemented such a design to distinguish diffuse from point-source pollution. Similarly, this study placed eight sampling sites along the Rákos Stream to ensure land use variation was captured at relevant hydrological breaks.

2.3.2 Temporal Strategy

Seasonal variation in rainfall, temperature, and land use practices (e.g., fertilizer application) necessitates regular sampling to capture pollutant fluctuations. Biweekly sampling, as adopted in this study (2019–2021), has been recommended by studies such as Zhang et al. (2018) and Locke (2023), allowing both baseflow and storm event responses to be observed. The dataset includes parameters like NO_3^-, NH_4^+, PO_4^{3-}, DO, EC, pH, and temperature, which are all sensitive to land use-driven changes.

2.3.3 Parameter Selection and Methodology

Nutrients (N, P), oxygen indicators (DO, BOD), and physical parameters (TSS, EC, pH) are widely recognized as key indicators in LULC–WQ research (Faruq et al., 2025). While advanced sensors are used in some contexts, manual grab sampling remains standard practice in long-term catchment studies, particularly in small streams or data-limited contexts like this one.

Surface water quality reflects a combination of physical, chemical, and biological characteristics (Obilonu et al., 2013), and is influenced by both point and non-point pollution sources (Liang et al., 2013; Puri et al., 2011). Major pollutants include nutrients, pathogens, and suspended solids, originating from industrial discharge, agricultural runoff, and urban wastewater.

Effective monitoring is essential to detect spatial and temporal changes in water quality. Parameters such as DO, pH, EC, temperature, and nutrients are often measured using field sensors or laboratory analysis (Johnson et al., 2006). Both manual and automated techniques are employed, depending on the study objectives and data availability.

In small streams such as Rákos, biweekly sampling ensures seasonal variability is captured. Monitoring frequency, equipment, and site selection are all crucial for reliable assessments (Johnson et al., 2006; Ribbe et al., 2008)

2.3.4 Regulatory Framework

The EU Water Framework Directive (WFD) mandates harmonized monitoring for achieving good ecological status in surface waters (European Commission, 2000). Hungary has adopted this approach by developing integrated monitoring plans, as noted by Halász et al. (2007), with catchments like Rákos and Galga serving as key case studies.

2.3.5 Data Integration

Combining water quality data with GIS-based land use information, hydrological measurements, and meteorological variables enhances the interpretation of pollutant dynamics (Arslan, 2009; Masood et al., 2022). In this study, stream discharge was calculated directly from field measurements of flow velocity and channel width at each sampling station. Precipitation and temperature data were also incorporated to capture seasonal variability and support dynamic modeling within the QUAL2K framework.

2.4 GIS and Remote Sensing Applications in LULC–Water Quality Studies

The use of Geographic Information Systems (GIS) and remote sensing technologies has significantly advanced research into the relationship between land use and surface water quality. These tools enable spatially explicit analyses that are critical for understanding how various land cover types influence pollutant generation, transport, and attenuation within catchments. Integrating geospatial datasets with

field-based water quality measurements improves the interpretability of results and supports evidence-based watershed management (Adami et al., 2012; Masood et al., 2022).

2.4.1 Buffer Analysis and Spatial Resolution

Recent studies emphasize the effectiveness of buffer-based land use analysis in identifying localized pollutant sources. Rather than relying on whole-catchment averages, researchers often calculate land use proportions within 100–500 meter buffers upstream of water quality sampling points (Mapili, 2005). This method enhances spatial specificity and improves correlation with stream water quality.

Following this approach, the current study delineated flow-relevant buffer zones based on stream direction and topography. Land use proportions within each buffer were extracted using GIS tools and linked with biweekly measurements of key water quality parameters. This enabled station-level assessment of LULC impacts with greater precision than catchment-scale summaries.

2.4.2 Spatial Metrics and Landscape Structure

In addition to land use composition, GIS enables the derivation of spatial metrics that describe landscape configuration and potential pollutant pathways. Commonly used indices include:

- Percentage of impervious surfaces, a key predictor of runoff volume and pollutant loads.
- Mean slope and elevation, which influence sediment transport potential.
- Distance from pollutant sources to the stream, affecting delivery efficiency.
- Land use fragmentation and connectivity metrics, which help assess cumulative impacts.

Incorporating such indicators, as done in Xu et al. (2021), improves the explanatory power of statistical and modeling analyses and provides a more complete picture of land use–water quality interactions.

2.4.3 Remote Sensing for Change Detection

Remote sensing supports the detection of land use change over time, which is particularly valuable in urbanizing or agriculturally expanding regions. Time-series satellite imagery from platforms such as Landsat or Sentinel-2 allows researchers to track deforestation, crop conversion, and urban sprawl and relate them to changes in water quality trends.

While this study applied a static land cover dataset (CORINE Land Cover dataset), similar research (Xu et al., 2021) demonstrates the utility of time-series analysis in explaining temporal shifts in

pollutant levels. Future work could integrate multi-year land cover change detection to further explore long-term impacts on stream quality.

2.4.4 Management and Policy Applications

Beyond scientific research, GIS-based outputs, such as land use maps, pollution hotspot identification, and vulnerability mapping, are widely used by watershed managers and policymakers. These visual tools help prioritize areas for intervention and support planning decisions such as riparian buffer restoration or zoning restrictions. Scenario modeling using GIS is also increasingly used to predict the outcomes of land use change or restoration projects on water quality.

In Hungary, the integration of GIS with water quality monitoring supports national compliance with the EU Water Framework Directive. Halász et al. (2007) demonstrated how spatial land use analysis contributed to the development of regional action plans and monitoring network optimization.

2.5 Statistical Approaches for Assessing LULC–Water Quality Relationships

Understanding the relationship between land use and land cover (LULC) and surface water quality requires the application of appropriate statistical tools capable of handling multivariate, spatial, and temporal data. Numerous statistical techniques have been employed in the literature to analyze the strength and nature of LULC–WQ interactions (Arslan, 2009; Masood et al., 2022).

2.5.1 Pearson Correlation Analysis

Pearson correlation is often the first analytical step used to assess linear relationships between land use percentages and individual water quality parameters. Its simplicity and interpretability make it a popular choice for exploratory analysis. For example, Locke and Winter (2024) used Pearson correlation to demonstrate a strong positive association between urban land cover and nitrate concentrations in South African catchments. However, this method assumes linearity and is not suitable for detecting non-linear interactions or accounting for multiple influencing factors.

2.5.2 Analysis of Variance (ANOVA)

ANOVA is frequently employed to test whether mean values of water quality indicators differ significantly across land use types or seasons. Welde and Gebremariam (2017), for instance, used one-way ANOVA to compare nutrient concentrations across agricultural, forested, and urban land covers in Ethiopian watersheds. Their findings showed significant differences ($p < 0.05$), with higher nutrient levels in agriculturally dominated areas. While widely used, ANOVA relies on assumptions of

normality and homogeneity of variance, and may not perform well when these assumptions are violated.

2.5.3 Principal Component Analysis (PCA)

PCA is a multivariate technique used to reduce the dimensionality of large datasets by identifying principal components that explain the greatest variance. This method is valuable for uncovering patterns and grouping similar water quality parameters. In their study of the Three Gorges Reservoir Basin, Zhang et al. (2020) applied PCA and found distinct clustering of nutrient-related parameters in association with urban land use, revealing underlying gradients in water chemistry. However, because PCA is an unconstrained technique, it does not explicitly incorporate external environmental variables such as land use.

2.5.4 Redundancy Analysis (RDA)

Redundancy Analysis (RDA) is a constrained ordination technique frequently used in LULC–water quality studies to assess how sets of environmental variables (e.g., land use composition, slope, landscape metrics) explain variation in multiple water quality parameters (Mo et al., 2023; Ye et al., 2009). In a study of the Daning River Basin in the Three Gorges Reservoir Region, Zhang, et al. (2020) applied RDA to assess land use effects at multiple spatial scales. Their results showed that watershed-scale land use had the strongest explanatory power in both wet and dry seasons, while riparian land use within 200–500 m buffers was more influential during the wet season. Among the predictors, water body percentage and Shannon's Diversity Index (SHDI) were most closely associated with nutrient levels, including TN, TDN, and TP. These findings highlight the utility of RDA for capturing spatially and seasonally variable land use impacts on riverine water quality.

2.5.5 Regression Models

Multiple linear regression (MLR) and stepwise regression techniques are commonly employed to predict water quality parameters based on land use metrics. These models enable researchers to quantify the relative influence of different land use types (e.g., agriculture, urban, forest) while accounting for potential interactions among variables. For example, Locke and Winter (2024b) demonstrated how stepwise regression models could identify dominant land use predictors of nitrate and phosphate concentrations in South African watersheds.

While regression models offer flexibility and interpretability, they require careful assumption testing, including normality, multicollinearity, and independence of residuals, and are typically more reliable with large datasets. Moreover, when spatial metrics such as proximity to streams or slope are incorporated, regression models become more robust in capturing the heterogeneity of landscape influences.

Recent studies have increasingly combined regression with spatially explicit data extracted from GIS, including percent impervious surface, buffer slope, and riparian land use composition. These integrated approaches improve the ability to detect spatial patterns in pollutant concentrations and inform land-use-based water quality management strategies (Aboelnour et al., 2021; Woldesenbet et al., 2017).

Each statistical method contributes unique insights into the complex relationship between LULC and surface water quality. Pearson correlation and ANOVA are effective for initial exploratory analysis and hypothesis testing, whereas PCA and RDA offer deeper understanding of data structure and the influence of multiple variables. Regression models, when appropriately designed, allow for robust predictions and scenario evaluations. Combining these methods enhances analytical rigor and ensures comprehensive interpretation of LULC–WQ interactions.

In this study, a combination of correlation analysis and ANOVA was employed to explore the linkages between LULC and water quality parameters in the Rákos Stream catchment.

2.6 Water Quality Modeling Approaches: Focus on QUAL2K

Understanding land use impacts on surface water quality requires not only statistical correlation but also process-based simulation of pollutant transport and transformation. QUAL2K, a one-dimensional, steady-state water quality model developed by the U.S. Environmental Protection Agency (Chapra, et al., 2013), provides a suitable framework for this purpose. It simulates flow, temperature, dissolved oxygen (DO), nutrients (NH_4^+, NO_3^-, PO_4^{3-}), algal dynamics, BOD, sediment oxygen demand (SOD), and pH, making it effective for streams with combined point and non-point sources.

Several studies have applied the QUAL2K model to investigate how land use influences river water quality under various environmental conditions. For instance, Santy et al. (2020) used QUAL2K to

evaluate the combined effects of land use and climate change on water quality in the Ganges River around the industrialized Kanpur region. Their findings underscored the model's effectiveness in capturing seasonal variations in nutrient concentrations and simulating pollutant transport in urbanized river segments. Similarly, implemented the QUAL2K model to assess the spatial distribution of pollutants in the Dez River, Iran, demonstrating how agricultural and urban inputs impacted water quality parameters such as BOD and nutrient loads.

In Brazil, Bottino et al. (2010) calibrated the QUAL2K model in a micro-watershed to analyze the influence of different land use types on stream water quality. Their study confirmed the model's capacity to simulate nutrient dynamics in response to varying landscape configurations. In Vietnam, Nguyen et al. (2019) developed an integrated modeling approach by coupling SWAT and QUAL2K to simulate both watershed hydrology and in-stream water quality. This integration proved valuable in data-scarce regions by enhancing spatial resolution and accuracy of nutrient transport predictions. Broader reviews by Yong and Chen (2002) and Hossain (2017) also support the use of QUAL2K as a practical and widely adopted tool for linking land use patterns to water quality outcomes in stream systems.

Overall, QUAL2K has demonstrated its suitability for modeling land use–driven water quality changes in small to medium-sized streams, particularly due to its flexibility in simulating nutrient cycles and dissolved oxygen dynamics. Its relatively simple structure, ease of calibration using biweekly field measurements of discharge, temperature, and pollutant concentrations, and proven success in both agricultural and urban settings have contributed to its widespread adoption (Bottino et al., 2010; Samaneh Abdeveis et al., 2020; Santy et al., 2020). Moreover, the model's compatibility with low-data environments and regulatory requirements, such as those defined by the European Union Water Framework Directive, makes it a practical choice for research and policy contexts. In the present study, QUAL2K was applied to simulate water quality along the Rákos Stream based on empirical measurements collected from eight monitoring stations. The model was calibrated and validated using data from 2019 to 2021, showing strong agreement with observed values and enabling spatial and seasonal interpretation of nutrient and dissolved oxygen patterns under varying land use conditions.

2.7 Knowledge Gaps and Research Contribution

Although numerous studies have explored the impact of land use and land cover (LULC) on surface water quality, several methodological and spatial-temporal limitations persist, particularly in the context of small peri-urban catchments in Central and Eastern Europe. Much of the existing research tends to focus on large-scale basins or highly regulated systems, often overlooking the fine-scale dynamics in smaller tributaries that may be more sensitive to land use pressures and local pollutant inputs. One of the key gaps in the literature is the limited integration of spatial, statistical, and process-based modeling approaches within a single framework. While many studies utilize remote sensing and GIS to classify LULC, they often fail to directly couple these land use patterns with in-situ water quality data or dynamic modeling. Conversely, modeling studies using tools such as QUAL2K sometimes rely on default parameters or secondary input data without field-based calibration, thereby limiting their ecological validity. Furthermore, the use of buffer-based LULC analysis, despite being recognized as more representative of local influences, is still not widely adopted in European research, where catchment-averaged metrics remain prevalent.

Another underexplored area is the incorporation of seasonal variability in assessing land use impacts. Studies employing annual or seasonal averages may obscure the short-term fluctuations in pollutant loads driven by rainfall events, agricultural practices, or changes in hydrological connectivity. Consequently, the nuanced relationships between land use and water quality across seasons remain poorly understood in many European catchments.

This study addresses these gaps by implementing a multi-method approach in the Rákos Stream catchment, a small, mixed-use watershed in the urbanizing region of Pest County, Hungary. The research integrates two years of biweekly field data with GIS-based analysis, statistical tools such as Pearson correlation, ANOVA, and dynamic water quality modeling using QUAL2K. Unlike previous studies, it places emphasis on localized LULC metrics, field-calibrated inputs, and seasonal water quality dynamics across a complete hydrological cycle.

Understanding the complex relationship between land use dynamics and water resources is essential for sustainable environmental management. This study contributes to the literature by assessing both water quality and quantity aspects in a peri-urban basin with heterogeneous land use. Specifically, the Rákos Stream catchment includes agricultural, forested, and urbanized areas, making it a representative case for analyzing diverse LULC influences.

The research integrates water quality modeling (QUAL2K), statistical analysis (correlation and ANOVA), and GIS-based analysis, offering a comprehensive view of pollutant dynamics. Findings from this study are expected to inform evidence-based land use planning and environmental policy, supporting the goals of the EU Water Framework Directive. Additionally, the research methodology can be adapted to similar data-limited regions undergoing urbanization.

3 MATERIALS AND METHODOLOGIES

The primary aim of this research was to evaluate the influence of land use on water quality in the Rákos Stream in Hungary and to investigate the relationship between selected water quality indicators and the surrounding land use characteristics.

This chapter presents the methodological framework used in the study, including an overview of the study area, sampling design, analytical methods, and modeling techniques.

3.1 Description of the Study Area

The Rákos Stream is a small watercourse located in central Hungary, extending approximately 44.3 kilometers in length and averaging 1 to 3 meters in width. It has a drainage area of approximately 185 km^2 and originates from the Gödöllő Hills, flowing into the Danube River north of Budapest, the largest river in Hungary. The streambed exhibits a mix of natural and artificial characteristics: the lower 22 kilometers, extending from the mouth to the edge of Budapest, are lined with concrete, pebbly, and rocky bed. The banks of the natural bed section are occupied by various plant species. Due to its proximity to the capital, the Rákos Stream flows through a range of land use zones, including residential neighborhoods, industrial facilities, agricultural lands, and forested areas. Agricultural activities are found around the source, and numerous fishponds that contribute wastewater are situated between Pécel and Gödöllő. Additionally, a milk factory at the boundary of Budapest and Gödöllő discharges wastewater into the stream (Figure 3-1).

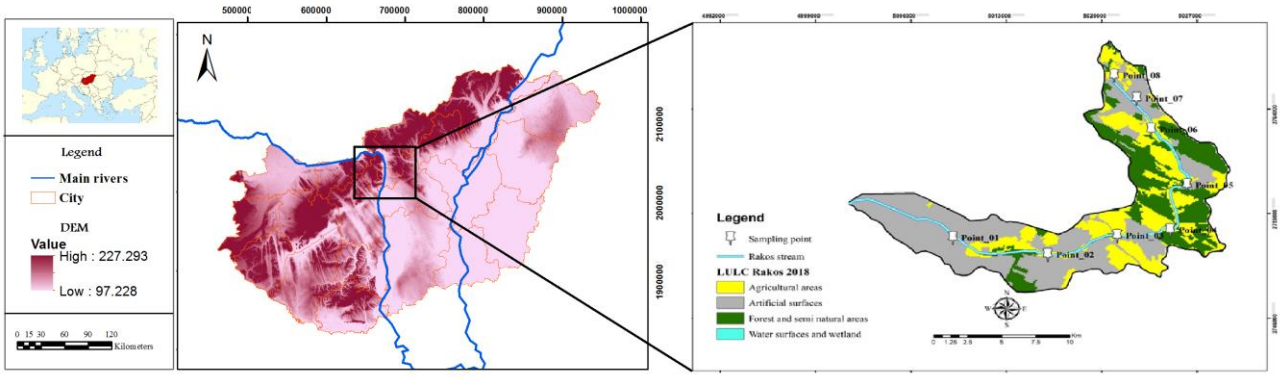

Figure 3-1 Study area location and sampling sites in the Rákos Catchment, Hungary

3.2 Conceptual Model

The conceptual framework of this study provides an overview of the integrated approach used to evaluate the influence of land use and land cover (LULC) on water quality in the Rákos Stream catchment.

As illustrated in Figure 3-2, the framework combines spatial datasets, field measurements, and analytical methods within a unified structure.

LULC classifications, derived from the CORINE database, were used to generate land use maps and delineate the watershed and river network. Field-based water quality monitoring campaigns provided data on both physical parameters (e.g., water temperature, dissolved oxygen) and chemical parameters (e.g., nitrate, ammonium, phosphate). Streamflow records were also compiled to support hydrodynamic and water quality modelling.

These datasets were integrated and analyzed using statistical methods—both univariate and multivariate—to identify patterns in water quality and their relationships with surrounding LULC. In parallel, the process-based QUAL2K model was applied to simulate present-day conditions in the stream and quantify the influence of land use on selected water quality indicators.

Overall, the conceptual model served as a methodological roadmap, linking data sources with analytical and modelling components, and guiding the systematic evaluation of LULC impacts on water quality in the study area.

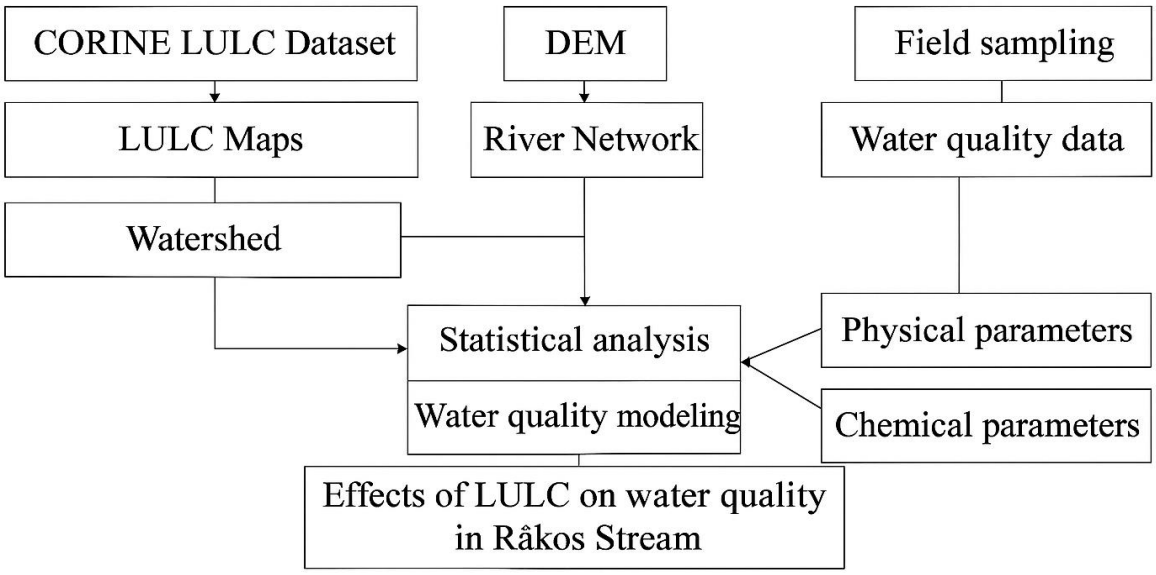

Figure 3-2 The conceptual model within the theoretical framework of the study

3.3 Sampling Design

A well-structured sampling design was developed prior to field data collection to ensure methodological consistency and spatial coverage. The subsequent subsections detail the main components of the design, including site selection, sampling frequency and duration, and the measured water quality parameters.

3.3.1 Sampling Site Selection

Eight sampling locations were strategically selected along the Rákos Stream to represent the spatial variation in water quality conditions. Site selection was informed by the dominant land use patterns and proximity to known or suspected pollution sources within the catchment. Table 3-1 summarizes the key characteristics of each sampling point.

Table 3-1 Characteristics of the Rákos stream sampling points

Sampling Point	Location	Land Use	Key Features
Point-01	Downstream, Budapest	Residential, artificially paved	Slightly sloping, little turbulence
Point-02	Régi akadémiatelep	Urban, artificially paved	Road bridge, downstream of bridge
Point-03	Pécel	Agricultural, weir	Wastewater treatment plant, odor
Point-04	Pécel	Forested	Steep, rocky bed, high turbulence
Point-05	Isaszeg	Forested, agricultural	Coarse sand bed, retaining wall
Point-07	Gödöllő	Urban, artificially paved	Footbridge
Point-08	Upstream	Pond, vegetation	Flat, shallow conditions

The geographic coordinates of each sampling point were recorded using a global positioning system (GPS) to ensure the consistent sampling locations throughout the study period.

3.3.2 Sampling Frequency and Duration

Sampling was conducted over a two-year period from November 2019 to October 2021, with samples collected every two weeks at eight fixed sampling sites. To ensure consistency, all samples were taken in the morning at approximately 8:15 AM.

3.3.3 Water Quality Parameters

At each sampling location, the following water quality parameters were assessed to provide a comprehensive profile of stream health:

Physical parameters: Temperature, electrical conductivity, EC, pH, and dissolved oxygen

Chemical parameters: Ammonium, phosphate, nitrate, and nitrite

Biological parameters: Chlorophyll-a

All physical and chemical parameters were measured in situ using portable field instruments to ensure data accuracy and consistency.

3.3.4 Sampling Procedures

The sampling protocol followed a standardized sequence of field operations to ensure consistency and data integrity:

- Flow conditions, site characteristics, and sampling time were recorded at each location.
- Collection of water samples in a clean, rinsed bucket, after rinsing the bucket with the sampled water.

- In-situ measurement of temperature, pH, electrical conductivity, and dissolved oxygen using portable field instruments.
- Measurement of chlorophyll-a using a portable algae torch instrument.
- Measurement of ammonium, nitrate, nitrite, and chloride concentrations using a compact photometer.

To ensure the accuracy and consistency of the measurements, various quality control measures were taken, such as washing the sampling equipment with distilled water between measurements and following the specific protocols and standard operating procedures for each water quality parameter. Table 3-2 summarizes the instruments and standardized analytical methods employed for each water quality parameter.

Table 3-2 Instruments and Standardized Analytical Methods Used for Water Quality Measurements

Parameter	Measuring Instrument	Standard Method Number	Unit
Temperature	Adwa, pH, conductivity, TDS and temperature meter	AD14 PH/ORP	˚C
Dissolved oxygen	DO meter	AD 630	%
Electric Conductivity	Electric conductivity sensor	DiST 3 (HI 98303)	µs
Ammonia	Compact photometer	PF-12Plus	mg/l
Nitrate	Compact photometer	PF-12Plus	mg/l
Nitrite	Compact photometer	PF-12Plus	mg/l
Chloride	Compact photometer	PF-12Plus	mg/l
pH	Adwa, pH, conductivity, TDS and temperature meter	AD14 PH/ORP	
Chlorophyl –a	Algae Torch (bbe)	ATo1009-156	mg/l

3.4 GIS-based Water Quality Assessment

QGIS version 2.18.15 was used for data input, spatial analysis, and mapping tasks throughout the study. Sampling locations were identified using Google Earth. A geodatabase was developed to store water quality parameters and the river network. Spatial analyses, interpolations, and map visualizations were performed using QGIS plugins. Sub-catchments were delineated for each sampling point, and the surrounding LULC was correlated with site-specific water quality data.

3.4.1 GIS Mapping Procedure

The Inverse Distance Weighted (IDW) interpolation method, available in QGIS, was used to interpolate water quality data. Field-sampled water quality data from eight locations were compiled in Excel and exported as a shapefile. The mean values of each parameter at the sampling points were

used to interpolate the raster cells, with the river network serving as a spatial mask. Raster cells within the Rákos watershed were interpolated based on these inputs, producing a spatial representation of water quality. Water quality classes were determined from the spatial distribution of pollutants and displayed in map legends corresponding to each parameter's value range.

3.4.2 GIS Interpolation

Spatial interpolation was performed using the Inverse Distance Weighting (IDW) method available in QGIS. IDW is a deterministic technique widely applied in environmental and geospatial studies for modelling continuous spatial data. It assumes that nearby points exert greater influence on an unknown location than those farther away, and estimates unknown values based on the proximity-weighted average of known samples (Jones et al., 2003). Estimation of unknown values is based on the proximity-weighted average of known sample points. The formula for IDW interpolation is presented in (Equation 1):

Equation 1: $$\hat{Z}(X_0) = \sum_{i=1}^{n} z\,(x_i).\, d_{ij} - p / \sum_{i=1}^{n} d_{ij} - p$$

where, Z is the interpolated value of a grid node, $\mathbf{Z_i}$ are the neighboring data points, and $\mathbf{d_{ij}}$ are the distances between the grid node and data points.

The IDW method was selected due to the spatial configuration of the monitoring network, consisting of eight sampling sites arranged linearly along the Rákos Stream, with biweekly sampling conducted over two years. Geostatistical techniques such as kriging typically requires a denser and more spatially dispersed network to ensure stable variogram modelling and reliable predictions. Spline doesn't need a variogram, but with few and linearly arranged points, it can over-smooth the results or produce unrealistic values. In contrast, IDW does not rely on variogram modelling, making it more suitable for datasets with limited, transect-aligned sampling points.

3.4.3 Accuracy Assessment

The accuracy of interpolation was evaluated using cross-validation methods. A leave-one-out approach (also known as jackknifing) excluded each data point in turn and estimated its value using the remaining data. The predicted values were then compared to the actual observations, and the discrepancies were assessed using cross-validation metrics (Wilk, 2006). This process was repeated for all data points, where n represents the total number of samples. The resulting metrics served as diagnostic tools to determine the reliability and appropriateness of the interpolation technique for map generation (Tanjung et al., 2022). Cross-validation outputs were generated using the Geostatistical

Analyst Toolbar in ArcGIS 10.3, providing diagnostic metrics and exploratory analysis (Wu et al., 2021).

Two cross-validation metrics were used to quantify the accuracy of interpolation: Mean Error (ME) and Root Mean Square Error (RMSE) (Shen et al., 2015). ME represents the average difference between predicted and actual values, while RMSE provides a measure of overall prediction accuracy, accounting for both variability and extreme values (Njeban, 2018). These metrics were computed using the following formulas (Equation 2 and 3):

Equation 2: $\text{RMSE}=\sqrt{\frac{1}{N}\sum_{i=1}^{N}(\hat{z}(x_i)-z(xi))^2}$

Equation 3: $ME = \frac{1}{N}\sum_{i=1}^{N}(\hat{z}\ (x_i) - z(x_i))$

3.5 Statistical Analysis

3.5.1 Data Preparation and Quality Control

Water quality data from the Rákos Stream were collected at eight sampling sites, representing varying upstream land use types. For statistical analysis, the biweekly data were averaged to obtain monthly values. The dataset included temperature (°C), dissolved oxygen (DO, mg/L), nitrite (NO_2, mg/L), nitrate (NO_3, mg/L), chloride (Cl^-, mg/L), ammonium (NH_4^+, mg/L), pH, orthophosphate (PO_4^{3-}, mg/L), and electrical conductivity (EC, µS/cm). Prior to statistical analysis, the dataset was screened for data quality. Missing values were handled using listwise deletion to ensure consistency across analyses. Outliers were identified using both boxplot inspection and standardized Z-scores ($|z| > 3$) and were excluded from the final dataset.

3.5.2 Normality and Transformation

The distribution of each variable was examined using the one-sample Kolmogorov–Smirnov (K–S) test, with both test statistics (D) and p-values reported. Where the assumption of normality was violated ($p < 0.05$), data were $\log_{10}$-transformed in accordance with Kim et al. (2014) to approximate a normal distribution. The normality of transformed variables was reassessed using the K–S test prior to further analysis.

3.5.3 Homogeneity of Variance

For all parametric tests, the assumption of homogeneity of variances was evaluated using Levene's test ($\alpha = 0.05$). Variables violating this assumption were analyzed using Welch's ANOVA, which does not require equal variances.

3.5.4 Correlation Analysis

Relationships between land use proportions and individual water quality parameters were evaluated using Pearson's correlation coefficient (r), with significance determined at $\alpha = 0.05$ (two-tailed). When data did not meet the assumptions of Pearson's test even after transformation, Spearman's rank correlation (ρ) was applied.

3.5.5 Analysis of Variance (ANOVA)

Spatial differences in water quality among the seven sites were tested using one-way ANOVA for variables meeting both normality and homogeneity assumptions. Welch's ANOVA was applied for variables with unequal variances. Significance was set at $\alpha = 0.05$. When significant differences were detected, post-hoc comparisons were conducted using Tukey's Honestly Significant Difference (HSD) test for equal variances and Duncan's Multiple Range Test for unequal variances, following the procedures outlined in Simedo et al. (2018) and Li and Wu (2019).

3.5.6 Temporal Aggregation

All analyses were conducted separately on monthly and seasonal averages to capture intra-annual variation in water quality. Seasonal averages were computed according to climatological definitions: winter, spring, summer, and autumn.

3.6 Assessing the Impact of Land-Use Types on Nutrient and Flow Dynamics Using QUAL2K Model

3.6.1 Model Description

The QUAL2K model was applied to simulate water quality conditions along the Rákos Stream in Hungary. QUAL2K is a one-dimensional, steady-state model developed by the U.S. Environmental Protection Agency for stream water quality simulation. It divides the stream into segments and calculates changes in water quality based on mass balance equations and reaction kinetics. The model simulates key processes such as reaeration, nutrient cycling, nitrification, and sediment oxygen demand.

This study configured the model to simulate core parameters such as streamflow, dissolved oxygen (DO), ammonium (NH_4^+), and phosphate (PO_4^{3-}).

3.6.2 Model Inputs

3.6.2.1 River Geometry

The modeled reach of the Rákos Stream extends for 30.73 km, from the headwaters near Gödöllő (222 m elevation) to the outlet (122 m elevation). The river was divided into seven computational segments to account for inflows, tributaries, and abstraction points. Geometric and topographic information was derived from digital elevation models (DEM) and topographic maps.

Seven key nodes were established along the mainstem to represent hydrology and pollutant dynamics (Figure 3-3):

- Gödöllő (km 32.50) – headwater entry, no lateral inflow or abstraction (0.000 m^3/s lateral, 0.030 m^3/s baseflow).
- Isaszeg (km 30.00) – mainstem headwater, zero lateral inflow, 0.040 m^3/s baseflow contribution.
- Pécel (km 23.00) – mid-reach node, zero lateral inflow, 0.015 m^3/s baseflow.
- Tributary2 (km 19) – a modeled reach with zero lateral inflow, 0.250 m^3/s baseflow.
- Tributary1 (km 1.50) – small tributary inlet supplying 0.300 m^3/s, no baseflow abstraction.
- Abstraction Point (km 23) – regulated withdrawal of 0.050 m^3/s, no lateral inflow.
- Tributary3 (km 19.5) – downstream reach, zero lateral inflow, 0.030 m^3/s baseflow.

These nodes captured both lateral inflows and human withdrawals, forming the structure of the distributed hydrological and water quality model. This detailed spatial setup—from agricultural headwaters to urban areas—enabled accurate calibration with field data and supported thorough analysis of how land use affects flow and pollutant movement.

In addition to inflows, outflows, and abstraction points, key hydraulic structures (e.g., weirs, sedimentation basins, and step-pools) were identified along the Rákos Stream and incorporated into the QUAL2K setup. Their locations were geo-referenced using kilometer stationing, ensuring that the model representation captured the influence of these structures on flow regulation, mixing processes,

and residence time.

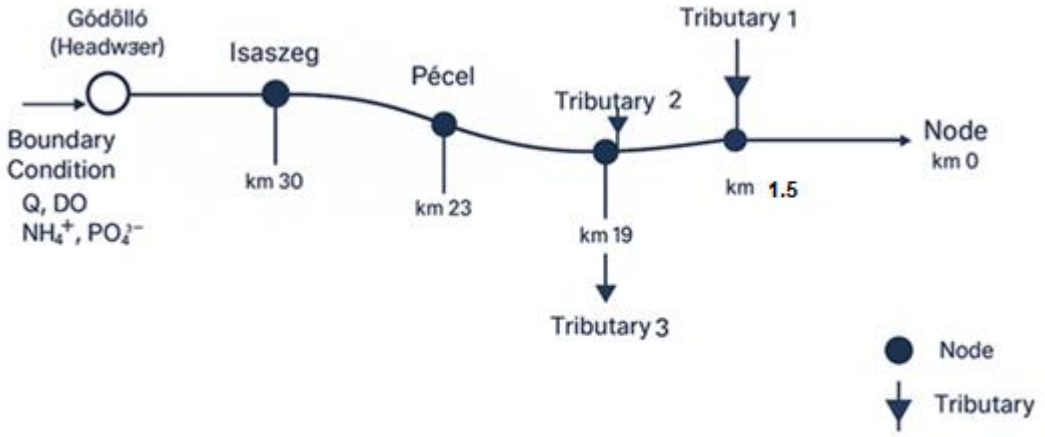

Figure 3-3 QUAL2K Reach Network for Rákos Stream

3.6.2.2 Hydrological Data

Observed streamflow data were used to characterize baseflow conditions and provide upstream boundary values. These measurements also supported calibration and validation of the model.

3.6.2.3 Meteorological Data

Daily air temperature and precipitation data were obtained from the Hungarian Meteorological Service, Meteorological Data Archive (https://odp.met.hu/). Air temperature data were used to estimate water temperature and simulate processes such as reaeration and decay, while precipitation records provided inputs for estimating non-point source runoff and lateral inflows. Two representative months were selected: July 2021 (the wettest month) for calibration and June 2021 (the driest month) for validation, thereby covering contrasting hydrological regimes.

3.6.2.4 Land Use Data

Land use and land cover maps of the study area, obtained from the CORINE Land Cover dataset, were reclassified into three primary categories: agricultural, artificial, and forest/semi-natural area. These reclassified datasets were then used to calculate non-point source runoff and pollutant contributions.

Each group encompassed specific CLC codes that denote particular land cover characteristics. The total area for each group was quantified in both square meters and hectares, and its proportional share was calculated relative to the study area's total size (190,060,656.6 m²) (**Error! Reference source not found.**). This classification provides a foundational understanding of the spatial distribution of land cover, which is essential for hydrological analysis and runoff estimation.

Main Category	CLC_CODE(s) Included	Area (m²)	Area (ha)	% of Total
Agricultural areas	211 (Non-irrigated arable land) 221 (Vineyards) 222 (Fruit trees) 231 (Pastures) 242 (Complex cultivation) 243 (Agro-natural mix)	52,972,918	5,297.29	27.88%
Artificial surfaces	112 (Urban fabric) 121 (Industrial units) 122 (Transport) 132 (Dump sites) 141 (Green urban) 142 (Leisure)	90,286,036	9,028.60	47.48%
Forest & semi-natural	311 (Broad-leaved forest) 312 (Coniferous) 313 (Mixed) 321 (Grasslands) 324 (Woodland-shrub)	47,032,856	4,703.29	24.74%

Table 3-3 Land use classification and area distribution

3.6.2.5 Non-point Source Runoff Estimation Across Land use Categories

Surface runoff from different land use types was estimated as non-point sources contributing to hydrological flows. Unlike point sources, these inputs originate from diffuse areas and are controlled mainly by land cover, rainfall, and surface characteristics.

Land use maps obtained from the CORINE Land Cover dataset were reclassified into three categories: agricultural, artificial, and forest/semi-natural.

Runoff volumes were calculated using the standard equation (Equation 4):

Equation 4: $\text{Runoff Volume (m}^3\text{)} = \text{Area (m}^2\text{)} \times \text{Rainfall (m)} \times \text{Runoff Coefficient}$

In this equation, 'Area' denotes the land surface covered by each land use type. 'Rainfall' refers to the precipitation depth over the period, given in meters. 'Runoff Coefficient' is a unitless value between 0 and 1 that reflects land surface properties like vegetation, infiltration capacity, and slope, influencing how much rainfall becomes runoff. To convert runoff volume into discharge, the following formula is

used:

Equation 5: $$Q(m^3/s) = \frac{Runoff\ Volume\ (m^3)}{Time\ (s)}$$

To reflect differences in land surface properties, runoff coefficients were assigned based on each land use category. In natural and agricultural areas, coefficients ranged from 0.10 to 0.20, indicating high infiltration and minimal surface sealing. Conversely, in urban and semi-urban zones characterized by impermeable surfaces like roads and buildings, coefficients ranged from 0.30 to 0.60, depending on development intensity (**Error! Reference source not found.**).

Table 3-4 Estimated Runoff and Manning's Roughness Coefficients by Land Use Type

Parameter	Area Type	Value
Runoff coefficient	Natural / Agricultural areas	0.10 – 0.20
Runoff coefficient	Urban / Semi-urban areas	0.30 – 0.60
Manning's roughness coefficient (n)	Natural areas	0.03– 0.05

For hydraulic modelling and flow resistance calculations, Manning's roughness coefficient (n) was also applied where necessary. In natural channels or vegetated areas, a Manning's *n* value between 0.03 and 0.05 was assumed, accounting for vegetation density, irregular banks, and natural obstructions (Table 3-4). The selection of these values was guided by the literature review. These parameters provide the necessary basis for estimating both the volume and velocity of runoff, particularly in flood-prone or hydrologically sensitive regions.

The composition of land use categories, their associated hydrological parameters, and the estimated runoff volumes for July 2021 (the wettest month, with a total precipitation of 34.7 mm) are summarized in Table 3-5.

Table 3-5 Estimated Runoff Volume by Land Use Type Using Rainfall and Runoff Coefficients

Land Use	Area (m²)	Runoff Coefficient	Precipitation (m)	Runoff Volume (m³)	m³/s
Agricultural areas	52,972,918	0.15	0.0347	52,972,918 × 0.0347 × 0.15 = 275,642.4	0.103
Artificial surfaces	90,286,036	0.45	0.0347	90,286,036 × 0.0347 × 0.45 = 1,410,741.6	0.527
Forest & semi-natural	47,032,856	0.15	0.0347	47,032,856 × 0.0347 × 0.15 = 245,073.3	0.0914

The estimated discharges from each land use category were incorporated into the QUAL2K model as lateral inflows, representing non-point source contributions along the modeled reaches.

3.6.2.6 Estimation of Point Source Runoff Based on Population

Municipal wastewater discharges from Gödöllő, Isaszeg, and Pécel were represented in the model as point sources. Wastewater generation was estimated using population data and a standard per capita wastewater production rate of 160 L/person/day (WHO, 2006), as summarized in (Table 3-6). Pollutant loads were then calculated using the QUAL2K default pollutant concentrations (Table 3-7) and the following equation:

Equation 6 Pollutant loading (μg/s) = Concentration (μg/L) × Discharge (m^3/s) × 1,000

Table 3-6 Point Source Wastewater Estimation Using Population Data and Per Capita Generation Rate

City	Population	Wastewater Production (m^3/day)	Wastewater per Capita (L/day)
Isaszeg	11,640	1,862.4	160
Pécel	17,377	2,780.3	160
Gödöllő	32,524	5,203.8	160

Table 3-7 Default Mean Concentrations of Wastewater Pollutants Used in QUAL2K Model Inputs

Parameter	Mean Value	Unit (QUAL2K)
Inorganic Suspended Solids	50,000	μg/L
Dissolved Oxygen (DO)	500	μg/L
Organic Nitrogen	25,000	μg N/L
Ammonia Nitrogen (NH_4–N)	35,000	μg N/L
Nitrate + Nitrite Nitrogen	500	μg N/L
Organic Phosphorus	4,000	μg P/L
Inorganic Phosphorus (PO_4–P)	6,000	μg P/L
Detritus	150,000	μg/L
Pathogen Indicator Bacteria	1.0×10^9	CFU/L
Alkalinity (as $CaCO_3$)	150,000	μg/L
Total Nitrogen (TN)	60,000	μg N/L
Total Phosphorus (TP)	10,000	μg P/L
Total Suspended Solids (TSS)	200,000	μg/L
pH	7.2	s.u.

This approach enabled the quantification of pollutant contributions from municipal point sources, which were incorporated into the overall model framework together with non-point source inputs.

3.6.2.7 Initial Conditions

Initial concentrations of key water quality parameters were defined using observed or estimated field data collected at the start of the simulation period:

- Dissolved Oxygen (DO): Assigned to represent natural background concentrations in the upstream section.

- Ammonium (NH_4^+) and Phosphate (PO_4^{3-}): Estimated using baseflow conditions with minimal upstream anthropogenic influence.

3.6.2.8 Boundary condition

The QUAL2K model incorporated both upstream and downstream boundary conditions to define the hydraulic and water quality characteristics of the stream segment.

Upstream Boundary (Headwater):

At the upstream boundary near Gödöllő, the model was initialized with flow rate and water quality concentrations for key parameters such as dissolved oxygen (DO), ammonium (NH_4^+), and phosphate (PO_4^{3-}), based on observed field data.

Downstream Boundary:

The downstream boundary was treated as a free outflow condition. No backwater effects or hydraulic constraints were assumed at the outlet, allowing water and pollutant transport to exit the modeled domain freely.

3.6.2.9 Lateral information

To realistically represent the pollutant dynamics along the Rákos stream, several lateral inflows and point sources were integrated into the QUAL2K model.

- **Point Sources:** Municipal wastewater discharges from the towns of Gödöllő, Isaszeg, and Pécel were modeled as point sources. These inflows contributed nutrients and organic matter to the stream, influencing concentrations of biochemical oxygen demand (BOD), ammonium, phosphate, and other parameters.
- **Lateral Inflows**: Three smaller tributaries were modeled as lateral inflows entering the main stream at different locations. Each tributary was represented with specific flow rates and associated pollutant concentrations. These lateral sources provided additional water and pollutant loads, affecting the water quality in localized sections of the stream. Each source was spatially and hydrologically positioned along the modeled reaches and calibrated to reflect field observations of flow and pollutant levels.

3.6.3 Model Calibration

The model was manually calibrated by adjusting pollutant loads and rate coefficients to align with observed water quality data along the stream. The calibration was done using data from July 2021, which was the wettest month with high flows and strong influence of runoff from both urban and agricultural areas.

During the calibration process, key model parameters related to pollutant decay and reaeration were adjusted to achieve the best fit between simulated and observed values. Table 3-8 presents the final calibrated values for ammonium decay rate (k_NH_4 (1/day), phosphate decay rate (k_PO_4 (1/day), and reaeration coefficients (1/day) for each reach. Initial values were set based on literature and QUAL2K default parameters, then iteratively modified within realistic ranges to minimize the NRMSE for dissolved oxygen, ammonium, and phosphate at all sampling points.

These values represent the final configuration of the model used for both calibration and validation runs.

Table 3-8 Calibrated Parameter Values for QUAL2K Model in the Rákos Stream

Reach	k_NH_4 (1/day)	k_PO_4 (1/day)	Reaeration Coef. (1/day)
1	0.35	0.25	1.8
2	0.32	0.22	1.7
3	0.30	0.20	1.6
4	0.28	0.18	1.5
5	0.27	0.16	1.4
6	0.26	0.15	1.3
7	0.25	0.14	1.2

3.6.4 Model Validation

The validation was conducted using data from June 2021, representing the driest month with low flows and minimal runoff influence, to test the model under contrasting hydrological conditions. No parameter adjustments were made after calibration; the calibrated parameters were applied unchanged to the validation dataset to ensure an independent assessment. Model performance was evaluated using the NRMSE for dissolved oxygen, ammonium, and phosphate across all sampling points. This approach allowed for a robust assessment of the model's predictive capability under different seasonal conditions.

3.6.5 Model Evaluation Using NRMSE

To assess the performance of the calibrated QUAL2K model, the Normalized Root Mean Square Error (NRMSE) was used as the primary evaluation metric. Unlike RMSE, which is influenced by the scale and units of the observed data, NRMSE standardizes the error by dividing it by the mean of the observed values. This produces a dimensionless value, allowing for meaningful comparisons across different variables and units.

The NRMSE was calculated using the following formula:

Equation 7: $$\text{NRMSE} = \frac{\text{RMSE}}{\text{Mean of Observed Data}}$$

This approach allowed for consistent evaluation of how well the model predicted concentrations of water quality parameters such as DO, ammonium, and phosphate across all sampling locations. A lower NRMSE value indicates a better model fit and greater predictive accuracy.

3.6.6 Load Contribution Analysis in the Rákos Stream

To quantify the contribution of different land use categories to pollutant loads in the Rákos Stream, GIS-based land use data were integrated with the calibrated QUAL2K model. Each land use type was assigned pollutant input values according to its area and typical nutrient characteristics. The QUAL2K model was then used to simulate the transport and transformation of these inputs along the stream network, accounting for flow conditions, mixing processes, and in-stream transformations. Model outputs were subsequently analyzed to determine the total pollutant load attributable to each land use type, which was expressed as a percentage of the overall catchment load.

This chapter presented the integrated methodological approach adopted in this study to investigate the relationship between land use and water quality in the Rákos Stream catchment. A multi-step framework was developed that included field-based water quality monitoring, GIS-based land use analysis, statistical evaluation, and hydrodynamic–water quality modeling using QUAL2K.

Water quality data were collected over a two-year period at eight sampling points selected to represent various land use conditions and pollution sources. These data included physical, chemical, and biological parameters. CORINE land cover datasets were used to assess land use change from 1990 to 2018, while GIS tools were applied to delineate sub-catchments, visualize spatial patterns, and estimate non-point source runoff contributions.

Statistical techniques such as Pearson's correlation and ANOVA were used to analyze spatial and seasonal variations, and to explore the relationships between land use/land cover and key water quality parameters. Finally, the QUAL2K model was applied to simulate the hydrodynamic and water quality behavior of the stream, integrating point and non-point source pollutant loads.

This combined approach provided a comprehensive understanding of the spatial and temporal effects of land use on stream water quality, forming the foundation for the subsequent analysis and discussion of results in the following chapter.

4 RESULTS AND DISCUSSION

This chapter presents the results of spatiotemporal variations in water quality across the Rákos Stream catchment over a two-year monitoring period (2019–2021). It integrates field-based measurements with spatial interpolation (Inverse Distance Weighting – IDW), statistical analyses, and process-based modeling using QUAL2K to examine how land use and hydrological dynamics influence pollutant behavior in the catchment.

First, spatial and seasonal variations in water quality parameters—such as ammonium, nitrate, phosphate, dissolved oxygen, total dissolved solids, and chlorophyll-a—are analyzed across eight sampling sites using GIS-based mapping and descriptive statistics. IDW interpolation is applied to visualize the spatial patterns of water quality across the catchment.

Second, land use and land cover (LULC) dynamics from 1990 to 2018 are evaluated to reveal trends in urbanization, agricultural expansion, and forest loss. The impact of these changes on water quality is then assessed through correlation analysis (Pearson and ANOVA) to quantify relationships between specific land use types and pollutant concentrations.

Finally, the QUAL2K model is employed to simulate hydrodynamics and water quality processes under current land use conditions. The model is calibrated and validated using observed field data, and applied to estimate pollutant loads from different land use types, assess in-stream attenuation zones, and evaluate the role of hydraulic structures in pollutant reduction.

Together, these analyses provide a comprehensive understanding of the factors shaping water quality in the Rákos Stream. The results offer evidence-based insights to support watershed planning, land use management, and future water quality monitoring efforts in similar peri-urban catchments.

4.1 Spatiotemporal patterns of water quality parameters

This section describes the spatial and temporal variability of key water quality parameters including pH, dissolved oxygen (DO), electrical conductivity (EC), and nutrient concentrations across the eight sampling locations from November 2019 to October 2021.

The results show clear seasonal and spatial differences in water quality conditions. Some parameters exhibit recurring seasonal trends (e.g., higher nutrient levels during warmer months), while others reflect spatial heterogeneity based on land use types surrounding each site. For example, urban and

agricultural areas are generally associated with higher nutrient and EC levels, whereas forested and natural areas tend to exhibit more stable and favorable water quality conditions.

Temporal variations across the sampling period indicate the influence of seasonal runoff, agricultural cycles, and possibly wastewater discharge patterns. Meanwhile, spatial differences suggest that land use and local pollution sources are key drivers of water quality dynamics.

Understanding these spatiotemporal patterns is essential for identifying hotspots of pollution, evaluating the influence of land use, and developing site-specific management strategies to improve water quality.

4.1.1 Analysis of NH_4^+ Concentrations

Figure 4-1 presents the spatiotemporal distribution of ammonium (NH_4^+) concentrations across eight sampling locations along the Rákos Stream during the monitoring period from November 2019 to October 2021. Overall, the dataset reveals substantial temporal fluctuations and spatial variability in NH_4^+ levels, with concentrations ranging from near-background values to peaks exceeding 3.5 mg/L. The timing and magnitude of these peaks differ notably among sampling points, reflecting localized pollution sources and environmental conditions.

The highest concentrations were consistently observed at Point-3 and Point-8, particularly during the summer of 2020 (e.g., June–August), when values surpassed 2 mg/L. These elevated levels likely result from increased runoff, urban wastewater inputs, and intensified microbial activity under warmer conditions. However, in contrast to this pattern, the summer of 2021 showed generally lower NH_4^+ concentrations across most sites, indicating potential changes in hydrological or land use dynamics.

Sampling points located in forested or less disturbed areas, such as Point-4 and Point-5, generally exhibited lower NH_4^+ concentrations throughout the study period. Nevertheless, occasional moderate increases were also observed at these sites, suggesting that even relatively undisturbed locations may experience short-term nutrient influxes under certain conditions.

These findings highlight both seasonal influences and land use effects on ammonium variability in the catchment. The spatial distribution suggests that monitoring and management efforts should prioritize areas with higher anthropogenic pressures, particularly during summer months when biological activity and runoff potential are elevated.

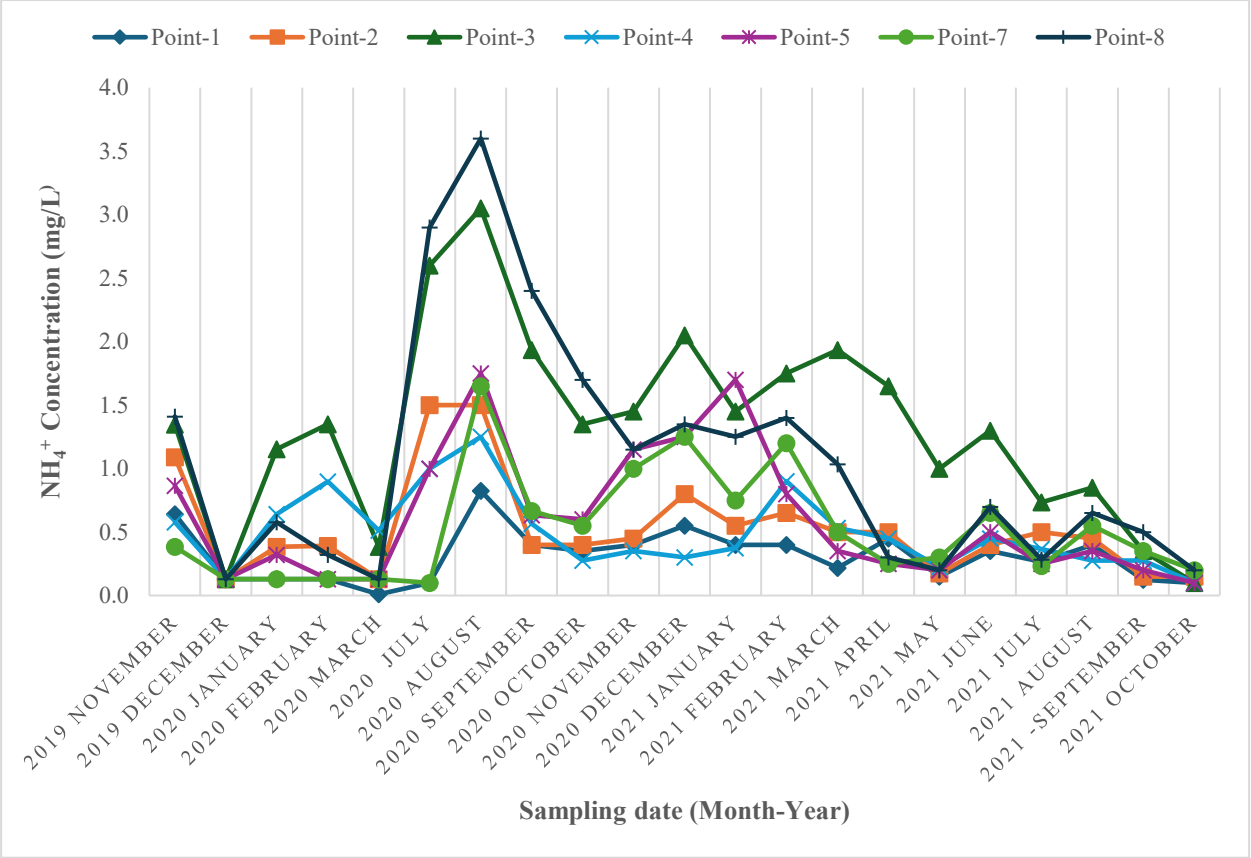

Figure 4-1 Spatiotemporal variations of Ammonium (NH_4^+) concentrations in the Rákos Stream

4.1.2 Analysis of NO_3- Concentrations

Figure 4-2 presents the spatiotemporal variations in nitrate (NO_3^-) concentrations across eight sampling points in the Rákos Stream from November 2019 to October 2021. The results reveal significant fluctuations over time and between locations, with some sites consistently exhibiting higher concentrations.

Sampling Points 1 and 3 recorded the highest nitrate concentrations, reaching peaks of approximately 105 mg/L and 85 mg/L, respectively. These sites are located in urban or agricultural zones, likely influenced by fertilizer use, stormwater runoff, and wastewater discharges.

In contrast, Point-4 generally showed lower nitrate concentrations, typically below 60 mg/L, although some variability was still observed.

The temporal trends also varied among sampling points, indicating that both land use and local hydrological conditions influence nitrate dynamics. For instance, the timing and intensity of rainfall

events, agricultural activity, and groundwater interactions may play roles in nitrate delivery and transport.

Overall, the nitrate data highlight a clear pattern of elevated concentrations in more developed areas, supporting the hypothesis that urbanization and intensive land use contribute significantly to nutrient enrichment in the stream. These findings underscore the importance of land use planning and pollution control measures in mitigating nitrate loading in surface waters.

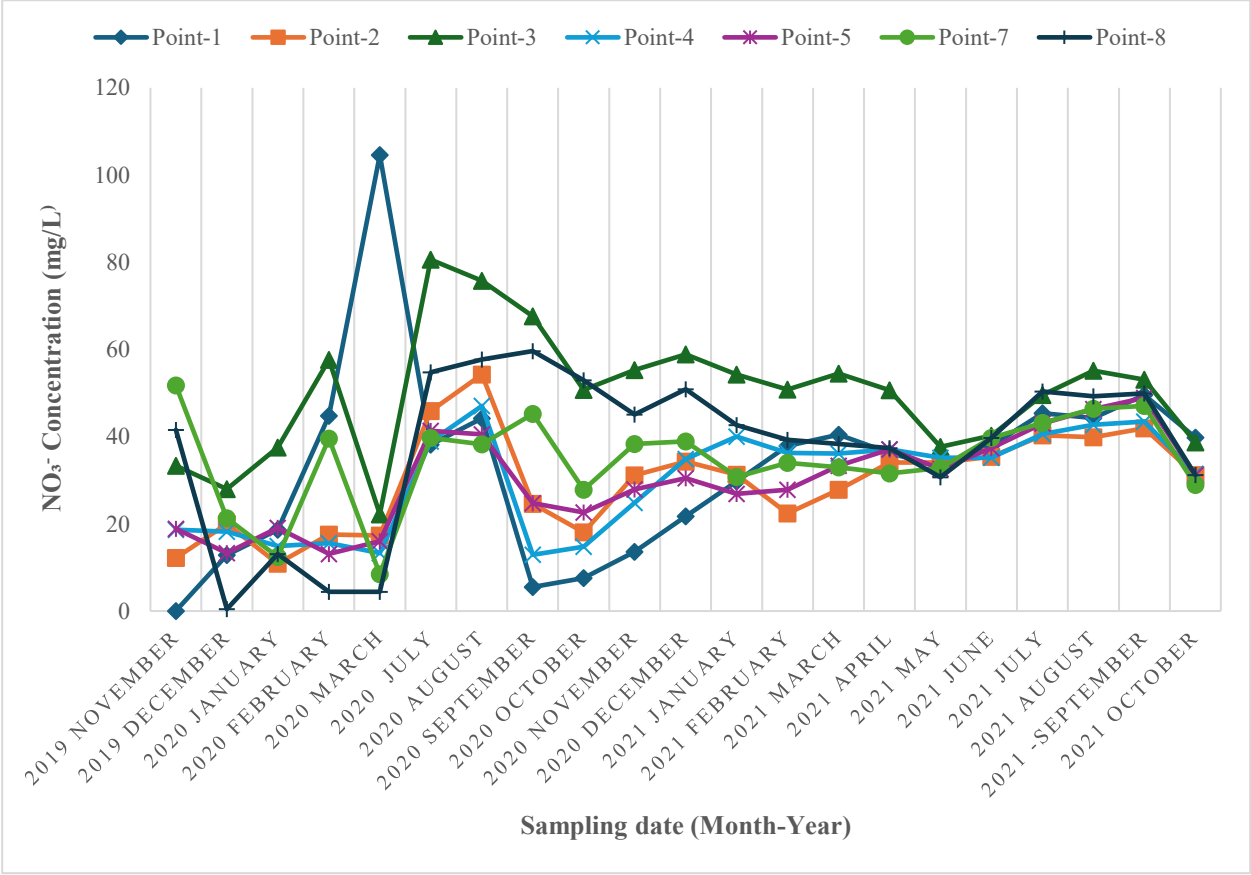

Figure 4-2 Spatiotemporal dynamics of Nitrate (NO_3-) concentrations in the Rákos Stream

4.1.3 Analysis of NO_2- Concentrations

Figure 4-3 illustrates the spatiotemporal variations in nitrite (NO_2^-) concentrations across eight sampling locations in the Rákos Stream during the monitoring period from November 2019 to October 2021. The results reveal distinct temporal patterns and pronounced spatial differences across the sites.

The highest NO_2^- level occurred at Point-3, reaching nearly 1.9 mg/L in January 2020. A noticeable increase was also observed at Point-1 in November 2019 (about 1.0 mg/L), and at Point-8 in October

2020 (~0.65 mg/L). These elevated levels are likely influenced by human activities such as urban runoff, agricultural practices, and potentially incomplete nitrification or denitrification processes near urban areas. Conversely, sampling points located in forested or less disturbed areas, such as Points 4, 5, and 7, generally maintained lower concentrations, often below 0.5 mg/L.

Nitrite concentrations are known to be sensitive to both pollution inputs and in-stream biochemical processes. The observed fluctuations across the monitoring stations suggest a combination of external inputs (e.g., wastewater discharge or fertilizer use) and internal dynamics (e.g., microbial transformations of nitrogen species) that vary with land use type and environmental conditions.

These findings demonstrate the relevance of both land-based pollution sources and in-stream nitrogen cycling in shaping NO_2^- dynamics. They emphasize the importance of monitoring intermediate nitrogen compounds like nitrite, which can serve as early indicators of disruptions in nitrogen transformation pathways and potential environmental stress in aquatic systems.

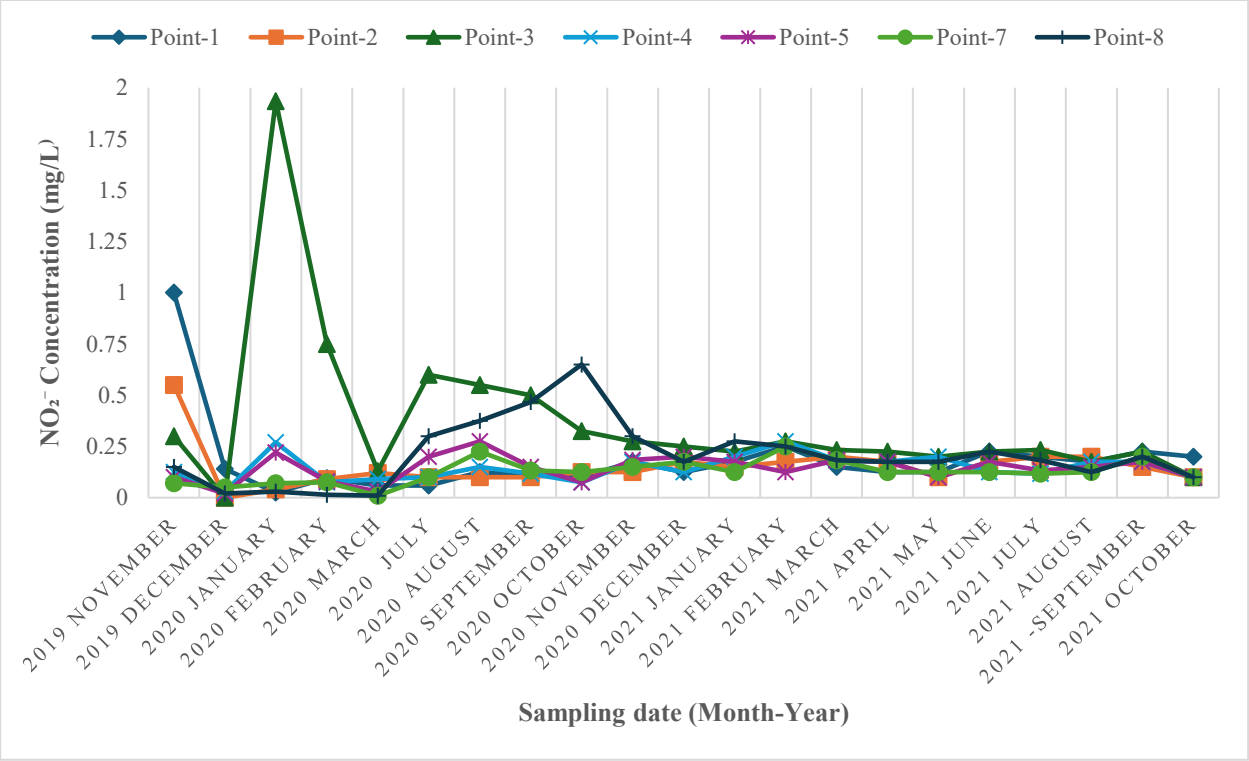

Figure 4-3 Spatiotemporal dynamics of Nitrite (NO_2^-) concentrations in the Rákos Stream

4.1.4 Analysis of Dissolved Oxygen Saturation

Figure 4-4 illustrates the spatiotemporal variability of dissolved oxygen (DO) saturation across eight sampling sites along the Rákos Stream from November 2019 to October 2021. Overall, DO saturation

ranged from values below 20% to peaks approaching 70%, with notable differences observed between sites and seasons.

Sampling Points 1 and 2, located in urbanized areas, generally recorded higher DO saturation during the early study period, although their advantage diminished over time. In contrast, Points 3 and 8 consistently exhibited lower saturation levels, accompanied by more pronounced fluctuations, potentially due to local pollution or hydrological disturbances.

DO saturation dynamics are influenced by various factors such as aeration, temperature, microbial activity, and organic matter decomposition. The observed temporal variability, especially the sharp declines at certain sites, may reflect the effects of increased biological oxygen demand (BOD) and urban runoff.

Meanwhile, less developed sites such as Point 4 demonstrated relatively stable DO levels, suggesting improved ecological conditions and limited anthropogenic impact. These results emphasize the crucial role of land use patterns in shaping oxygen availability and overall stream health.

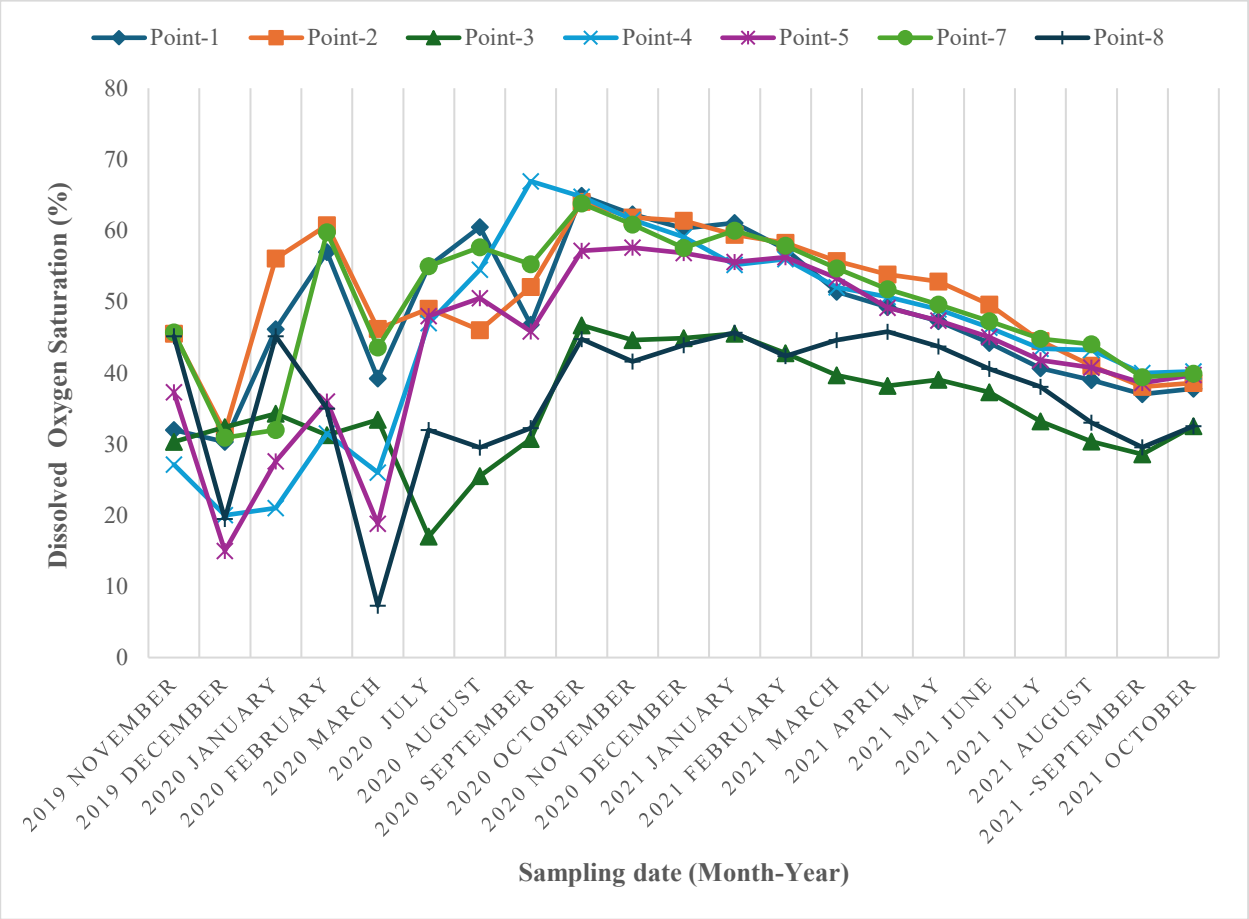

Figure 4-4 Spatiotemporal variations in Dissolved Oxygen (DO) Saturation levels in the Rákos Stream

4.1.5 Analysis of Chl-a Concentrations

Figure 4-5 illustrates the spatiotemporal variability of chlorophyll-a (Chl-a) concentrations across eight sampling locations in the Rákos Stream between November 2019 and October 2021. Chl-a serves as a key indicator of phytoplankton biomass and nutrient enrichment, thereby reflecting potential eutrophication in aquatic ecosystems.

The data reveal marked variability in both time and space. A pronounced peak was observed at Point 7 in December 2019 (~650 µg/L), followed by elevated levels at Point 1 in early 2020 (~300 µg/L) and at Point 2 in late 2021 (~400 µg/L). These values suggest localized algal blooms, likely driven by nutrient enrichment from adjacent land uses.

In contrast, Points 3, 4, 5, and 8 generally recorded lower concentrations, mostly below 200 µg/L, though short-term fluctuations were still evident.

Temporal variations in Chl-a concentration likely reflect shifts in nutrient loading, water temperature, solar radiation, and streamflow dynamics. The patterns observed highlight the role of anthropogenic inputs, particularly from urban and agricultural sources, in stimulating algal productivity. Meanwhile, relatively stable and low concentrations at less disturbed or forested sites imply limited nutrient input and better ecological conditions.

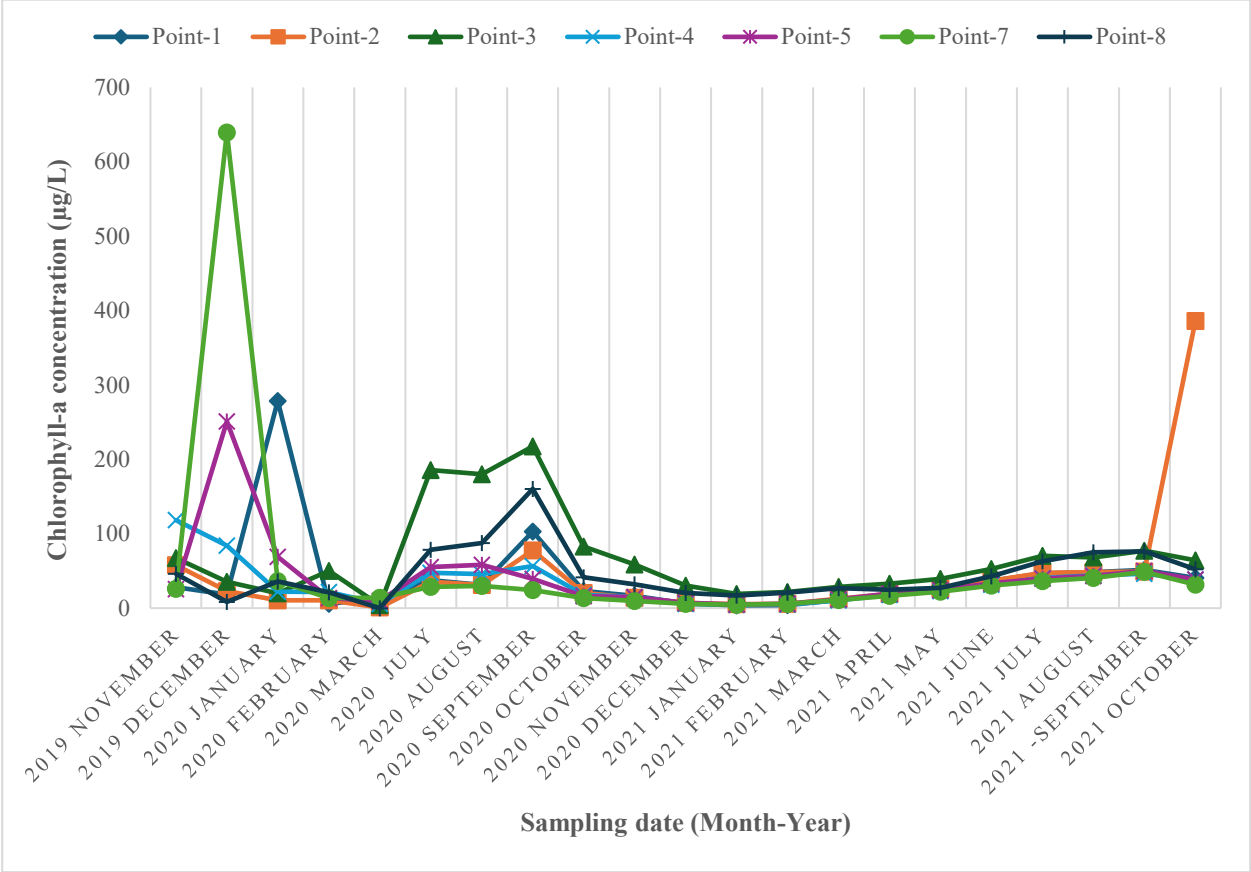

Figure 4-5 Spatiotemporal patterns of Chlorophyll-a (Chl-a) concentrations in the Rákos Stream

4.1.6 Analysis of pH Variations

Figure 4-6 presents the spatiotemporal variations in pH values across eight sampling locations along the Rákos Stream from November 2019 to October 2021. pH serves as a critical parameter reflecting the chemical balance of surface water, influenced by natural processes (e.g., mineral weathering, biological activity) and anthropogenic discharges.

The results reveal both spatial and temporal fluctuations in pH. The most pronounced variability was observed at Point 3 (Pécel), where pH values exceeded 8.5 at times, suggesting the influence of urban runoff, fertilizers, or wastewater discharge. A sharp peak at Point 8 in mid-2020 (~10.5) also indicates a potential episodic event affecting water chemistry.

In contrast, Points 4 and 5 exhibited more stable and slightly lower pH values, typically between 7.2 and 8.0, suggesting buffered conditions with limited human impact.

These spatial differences highlight the influence of land use on acid–base dynamics in the stream. Continuous monitoring of pH is essential, as deviations from neutral values can disrupt aquatic ecosystems and modify the behavior of other pollutants, such as metals and nutrients.

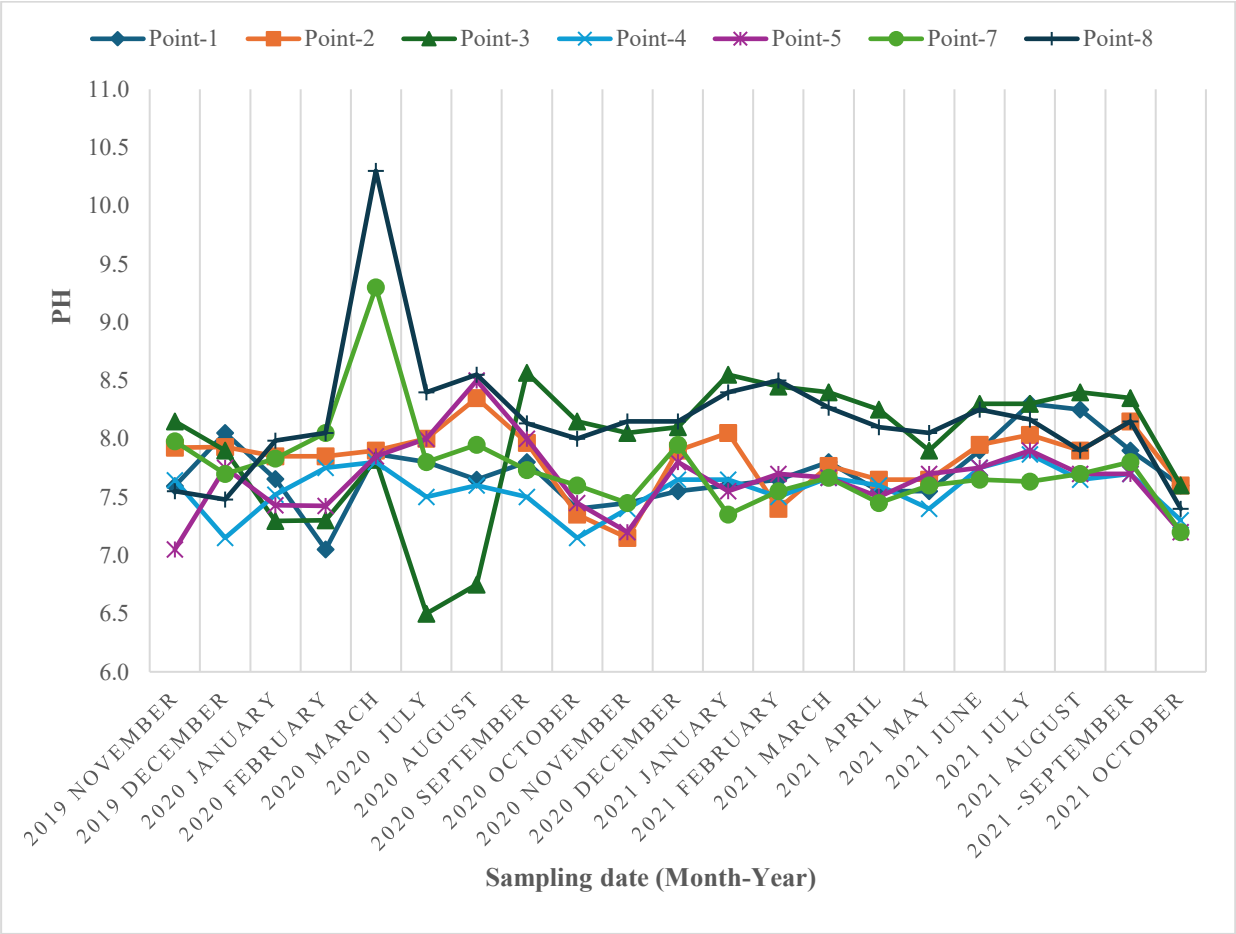

Figure 4-6 Spatiotemporal variations in pH in the Rákos Stream

4.1.7 Analysis of PO_4^{3-} Concentrations

Figure 4-7 shows the spatiotemporal distribution of phosphate (PO_4^{3-}) concentrations across the eight sampling locations in the Rákos Stream during the monitoring period from November 2019 to October 2021. Phosphate is a key nutrient in aquatic systems and often originates from both natural sources and human activities such as fertilizer runoff, wastewater discharge, and detergent use.

The results reveal pronounced spatial and temporal variability in PO_4^{3-} concentrations. Elevated phosphate levels were recorded at several urban and agricultural locations especially Points 8 and 3 (Pécel) indicating the likely influence of anthropogenic inputs from nearby residential and farming areas.

Interestingly, some forested or less developed areas such as Points 4 and 7 also exhibited occasional spikes in phosphate concentrations. These anomalies could be attributed to natural processes like internal loading from sediments, decaying organic matter, or transient hydrological conditions.

The temporal patterns show that phosphate concentrations often peaked during warmer months, possibly due to enhanced biological activity, surface runoff, or increased wastewater discharge during this period. The spatial differences highlight how land use types, local hydrology, and nutrient transport processes collectively shape phosphorus dynamics in the stream.

Understanding phosphate fluctuations is essential, as excessive PO_4^{3-} levels can lead to eutrophication, resulting in algal blooms and oxygen depletion. The findings underscore the importance of regulating both point and non-point phosphorus sources to maintain ecological balance in the Rákos catchment.

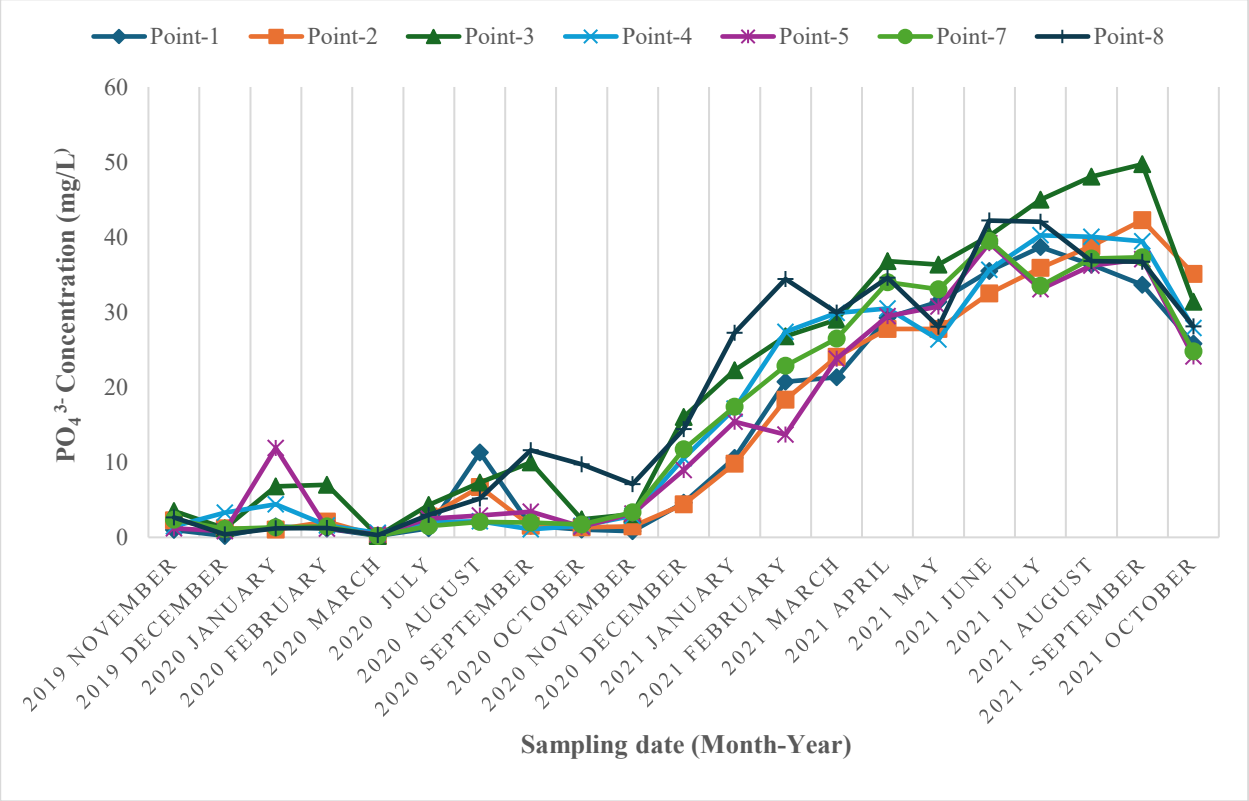

Figure 4-7 Spatiotemporal Dynamics of Phosphate (PO_4^{3-}) Concentrations in the Rákos Stream

4.1.8 Analysis of Electrical Conductivity (EC)

Error! Reference source not found. presents the spatiotemporal variations of electrical conductivity (EC) across eight sampling sites in the Rákos Stream from November 2019 to October 2021. EC

reflects the water's ability to conduct electrical current, which is primarily determined by the concentration of dissolved ionic substances such as salts, minerals, and other charged particles. It serves as a general indicator of water quality and salinity.

The results demonstrate considerable spatial and temporal variability in EC values across the catchment. Urban and agricultural areas, particularly Points 8 and 3 (Pécel) exhibited consistently higher EC levels. This pattern suggests the influence of urban runoff, wastewater discharge, and fertilizer application in these zones, which may contribute significant amounts of dissolved ions to the stream.

In contrast, forested and less developed sites, such as Points 4 (Pécel), 5, and 7, generally showed lower and more stable EC values. These areas are likely less exposed to anthropogenic pollution sources, and the surrounding vegetation and soils may promote better filtration and retention of dissolved constituents.

Temporal trends in EC varied across the sampling sites, with some locations showing seasonal peaks. These fluctuations could be influenced by precipitation events, surface runoff intensity, evapotranspiration rates, and changes in streamflow or baseflow contributions.

Elevated EC values may indicate increased salinity or pollution loads and can affect aquatic life, particularly species sensitive to ionic strength or osmotic stress. The findings emphasize the importance of monitoring EC as a surrogate for dissolved pollutant input and highlight the need to manage urban and agricultural sources to protect water quality in the Rákos Stream.

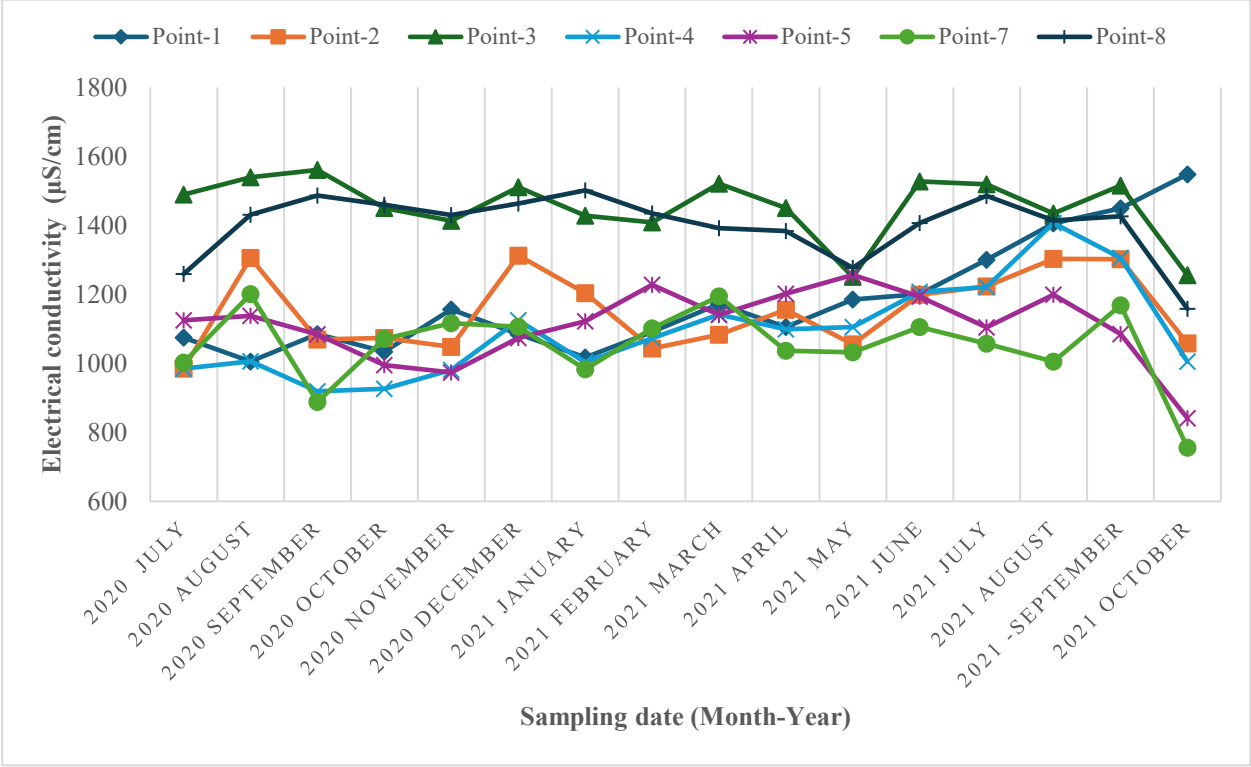

Figure 4-8 Spatiotemporal variations in electrical conductivity (EC) in the Rákos Stream

In summary, the spatiotemporal analysis of water quality parameters in the Rákos Stream revealed clear patterns associated with both seasonal variation and surrounding land use types. Urban and agricultural sites, particularly Points 8 and 3, consistently exhibited higher concentrations of nutrients (NH_4^+, NO_3^-, NO_2^-, PO_4^{3-}), elevated EC, and fluctuating DO and pH levels, suggesting substantial anthropogenic influence from urban runoff, wastewater discharges, and farming practices. In contrast, forested and natural areas such as Points 4 and 5 maintained relatively lower and more stable values across most parameters, reflecting more pristine environmental conditions. These observations emphasize the critical role of land use in shaping water quality dynamics and highlight the spatial complexity of pollutant distribution within the catchment. The next section further explores the statistical correlations between land use categories and water quality indicators to better understand the underlying relationships and dominant pollution sources.

4.2 The relationship between different water quality parameters

This section explores the interrelationships among water quality parameters based on a two-stage analysis: descriptive statistics and inferential correlation. The descriptive statistics (Table 4-1) provide

essential context for understanding spatial and temporal trends in measured indicators, while correlation and ANOVA tests reveal statistically significant associations between variables.

After performing ANOVA analysis, Duncan and Tukey statistics were used to compare the means. The results of these tests are presented in the appendices.

Table 4-1 Descriptive Statistics of Key Water Quality Parameters in Rákos Catchment

		N	Mean	Std. Deviation	Std. Error	95% Confidence Interval for Mean		Minimum	Maximum
						Lower Bound	Upper Bound		
Temperature	1	21	13.60	7.34	1.60	10.26	16.94	3.25	25.25
	2	21	13.27	7.21	1.57	9.99	16.55	3.15	24.50
	3	21	14.80	7.55	1.65	11.37	18.24	4.00	26.10
	4	21	13.03	7.38	1.61	9.68	16.39	2.60	24.35
	5	21	12.91	6.95	1.52	9.75	16.07	3.35	24.35
	7	21	12.94	6.50	1.42	9.99	15.90	5.40	24.50
	8	21	14.37	7.74	1.69	10.84	17.89	3.25	27.00
	Total	147	13.56	7.13	0.59	12.40	14.72	2.60	27.00
DO	1	21	48.54	10.53	2.30	43.75	53.34	30.30	64.90
	2	21	50.79	8.93	1.95	46.72	54.85	31.70	64.05
	3	21	35.15	7.42	1.62	31.77	38.53	17.00	46.70
	4	21	45.50	13.92	3.04	39.16	51.83	20.00	66.93
	5	21	43.72	12.07	2.63	38.23	49.21	15.00	57.60
	7	21	50.07	9.46	2.07	45.76	54.37	30.90	63.80
	8	21	36.76	9.86	2.15	32.27	41.25	7.30	45.80
	Total	147	44.36	11.82	0.97	42.43	46.29	7.30	66.93
NO_2^-	1	21	0.19	0.20	0.04	0.10	0.28	0.03	1.00
	2	21	0.16	0.10	0.02	0.11	0.20	0.04	0.55
	3	21	0.38	0.39	0.09	0.20	0.56	0.10	1.94
	4	21	0.15	0.06	0.01	0.12	0.18	0.03	0.28
	5	21	0.15	0.06	0.01	0.12	0.17	0.02	0.28
	7	21	0.13	0.06	0.01	0.10	0.15	0.01	0.25
	8	21	0.21	0.16	0.03	0.14	0.28	0.01	0.65
	Total	147	0.19	0.20	0.02	0.16	0.23	0.01	1.94
NO_3^-	1	21	33.61	22.07	4.82	23.57	43.66	0.04	104.61
	2	21	29.74	11.40	2.49	24.55	34.93	10.88	54.25
	3	21	50.10	14.52	3.17	43.49	56.71	22.21	80.60
	4	21	30.09	11.54	2.52	24.84	35.35	12.90	47.05
	5	21	30.11	10.62	2.32	25.28	34.95	13.11	48.90

	7	21	34.72	10.86	2.37	29.78	39.67	8.44	51.76
	8	21	37.80	17.92	3.91	29.64	45.96	0.44	59.63
	Total	147	35.17	15.88	1.31	32.58	37.76	0.04	104.61
CLA	1	21	40.30	59.08	12.89	13.40	67.19	3.75	278.45
	2	21	44.15	80.86	17.65	7.34	80.96	0.90	386.00
	3	21	66.92	57.74	12.60	40.64	93.20	3.90	217.47
	4	21	33.46	28.18	6.15	20.63	46.28	4.65	118.35
	5	21	39.59	51.97	11.34	15.94	63.25	4.85	251.00
	7	21	51.83	135.23	29.51	-9.72	113.39	4.60	639.50
	8	21	45.61	35.88	7.83	29.28	61.95	0.00	160.37
	Total	147	45.98	71.36	5.89	34.35	57.61	0.00	639.50
NH_4^+	1	21	0.31	0.21	0.04	0.22	0.40	0.01	0.83
	2	21	0.53	0.40	0.09	0.35	0.71	0.13	1.50
	3	21	1.33	0.76	0.17	0.98	1.68	0.10	3.05
	4	21	0.50	0.30	0.07	0.36	0.63	0.10	1.25
	5	21	0.60	0.51	0.11	0.37	0.84	0.10	1.75
	7	21	0.53	0.43	0.09	0.33	0.73	0.10	1.65
	8	21	1.06	0.95	0.21	0.62	1.49	0.13	3.60
	Total	147	0.69	0.65	0.05	0.59	0.80	0.01	3.60
Ph	1	21	7.71	0.28	0.06	7.58	7.84	7.05	8.30
	2	21	7.83	0.28	0.06	7.70	7.95	7.15	8.35
	3	21	7.96	0.57	0.12	7.70	8.22	6.50	8.57
	4	21	7.56	0.20	0.04	7.47	7.65	7.15	7.87
	5	21	7.66	0.32	0.07	7.51	7.80	7.05	8.50
	7	21	7.76	0.41	0.09	7.57	7.95	7.20	9.30
	8	21	8.19	0.57	0.12	7.93	8.45	7.40	10.30
	Total	147	7.81	0.44	0.04	7.74	7.88	6.50	10.30
PO_4^{3-}	1	21	14.66	14.77	3.22	7.94	21.38	0.20	38.67
	2	21	15.11	15.35	3.35	8.12	22.10	0.20	42.25
	3	21	20.35	17.30	3.78	12.47	28.22	0.20	49.70
	4	21	16.48	15.58	3.40	9.39	23.57	0.60	40.23
	5	21	15.26	14.26	3.11	8.77	21.76	0.40	39.20
	7	21	15.94	15.30	3.34	8.98	22.91	0.20	39.50
	8	21	18.90	15.62	3.41	11.79	26.01	0.30	42.20
	Total	147	16.67	15.29	1.26	14.18	19.16	0.20	49.70
EC	1	16	1,182.12	162.28	40.57	1,095.64	1,268.59	1,006	1,548
	2	16	1,151.20	112.85	28.21	1,091.06	1,211.33	985	1,313
	3	16	1,454.68	91.74	22.94	1,405.79	1,503.56	1,251	1,561
	4	16	1,094.34	137.34	34.34	1,021.16	1,167.53	919	1,407
	5	16	1,110.02	105.71	26.43	1,053.69	1,166.35	841	1,257

7	16	1,051.59	113.45	28.36	991.14	1,112.04	756	1,201
8	16	1,400.54	93.28	23.32	1,350.84	1,450.25	1,158	1,502
Total	112	1,206.36	186.65	17.64	1,171.41	1,241.30	756	1,561

The descriptive statistics revealed notable variability in water quality across the sampling sites. Temperature ranged from 2.6°C to 27.0°C, with a mean of 13.56°C, indicating seasonal and spatial fluctuations. Dissolved oxygen (DO) levels varied widely, from 7.3 mg/L to 66.93 mg/L, averaging 44.36 mg/L, reflecting dynamic biological and chemical processes in the stream. Nitrate (NO_3^-) concentrations showed considerable spatial differences, with an average of 35.17 mg/L and peaks exceeding 100 mg/L in agricultural and urban areas. Nitrite (NO_2^-) and ammonium (NH_4^+) averaged 0.19 mg/L and 0.69 mg/L, respectively, with occasional high values pointing to localized pollution events. Phosphate (PO_4^{3-}) levels averaged 16.67 mg/L, with maxima approaching 50 mg/L, while chlorophyll-a (Chl-a) exhibited sharp fluctuations, reaching up to 639.5 µg/L likely associated with episodic algal blooms. Electrical conductivity (EC) averaged 1206.36 µS/cm, with a high standard deviation (186.65), highlighting significant differences in ionic strength across the catchment. The pH ranged from 6.5 to 10.3, indicating generally neutral to slightly alkaline conditions.

The Pearson correlation analysis (Table 4-2) showed several significant relationships among the water quality parameters, providing insights into nutrient dynamics and pollution processes.

- **Temperature** was positively correlated with NO_3^-, PO_4^{3-}, pH, and EC, suggesting that warmer conditions may enhance nutrient level and electrical conductivity.
- **Dissolved oxygen (DO)** showed negative correlations with NO_2^-, Chl-a, EC, and pH, indicating that higher nutrient and algal activity is associated with lower oxygen levels.
- **Nitrite (NO_2^-)** was positively correlated with NO_3^-, NH_4^+, and EC, but negatively with DO, reflecting co-occurrence of nitrogen forms under oxygen-depleted conditions.
- **Nitrate (NO_3^-)** had strong positive correlations with PO_4^{3-}, NH_4^+, and EC, highlighting the simultaneous accumulation of multiple nutrients in impacted areas.
- **Chlorophyll-a** correlated positively with EC and negatively with DO, emphasizing the role of algal growth in altering water chemistry.
- **Ammonium (NH_4^+)** showed positive correlations with NO_3^-, NO_2^-, and EC, suggesting overlapping sources or transformation pathways.

- **pH** was positively related to temperature and EC, and negatively with DO, indicating increased alkalinity under low-oxygen, high-solute conditions.
- **Phosphate (PO_4^{3-})** correlated positively with NO_3^-, temperature, and EC, supporting the notion of nutrient co-mobilization.
- **EC** showed positive correlations with most parameters (except DO), confirming its integrative role in reflecting the overall water quality status.

Table 4-2 Pearson's correlation between different water quality parameters, in the Rákos River basin

		Temperature	DO	NO_2^-	NO_3^-	CLA	NH_4^+	PH	PO_4^{3-}	EC
Temperature	Pearson Correlation	1	-0.136	-0.010	.512**	0.109	0.152	.163*	.535**	.239*
	Sig. (2-tailed)		0.101	0.906	0.000	0.190	0.066	0.048	0.000	0.011
	N	147	147	147	147	147	147	147	147	112
DO	Pearson Correlation	-0.136	1	-.163*	-0.073	-.347**	-0.096	-.243**	-0.078	-.641**
	Sig. (2-tailed)	0.101		0.049	0.380	0.000	0.248	0.003	0.345	0.000
	N	147	147	147	147	147	147	147	147	112
NO_2^-	Pearson Correlation	-0.010	-.163*	1	.246**	0.030	.428**	-0.080	-0.016	.599**
	Sig. (2-tailed)	0.906	0.049		0.003	0.722	0.000	0.334	0.849	0.000
	N	147	147	147	147	147	147	147	147	112
NO_3^-	Pearson Correlation	.512**	-0.073	.246**	1	0.088	.481**	0.100	.361**	.659**
	Sig. (2-tailed)	0.000	0.380	0.003		0.292	0.000	0.230	0.000	0.000
	N	147	147	147	147	147	147	147	147	112
CLA	Pearson Correlation	0.109	-.347**	0.030	0.088	1	0.096	-0.034	-0.038	.290**
	Sig. (2-tailed)	0.190	0.000	0.722	0.292		0.249	0.679	0.650	0.002
	N	147	147	147	147	147	147	147	147	112
NH_4^+	Pearson Correlation	0.152	-0.096	.428**	.481**	0.096	1	0.155	-0.147	.439**
	Sig. (2-tailed)	0.066	0.248	0.000	0.000	0.249		0.061	0.076	0.000
	N	147	147	147	147	147	147	147	147	112
PH	Pearson Correlation	.163*	-.243**	-0.080	0.100	-0.034	0.155	1	0.127	.584**
	Sig. (2-tailed)	0.048	0.003	0.334	0.230	0.679	0.061		0.126	0.000
	N	147	147	147	147	147	147	147	147	112
PO_4^{3-}	Pearson Correlation	.535**	-0.078	-0.016	.361**	-0.038	-0.147	0.127	1	.324**
	Sig. (2-tailed)	0.000	0.345	0.849	0.000	0.650	0.076	0.126		0.000
	N	147	147	147	147	147	147	147	147	112
EC	Pearson Correlation	.239*	-.641**	.599**	.659**	.290**	.439**	.584**	.324**	1
	Sig. (2-tailed)	0.011	0.000	0.000	0.000	0.002	0.000	0.000	0.000	
	N	112	112	112	112	112	112	112	112	112

****. Correlation is significant at the 0.01 level (2-tailed).**

***. Correlation is significant at the 0.05 level (2-tailed).**

The ANOVA results (Table 4-3) confirmed statistically significant spatial variability for several parameters. Dissolved oxygen (DO), nitrate (NO_3^-), ammonium (NH_4^+), nitrite (NO_2^-), pH, and electrical conductivity (EC) all exhibited significant differences across the sampling sites ($p < 0.001$). In contrast, temperature, chlorophyll-a (Chl-a), and phosphate (PO_4^{3-}) did not show significant spatial variation, likely due to uniform distributions or buffering mechanisms. The particularly high F-value for EC ($F = 28.03$) highlights its utility as a sensitive indicator of spatial variation in ionic content and pollution gradients across the catchment.

Table 4-3 ANOVA Results for Spatial Differences in Water Quality Parameters Across Sampling Sites

		Sum of Squares	df	Mean Square	F	Sig.
Temperature	Between Groups	70.76	6	11.79	0.22	0.97
	Within Groups	7352.60	140	52.52		
	Total	7423.35	146			
DO	Between Groups	4950.57	6	825.09	7.48	0.00
	Within Groups	15439.86	140	110.28		
	Total	20390.43	146			
NO_2^-	Between Groups	0.91	6	0.15	4.45	0.00
	Within Groups	4.79	140	0.03		
	Total	5.71	146			
NO_3^-	Between Groups	6578.39	6	1096.40	5.07	0.00
	Within Groups	30254.69	140	216.11		
	Total	36833.08	146			
CLA	Between Groups	14828.40	6	2471.40	0.48	0.83
	Within Groups	728643.68	140	5204.60		
	Total	743472.08	146			
NH_4^+	Between Groups	16.37	6	2.73	8.57	0.00
	Within Groups	44.56	140	0.32		
	Total	60.94	146			
PH	Between Groups	5.50	6	0.92	5.71	0.00
	Within Groups	22.44	140	0.16		
	Total	27.94	146			
PO_4^{3-}	Between Groups	577.84	6	96.31	0.40	0.88
	Within Groups	33544.92	140	239.61		
	Total	34122.76	146			
EC	Between Groups	2380485.46	6	396747.58	28.03	0.00
	Within Groups	1486460.08	105	14156.76		
	Total	3866945.55	111			

Overall, the statistical analyses, including descriptive summaries, Pearson correlation, and ANOVA, demonstrated clear interactions among water quality parameters and significant spatial variability across the Rákos Stream catchment. Parameters such as DO, NO_3^-, NH_4^+, NO_2^-, and EC were

especially sensitive to changes in land use and site conditions. These findings underscore the need for targeted monitoring and management strategies focusing on areas with elevated nutrient and solute levels. The following section further explores how different land use types influence water quality patterns in the catchment.

4.3 LULC composition

The distribution of land use and land cover (LULC) types varied noticeably across the sub-catchments of the Rákos Stream (Table 4-4, Figure 4-9). Site S1 was dominated by artificial surfaces, comprising 65.51% of its area, substantially higher than at any other site. In contrast, Site S4 exhibited the lowest proportion of artificial surfaces (0.88%) and had the highest coverage of forest and semi-natural areas at 64.40%.

Agricultural land was most extensive at Site S3 (49.09%), followed by Site S2 (42.28%). By comparison, Site S1 had a much smaller agricultural footprint (20.49%). Sites S5 and S6–7 had moderate shares of agricultural areas at 28.22% and 37.45%, respectively.

Forested and semi-natural areas were concentrated primarily at Site S4, while Site S2 had the least forest cover, with only 0.14%. Site S3 also had a notable forest proportion (20.09%).

Wetlands and water bodies were generally scarce across the study area. Site S5 was the only location with both wetland (0.74%) and surface water (2.30%), whereas no such features were recorded at the other sites.

In summary, the analysis highlights distinct land use patterns within the Rákos catchment. Site S1 represents a highly urbanized area, while Site S4 is characterized by its natural landscape. The agricultural zones were primarily concentrated in Sites S2 and S3, reflecting the spatial heterogeneity in land use across the catchment.

Table 4-4 Land use/land cover (%) in the eight sub catchments, in the Rákos Stream basin

Site	Artificial surfaces	Agricultural areas	Forest and semi natural areas	Wetland	Water bodies
S1	65.51	20.49	14		
S2	57.59	42.28	0.14		
S3	30.81	49.09	20.09		
S4	0.88	34.72	64.40		
S5	28.85	28.22	39.88	0.74	2.30
S6,7	49.55	37.45	12.99		
S8	48.52	36.72	14.75		

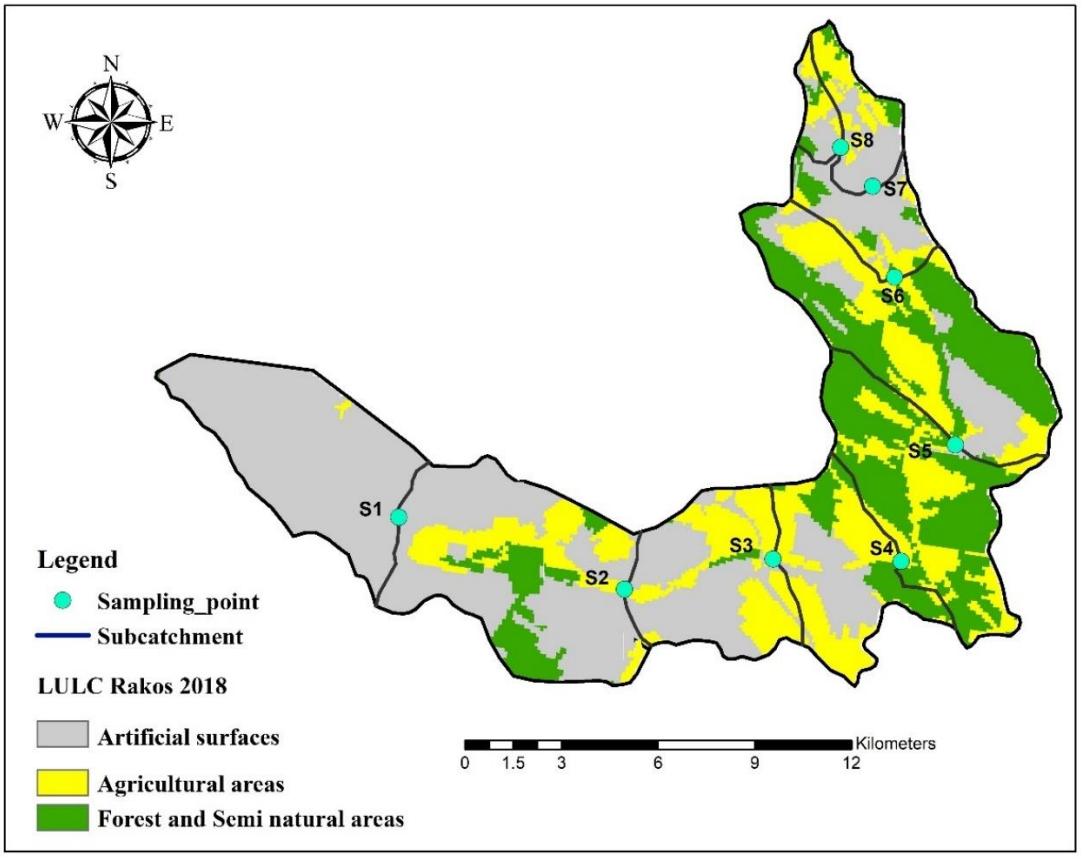

Figure 4-9 Sub-catchments of the Rákos Stream with corresponding sampling and LULC classes

4.4 Impacts of LULC on water quality

Before performing correlation and ANOVA statistical analyses, the preconditions for these analyses, including data normality and homogeneity of variances, were performed through Kolmogorov-Smirnov and Levene Statistic, the results of which are presented in the appendices. The Pearson correlation analysis provided insights into the statistical relationships between land use and land cover (LULC) types and water quality parameters in the Rákos Stream. These correlations indicate associations but do not imply direct causation. The analysis was conducted using monthly average water quality data, and the strength and significance levels of the correlations are reported to ensure transparent interpretation (Table 4-5).

The proportion of heterogeneous agricultural areas showed statistically significant positive correlations with nitrite (NO_2^-, $r = 0.230$, $p < 0.01$), ammonium (NH_4^+, $r = 0.286$, $p < 0.001$), and electrical conductivity (EC, $r = 0.381$, $p < 0.001$), and a significant negative correlation with dissolved oxygen (DO, $r = –0.203$, $p < 0.05$). These patterns are consistent with established findings that

heterogeneous agricultural land can contribute to nutrient enrichment and ionic concentration in streams, likely due to fertilizer runoff, soil erosion, and nutrient leaching.

Pasture areas displayed negative correlations with nitrate (NO_3^-, $r = –0.176$, $p < 0.05$) and ammonium (NH_4^+, $r = –0.243$, $p < 0.01$), both statistically significant. Weak negative correlations were also observed with pH ($r = –0.089$, $p > 0.05$) and EC ($r = –0.102$, $p > 0.05$), though these were not statistically significant.

EC exhibited significant negative correlations with Industrial/Commercial areas ($r = –0.229$, $p < 0.01$), Urban Fabric ($r = –0.217$, $p < 0.01$), and Arable Land ($r = –0.352$, $p < 0.001$), and a weak, non-significant negative correlation with Pasture. In contrast, EC had significant positive correlations with Heterogeneous Agricultural areas ($r = 0.381$, $p < 0.001$), Dumpsites ($r = 0.217$, $p < 0.01$), and Transitional Woodland ($r = 0.341$, $p < 0.001$), as well as with Forest ($r = 0.341$, $p < 0.001$), indicating potential ionic enrichment in areas with both disturbed and certain vegetated land covers.

A positive and significant correlation was observed between green urban areas and DO ($r = 0.260$, $p < 0.01$), suggesting that vegetated urban spaces may help sustain or improve oxygen availability in stream ecosystems.

These results highlight that while some land use types, particularly heterogeneous agricultural areas and dumpsites, are associated with elevated nutrient concentrations and increased EC, others, such as green urban areas and certain pasturelands, may have a more neutral or potentially beneficial influence on water quality.

Table 4-5 Pearson's correlation between land use/land cover (LULC) and water quality parameters (Monthly), in Rákos River basin

		Industrial Commercial	Urban Fabric	forest	Transitional Woodland	Green Urban	Arable land	Pasture	Permanent Crops	Heterogeneous	Dumpsites
Temperature	Pearson Correlation	-0.039	-0.037	-0.037	0.036	-0.005	-0.028	-0.043	0.002	0.040	0.037
	Sig. (2-tailed)	0.641	0.653	0.653	0.668	0.950	0.738	0.606	0.980	0.628	0.656
	N	147	147	147	147	147	147	147	147	147	147
DO	Pearson Correlation	-0.016	-0.022	-0.022	-0.151	.260**	-0.094	0.043	0.145	-.203*	-0.031
	Sig. (2-tailed)	0.851	0.790	0.790	0.068	0.001	0.256	0.608	0.080	0.014	0.713
	N	147	147	147	147	147	147	147	147	147	147
NO_2^-	Pearson Correlation	-0.104	-0.099	-0.099	-0.013	-0.008	-0.060	-0.106	-0.016	.230**	.218**
	Sig. (2-tailed)	0.212	0.235	0.235	0.872	0.924	0.470	0.202	0.850	0.005	0.008
	N	147	147	147	147	147	147	147	147	147	147
NO_3^-	Pearson Correlation	-0.131	-0.130	-0.130	-0.006	0.019	-0.081	-.176*	-0.040	0.145	0.158
	Sig. (2-tailed)	0.113	0.115	0.115	0.943	0.823	0.327	0.033	0.630	0.079	0.057
	N	147	147	147	147	147	147	147	147	147	147
CLA	Pearson Correlation	-0.036	-0.037	-0.037	-0.027	0.052	-0.060	-0.086	-0.033	0.050	0.048
	Sig. (2-tailed)	0.667	0.659	0.659	0.744	0.533	0.473	0.298	0.695	0.548	0.564
	N	147	147	147	147	147	147	147	147	147	147
NH_4^+	Pearson Correlation	-0.062	-0.058	-0.058	0.072	-0.119	-0.035	-.177*	-.243**	.286**	0.036
	Sig. (2-tailed)	0.458	0.486	0.486	0.383	0.149	0.673	0.032	0.003	0.000	0.669
	N	147	147	147	147	147	147	147	147	147	147
pH	Pearson Correlation	-0.143	-0.141	-0.141	.289**	0.034	-.231**	-.325**	-0.089	0.094	-0.014
	Sig. (2-tailed)	0.084	0.089	0.089	0.000	0.687	0.005	0.000	0.282	0.259	0.870
	N	147	147	147	147	147	147	147	147	147	147
PO_4^{3-}	Pearson Correlation	-0.039	-0.038	-0.038	0.015	-0.042	0.008	-0.031	-0.054	0.057	-0.003
	Sig. (2-tailed)	0.643	0.650	0.650	0.853	0.610	0.927	0.705	0.516	0.495	0.974
	N	147	147	147	147	147	147	147	147	147	147
EC	Pearson Correlation	-.229**	-.217**	-.217**	.341**	-0.115	-.201*	-.352**	-0.102	.381**	.217**
	Sig. (2-tailed)	0.005	0.008	0.008	0.000	0.166	0.015	0.000	0.219	0.000	0.008
	N	147	147	147	147	147	147	147	147	147	147

The seasonal Pearson correlation analysis offers additional insight into how land use and land cover (LULC) types influence water quality in the Rákos Stream (Table 4-6). Among the notable findings, heterogeneous agricultural areas and dumpsites showed significant positive correlations with nitrite (NO_2^-; $r = 0.436$ and $r = 0.438$, $p < 0.05$, respectively) and ammonium (NH_4^+; $r = 0.595$, $p < 0.01$ for heterogeneous agriculture). EC was also positively correlated with heterogeneous agriculture ($r = 0.462$, $p < 0.05$), suggesting that these land uses are associated with higher nutrient and dissolved solids levels, potentially due to runoff and leaching.

Permanent crops exhibited a significant negative correlation with NH_4^+ ($r = –0.385$, $p < 0.05$), while pasture areas were strongly negatively correlated with pH ($r = –0.504$, $p < 0.01$), indicating that these land uses may help moderate nutrient enrichment and stabilize stream water chemistry.

Dissolved oxygen (DO) showed a positive, borderline significant relationship with green urban areas ($r = 0.371$, $p = 0.057$), but a negative correlation with permanent crops ($r = –0.380$, $p = 0.050$), which may reflect oxygen depletion in more intensively cultivated areas.

It is important to note that these results indicate statistical associations rather than direct causal effects. Seasonal variability in hydrological conditions, rainfall patterns, and possible point-source discharges could also contribute to the observed correlations. Further analyses integrating hydrological connectivity and potential pollution sources would be needed to establish causal pathways.

Overall, the seasonal analysis is consistent with the monthly results, highlighting that heterogeneous agricultural areas and dumpsites are persistently linked with degraded water quality, while some land uses, such as pasture and permanent crops, may play a mitigating role in nutrient loading.

Table 4-6 Pearson's correlation between land use/land cover (LULC) and water quality parameters (Seasonal), in Rákos River basin

		Industrial Commercial	Urban Fabric	Forest	Transitional Woodland	Green Urban	Arable land	Pasture	Permanent Crops	Heterogeneous	Dumpsites
Temperature	Pearson Correlation	-0.022	-0.017	-0.017	0.03	-0.04	-0.004	0.008	0.026	0.123	0.11
	Sig. (2-tailed)	0.913	0.932	0.932	0.882	0.845	0.983	0.969	0.898	0.541	0.585
	N	27	27	27	27	27	27	27	27	27	27
DO	Pearson Correlation	-0.055	-0.064	-0.064	-0.044	0.371	-0.19	0.021	0.222	-0.38	-0.163
	Sig. (2-tailed)	0.784	0.752	0.752	0.827	0.057	0.342	0.915	0.266	0.05	0.417
	N	27	27	27	27	27	27	27	27	27	27
NO_2^-	Pearson Correlation	-0.176	-0.169	-0.169	-0.123	0.023	-0.093	-0.161	-0.018	.436*	.438*
	Sig. (2-tailed)	0.379	0.4	0.4	0.543	0.908	0.643	0.423	0.928	0.023	0.022
	N	27	27	27	27	27	27	27	27	27	27
NO_3^-	Pearson Correlation	-0.164	-0.16	-0.16	-0.075	0.02	-0.086	-0.191	-0.032	0.29	0.315
	Sig. (2-tailed)	0.415	0.425	0.425	0.709	0.919	0.669	0.339	0.873	0.143	0.11
	N	27	27	27	27	27	27	27	27	27	27
CLA	Pearson Correlation	-0.056	-0.06	-0.06	-0.21	0.18	-0.115	-0.143	-0.05	0.134	0.179
	Sig. (2-tailed)	0.78	0.767	0.767	0.294	0.37	0.567	0.478	0.804	0.506	0.372
	N	27	27	27	27	27	27	27	27	27	27
NH_4^+	Pearson Correlation	-0.081	-0.077	-0.077	-0.177	-0.096	-0.027	-0.217	-.385*	.595**	0.234
	Sig. (2-tailed)	0.686	0.704	0.704	0.378	0.633	0.892	0.276	0.047	0.001	0.239
	N	27	27	27	27	27	27	27	27	27	27
pH	Pearson Correlation	-0.222	-0.218	-0.218	0.358	0.094	-0.368	-.504**	-0.137	0.223	0.066
	Sig. (2-tailed)	0.266	0.274	0.274	0.067	0.64	0.059	0.007	0.497	0.264	0.742
	N	27	27	27	27	27	27	27	27	27	27
PO_4^{3-}	Pearson Correlation	-0.046	-0.046	-0.046	-0.005	-0.049	0.013	-0.045	-0.073	0.082	0.013
	Sig. (2-tailed)	0.818	0.821	0.821	0.981	0.808	0.95	0.825	0.718	0.683	0.949
	N	27	27	27	27	27	27	27	27	27	27
EC	Pearson Correlation	-0.224	-0.214	-0.214	0.201	-0.053	-0.21	-0.363	-0.106	.462*	0.328
	Sig. (2-tailed)	0.261	0.284	0.284	0.314	0.793	0.293	0.063	0.597	0.015	0.095
	N	27	27	27	27	27	27	27	27	27	27

In summary, both the monthly and seasonal correlation analyses revealed consistent and statistically meaningful relationships between specific land use types and water quality indicators in the Rákos Stream. Agricultural areas, particularly heterogeneous agricultural land, and dumpsites emerged as key contributors to elevated nutrient levels and increased total dissolved solids, indicating persistent anthropogenic pressures throughout the year. In contrast, land uses such as pastures, permanent crops, forests, and green urban areas demonstrated associations with improved water quality conditions. These findings emphasize the importance of incorporating land use planning and environmental management strategies to mitigate pollution sources and enhance the ecological integrity of the stream.

4.5 GIS Interpolation, IDW

The spatial distribution of water quality parameters was analyzed using Inverse Distance Weighting (IDW) interpolation within a GIS environment (Figure 4-10). The resulting maps effectively visualize the spatial variation of physico-chemical pollutants across the Rákos stream catchment and are consistent with the trends identified in the statistical analyses. The color gradients in the IDW maps highlight zones of varying water quality, with red representing higher pollutant concentrations and green indicating relatively clean areas. The maps show clear spatial trends, where parameters such as ammonium (NH_4^+), nitrite (NO_2^-), nitrate (NO_3^-), phosphate (PO_4^{3-}), electrical conductivity (EC), and chlorophyll-a (Chl-a) are elevated in areas like Point_03 and Point_08. These locations correspond to regions influenced by heterogeneous agricultural land and dumpsites, as previously revealed through the Pearson correlation analysis. In contrast, the lowest concentrations for many parameters are observed in upstream and midstream regions, where pasture and natural land cover types are more dominant. This spatial distribution aligns with the earlier statistical findings, suggesting that land use types significantly influence water quality conditions across the catchment.

Overall, the spatial interpolation confirms that pollutant concentrations vary progressively along the stream, supporting the conclusion that land use management and pollution control measures should be spatially targeted to areas with the highest contamination levels. The accuracy assessment in this study demonstrated that IDW achieved satisfactory predictive performance for all assessed parameters, confirming its suitability for mapping spatial variations in water quality within the Rákos Stream catchment.

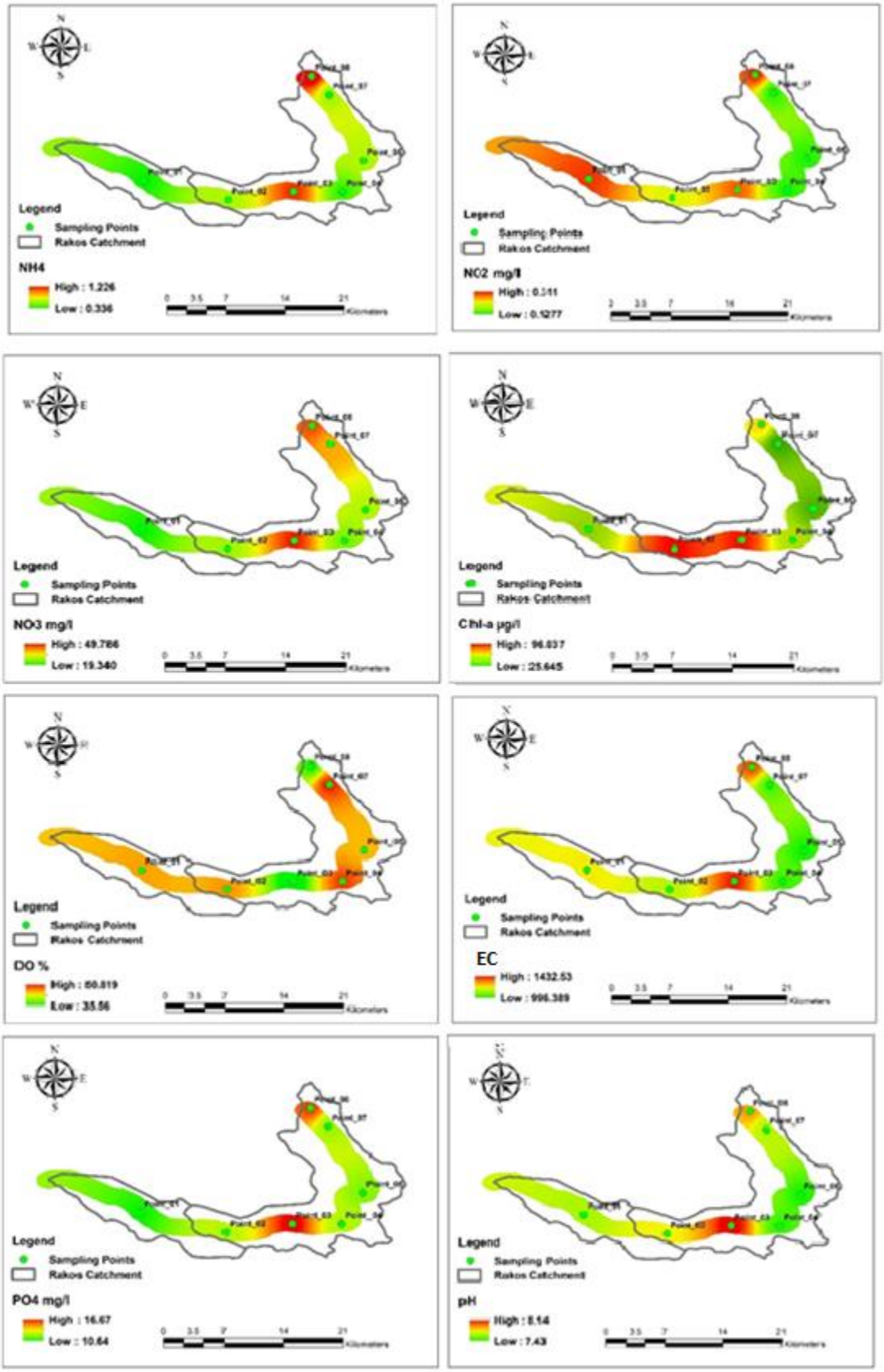

Figure 4-10 Spatial distribution of water quality parameter in the Rákos catchment, Hungary

4.6 Accuracy assessment and cross validation

Accuracy assessment is essential for evaluating the reliability of spatial interpolation methods. A more accurate interpolation approach produces predicted values that closely reflect the observed data, minimizing smoothing effects and preserving spatial variability (Sekulić et al., 2020). In this study, the accuracy of the Inverse Distance Weighting (IDW) interpolation method, applied to assess the surface water quality in the Rákos Stream, was evaluated using two widely accepted statistical indicators: Mean Error (ME) and Root Mean Square Error (RMSE**)** (Table 4-7).

Table 4-7 General results of cross validation analysis for IDW interpolation method used to assess Rákos Stream surface water quality

Criteria	ME	RMSE
NO_3^-	1.83	11.83
NO_2^-	-0.012	0.108
NH_4^+	0.031	0.45
PO_4^{3-}	0.27	2.8
DO	-0.009	8.53
EC	-9.68	239.70
PH	0.002	0.28
Chl-a	-0.55	32.27

The performance of the IDW method was assessed based on how closely ME values approached zero and how small the RMSE values were, as recommended by Njeban (2018). The results demonstrate satisfactory predictive accuracy across all assessed parameters, indicating that the IDW interpolation reasonably captured the spatial variation in water quality within the catchment.

The ME values, which are near zero for most parameters, suggest that the model estimates generally align well with observed values, reflecting a good spatial fit. However, as emphasized by Ishtiaque et al., (2017) ME may underrepresent true error magnitudes since positive and negative deviations can cancel each other out. Therefore, RMSE, being more sensitive to outliers (Yavuz & Erdoğan, 2012), is often considered a more robust indicator of overall predictive error.

The relatively low RMSE values across most parameters (with the exception of EC and Chl-a, which are naturally more variable) indicate limited occurrence of extreme deviations, suggesting that the IDW method performs well in reproducing spatial patterns of physicochemical parameters in the Rákos Stream.

4.7 Water Quality and Hydrodynamic Modelling

4.7.1 QUAL2K Model Calibration and Validation

Calibration and validation are essential steps in water quality modelling to ensure that the simulated outputs reliably represent observed conditions. In this study, the QUAL2K model was calibrated using data from July 2021, which represented the wettest month, characterized by high flows and strong runoff contributions from both urban and agricultural areas. The validation was subsequently carried out with data from June 2021, the driest month, to capture low-flow conditions with minimal runoff influence. This approach allowed the model performance to be evaluated under contrasting hydrological conditions, thereby ensuring the robustness of the simulations.

The results are presented in two main sections: (i) the modelled discharge (Q) profile and pollutant concentrations, which include the simulated longitudinal distribution of discharge and key pollutants—phosphate (PO_4^{3-}), ammonium (NH_4^+), and dissolved oxygen (DO)—along the stream during the calibration and validation period; and (ii) the land use contribution analysis, which highlights the percentage contributions of urban, agricultural, and natural land covers to pollutant loads, demonstrating the influence of land use on water quality.

4.7.2 Spatial Analysis of Discharge Variations in the Rákos Stream: A Model–Observation Comparison

Figure 4-11 illustrates the comparison between simulated discharge (green line) and observed flow data (black dots) along the 33.8 km stretch of the Rákos Stream, from the upstream section (km ~34) to its confluence with the Danube (km 0). The results reflect both natural inflows and anthropogenic influences shaping the stream's hydrology.

In the upstream section (km ~34 to km 30), the discharge gradually increases from around 0.22 m^3/s to 0.29 m^3/s, likely due to contributions from baseflow and small tributaries draining nearby agricultural areas (approx. 47.53–47.55°N, 19.07–19.10°E). Model outputs closely match observed data in this reach, validating the calibration process.

Between km 30 and km 23, a decline in discharge from 0.30 m^3/s to 0.24 m^3/s is observed. This reduction is associated with hydraulic structures (e.g., stilling basins, weirs) that slow flow, enhance sedimentation, and attenuate pollutant transport.

Downstream of km 23, a sharp increase in flow up to 0.53 m³/s occurs after the confluence with a major tributary near urbanized areas such as Gödöllő and Pécel. From km 20 to km 5, the flow remains relatively stable (0.53–0.55 m³/s), suggesting no major inflows or abstractions.

Finally, in the lower reach (km 5 to km 0), the discharge decreases again to ~0.24 m³/s as the stream approaches the Danube. This is attributed to flow diversion at the Rákos overflow weir into adjacent wetlands and floodplains, which play a role in regulating downstream peaks.

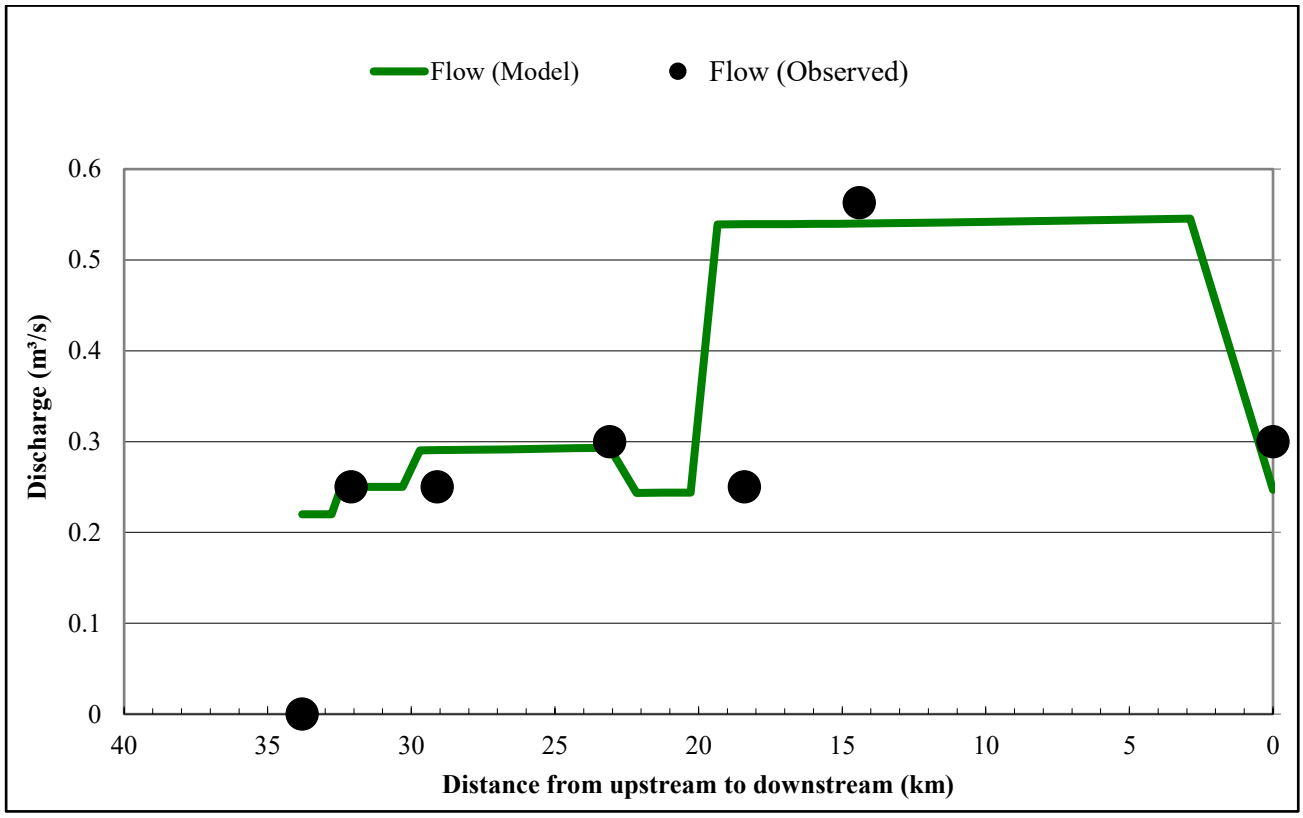

Figure 4-11 Discharge (Q) profile in the Rákos Stream

4.7.3 Dissolved Oxygen (DO) Dynamics and Spatial Variation Along the Rákos Stream

The dissolved oxygen (DO) profile along the Rákos Stream on 15 July 2021 (Figure 4-12) shows how various physical and biological processes interact to shape oxygen availability throughout the system. DO levels in the upstream section (km 35–32) were relatively low, ranging between 3.2 and 3.5 mg O_2/L, which is significantly below the theoretical saturation level of around 8 mg O_2/L. This oxygen

deficit is likely caused by high biological oxygen demand due to organic matter inputs from nearby agricultural areas near Isaszeg (≈47.54 N, 19.06 E).

A distinct drop in DO is observed at km 31, where concentrations fall to approximately 2.8 mg O_2/L. This coincides with a slow-moving section just downstream of a small diversion weir (47.53 N, 19.08 E). In this area, reduced flow velocity and turbulence appear to limit re-aeration, while promoting microbial respiration and oxygen consumption.

Between km 30 and km 25, DO levels increase sharply to about 3.8 mg O_2/L. This improvement is likely due to enhanced mixing and air–water exchange caused by engineered structures such as riffles and step-pools near Gödöllő (≈47.58 N, 19.11 E). In the following section (km 25–20), the DO profile stabilizes around 3.5 mg O_2/L, as the stream passes through a series of settling ponds (≈47.52 N, 19.15 E) that provide moderate but sustained re-aeration.

Further downstream (km 20–10), DO concentrations gradually increase to around 4.0 mg O_2/L. This rise suggests the influence of additional oxygen inputs from smaller riffles and vegetated bank areas, which likely serve as localized re-aeration zones. Near the end of the reach, a final weir at km 5 diverts part of the flow toward floodplain wetlands, contributing further to DO recovery through contact with oxygen-rich vegetation zones.

Overall, the observed DO concentrations (black squares) remained within the modeled uncertainty range, indicating good agreement between measured and simulated values. These results highlight the important role of hydraulic structures—such as riffles, step-pools, and floodplain wetlands—in supporting re-aeration and reducing the impact of oxygen demand in the stream. Maintaining and enhancing these features, particularly in the upstream reaches, can be beneficial for improving water quality and reducing the risk of oxygen stress in aquatic habitats.

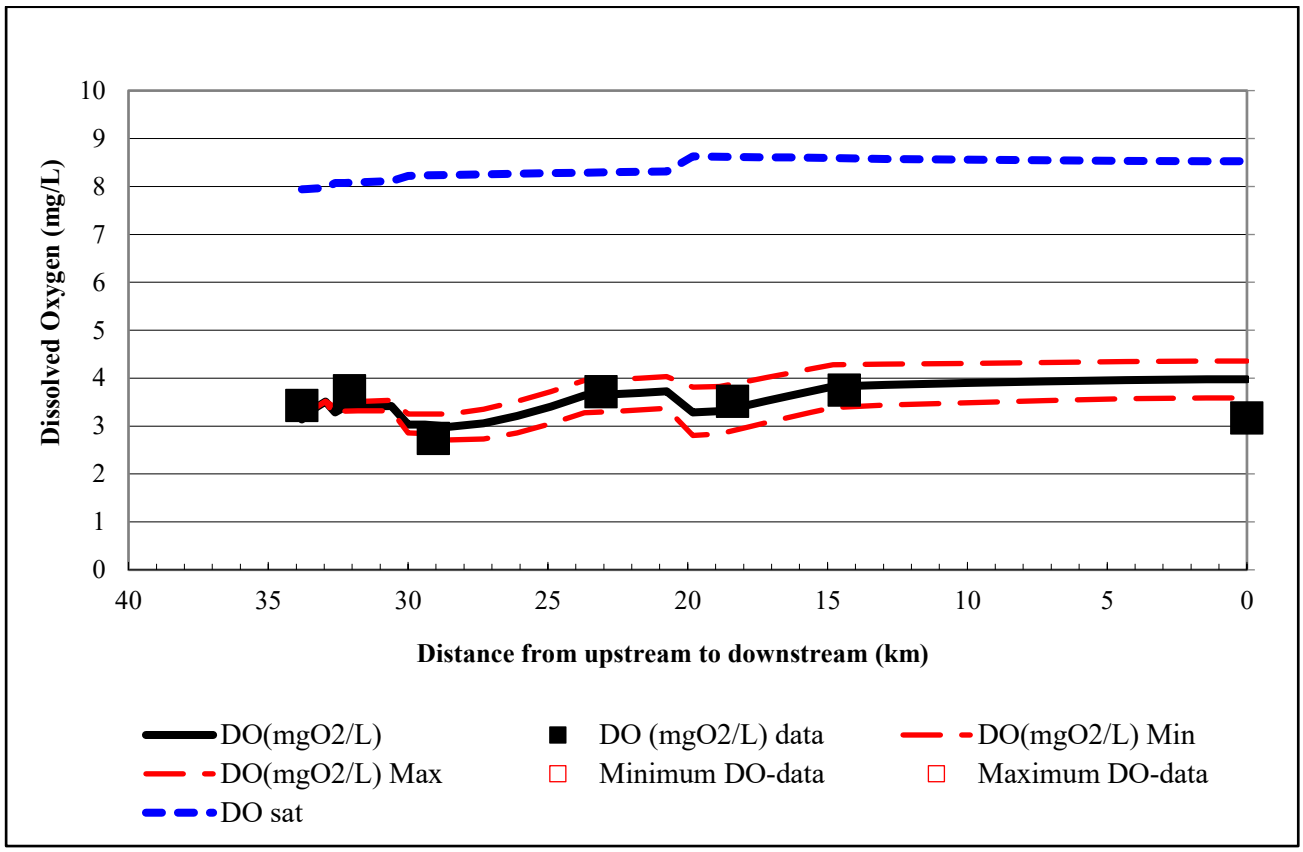

Figure 4-12 DO profile in the Rákos Stream, Calibration period (July 2021)

The validation results (June 2021) reproduced the general longitudinal pattern of DO concentrations along the Rákos Stream (Figure 4-13). Observed and simulated values showed close agreement in both the upstream and downstream sections, while a noticeable deviation occurred in the midstream reach (around km 30), where the measured DO dropped more sharply than the model predictions. Despite this local difference, most observed values fell within the model's uncertainty bounds, supporting the robustness of the calibration and confirming that the model can reliably represent DO dynamics under independent conditions.

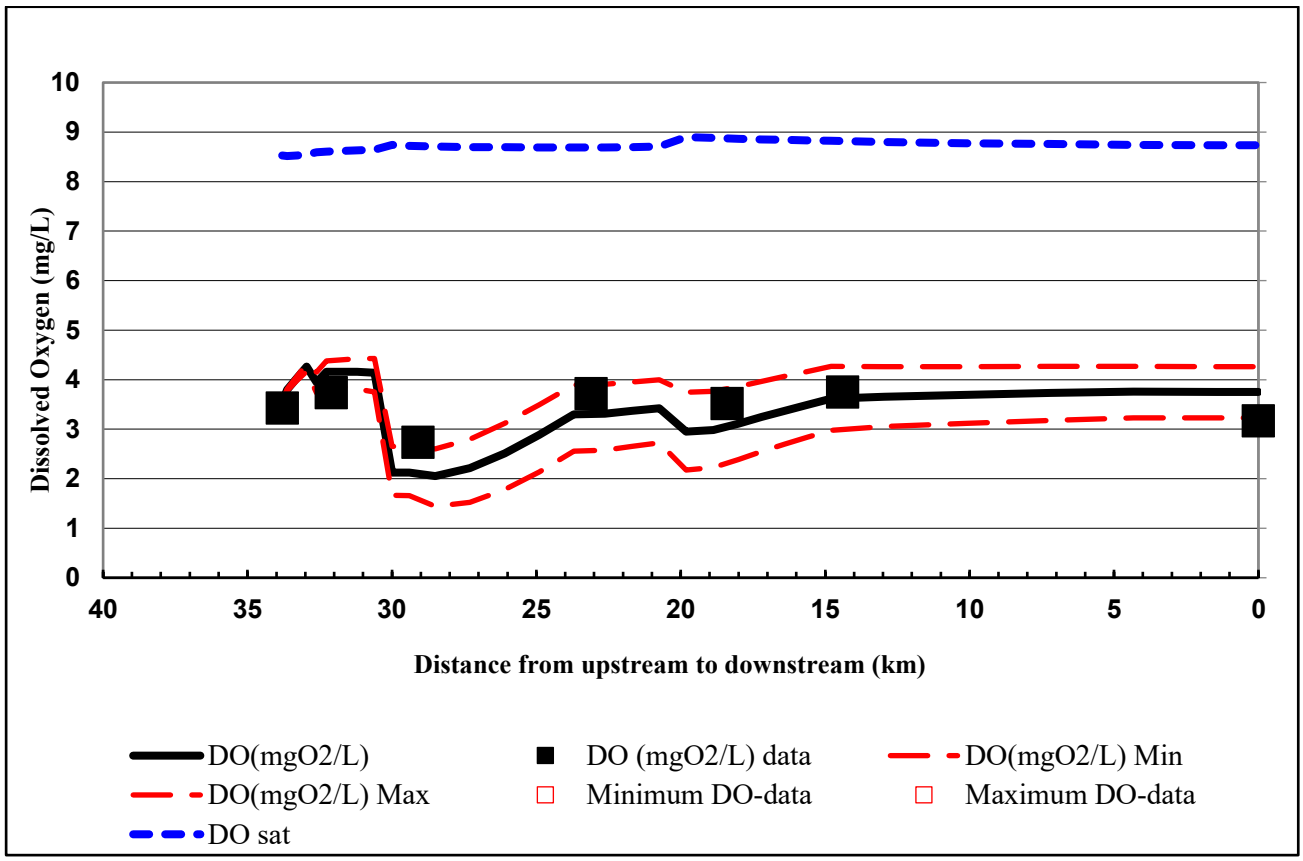

Figure 4-13 DO profile in the Rákos Stream, Validation period (June 2021)

4.7.4 Spatial Variation Ammonium (NH_4^+) Concentrations in the Rákos Stream

Figure 4-14 displays the longitudinal profile of ammonium (NH_4^+) concentrations along the Rákos Stream on 15 July 2021. The x-axis represents the river transect (from km 40 at the headwaters to km 0 at the confluence), while the y-axis shows NH_4^+ concentrations in µgN/L. The black line indicates modelled concentrations, red dashed lines show model uncertainty bounds, and black squares denote observed data points used for calibration and validation.

- **Upstream Increase and Peak Concentration**

Between km 35 and km 29, NH_4^+ concentrations increase sharply from approximately 220 µgN/L to over 550 µgN/L. This elevated level is likely linked to external loading from agricultural runoff and adjacent artificial surfaces. The spike may have been exacerbated by a recent rainfall event or localized point-source discharges.

- **Sharp Decline and Sedimentation Zone**

A pronounced decline in NH_4^+ concentration occurs between km 29 and km 23, where levels drop to below 150 µgN/L. This section includes multiple hydraulic structures such as weirs, settling basins, and engineered impoundments. These features reduce flow velocity, enhance retention time, and promote the deposition of both particulate and dissolved ammonium, effectively functioning as a buffer zone that limits downstream transport of nitrogenous pollutants.

- **Moderate Rebound and Stabilization**

Downstream of km 23, concentrations slightly rebound to around 200 µgN/L and then stabilize through the lower reaches (km 20 to km 0). This suggests that ammonium input and removal processes (e.g., nitrification, sedimentation) reach an approximate balance, leading to a steady-state condition. Minor fluctuations are likely due to low-level contributions from forested areas or diffuse urban runoff.

- **Geospatial Context**

The segment with the greatest decrease in NH_4^+ (km 29 to km 23) corresponds to the midstream region of the watershed, encompassing municipalities such as Gödöllő and Isaszeg. Located between latitudes 47.5800–47.6000 and longitudes 19.3600–19.4000, this zone includes several channel modifications and wider stream sections that support pollutant attenuation and enhance ecological resilience before the stream enters its more urbanized downstream corridor.

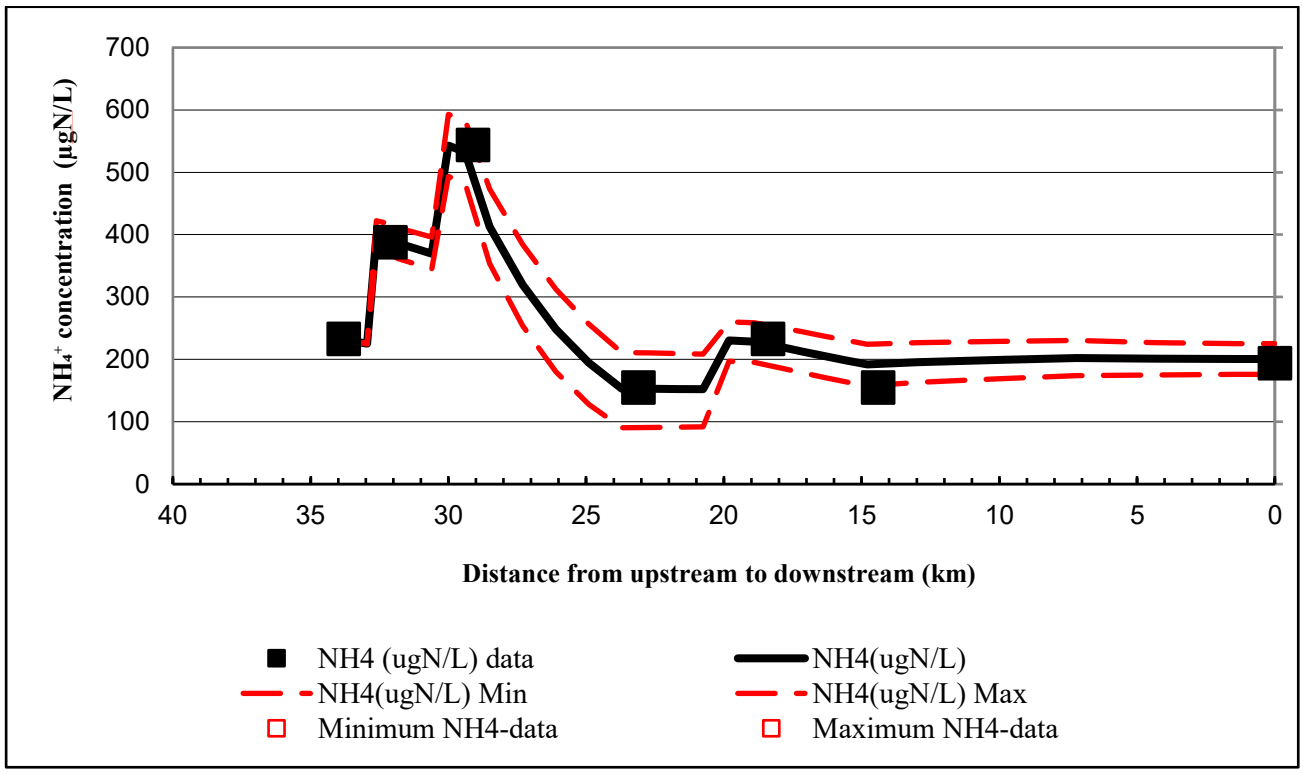

Figure 4-14 NH_4^+ concentration profile in the Rákos Stream, Calibration period (July 2021)

The validation run (June 2021) reproduced the general spatial pattern of ammonium concentrations in the Rákos Stream (Figure 4-15). The model successfully captured the upstream increase and the subsequent downstream decline, although the observed peak at km ~30 (≈900 µgN/L) was underestimated by the simulation. In the mid- and lower reaches, simulated concentrations closely followed the decreasing trend of the measurements, with most values remaining within the model's uncertainty bounds. Despite some underestimation at the downstream outlet, the overall agreement indicates that the model provides a reliable representation of NH_4^+ dynamics under validation conditions.

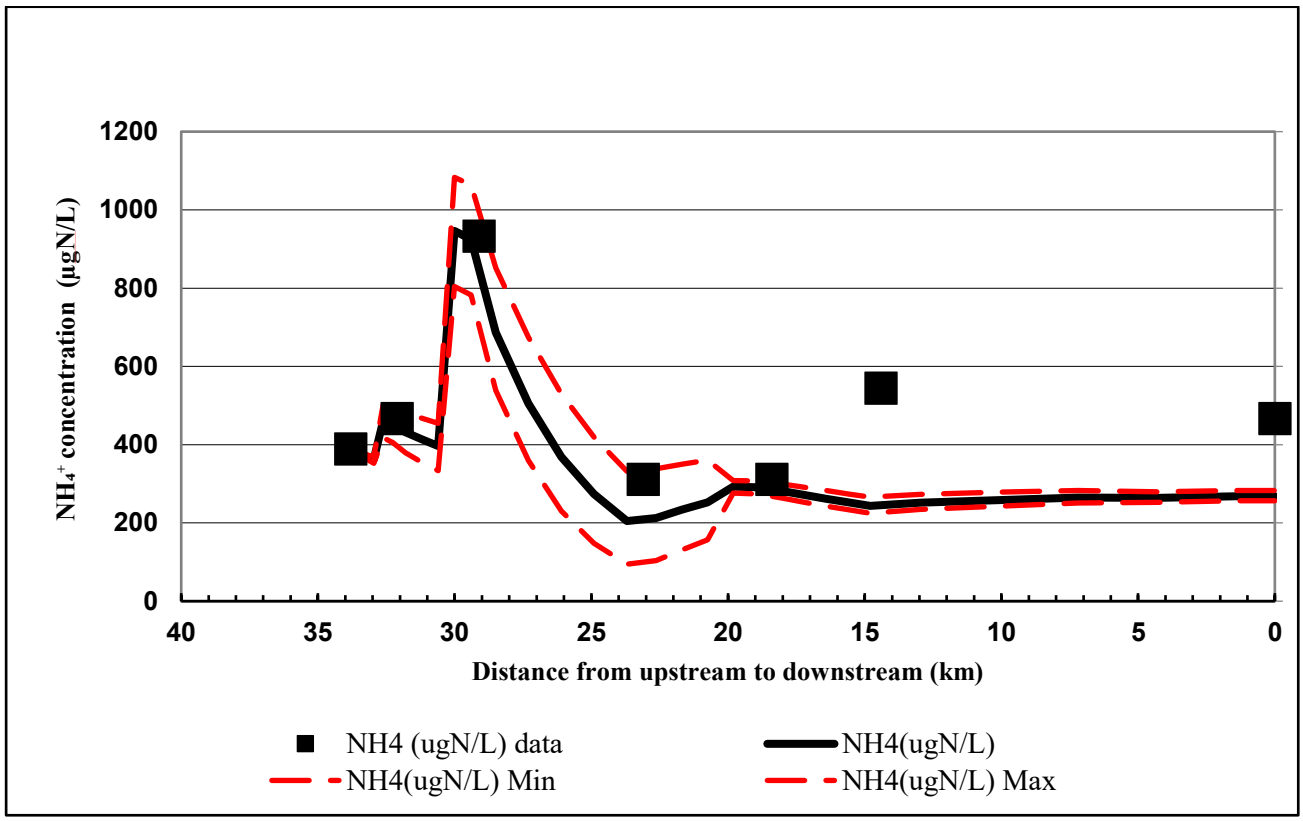

Figure 4-15 NH_4^+ concentration profile in the Rákos Stream, Validation period (June 2021)

4.7.5 Spatial Variation of Phosphate (PO_4^{3-}) Concentrations in the Rákos Stream

Figure 4-16 illustrates the spatial distribution of phosphate (PO_4^{3-}) concentrations along the Rákos Stream on 15 July 2021. The x-axis represents the river transect from km 40 (headwaters) to km 0 (confluence), and the y-axis shows PO_4^{3-} concentrations in µgP/L. The black line denotes simulated values, the dashed red lines indicate model uncertainty bounds, and black squares represent observed measurements used for calibration and validation.

- **Upstream Concentration Increase**

In the upstream segment (km 35–32), PO_4^{3-} concentrations gradually increase from approximately 12,500 µgP/L to around 13,000 µgP/L. This trend likely reflects diffuse nutrient input from agricultural runoff and minor urban discharges near Isaszeg (≈47.54 N, 19.06 E). However, natural attenuation by tributaries and riparian vegetation appears to partly buffer these effects.

- **Phosphate Peak near Gödöllő Confluence**

A sharp peak occurs between km 32 and km 30, where concentrations rise to approximately 14,600 µgP/L. This hotspot corresponds to the confluence with the Gödöllő tributary (≈47.59 N, 19.11 E),

which likely carries nutrient-rich inflows from stormwater outlets and urban maintenance zones. Modelled and observed data both indicate this location as a critical point of elevated phosphate loading.

- **Mid-Reach Decline and Retention Effects**

Further downstream (km 30–20), PO_4^{3-} levels decline to about 12,000 µgP/L. This section includes hydraulic features such as retention basins, low-flow channels, and sedimentation ponds (≈47.52 N, 19.15 E). These structures slow water movement, enhancing sedimentation and biological uptake by aquatic flora, particularly during periods of reduced flow velocity (< 0.3 m/s). Observed values generally fall within model uncertainty bounds, indicating effective representation of retention processes.

- **Stabilization in Lower Reaches**

Between km 20 and the river mouth (km 0), phosphate concentrations remain relatively stable between 12,000 and 12,500 µgP/L. This plateau likely reflects a balance between low-level nutrient inputs from forested and semi-natural landscapes and in-stream biogeochemical processes such as microbial immobilization and uptake by phytoplankton.

- **Implications for Watershed Management**

- **Targeted nutrient reduction** at the Gödöllő confluence is necessary to mitigate high phosphate loads.
- **Preservation and expansion** of mid-reach retention structures can enhance nutrient removal efficiency.
- **Strengthening downstream riparian buffers** may help maintain phosphate equilibrium and prevent resuspension during storm events.

These measures are essential to sustain water quality in the Rákos Stream and minimize nutrient export to the Danube River.

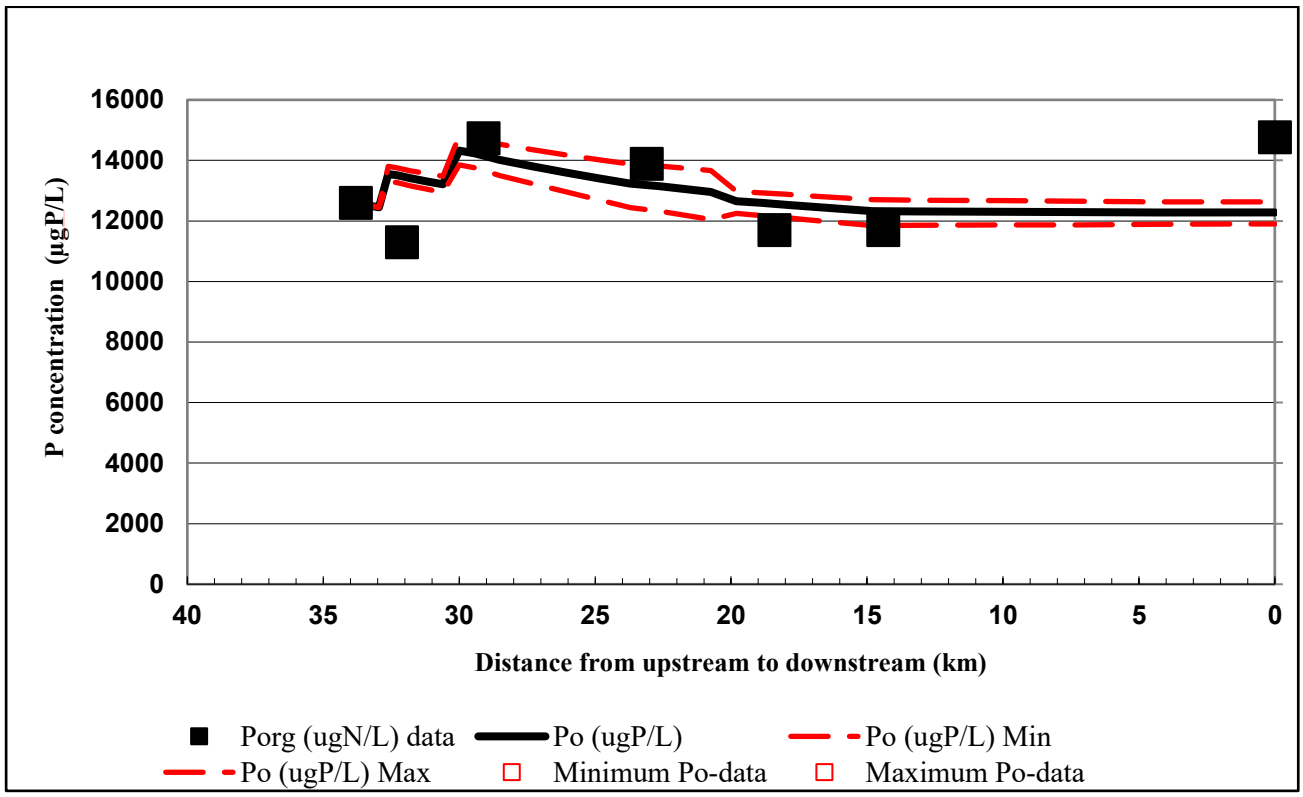

Figure 4-16 Phosphate concentration profile in the Rákos Stream, Calibration period (July 2021)

The validation results (June 2021) confirmed that the model reproduced the overall longitudinal pattern of phosphate concentrations in the Rákos Stream (Figure 4-17). The observed upstream increase and midstream peak (~14,500 µgP/L) were well represented, although the simulated values slightly underestimated the magnitude of this spike. Downstream of km 25, both observed and simulated concentrations declined to ~12,000 µgP/L, showing close agreement throughout the mid-reach. At the outlet, measured phosphate levels rose again, whereas the model predicted lower concentrations. Despite this underestimation, most observed data points remained within the model's uncertainty bounds, supporting the reliability of the model in simulating phosphate dynamics under independent validation conditions.

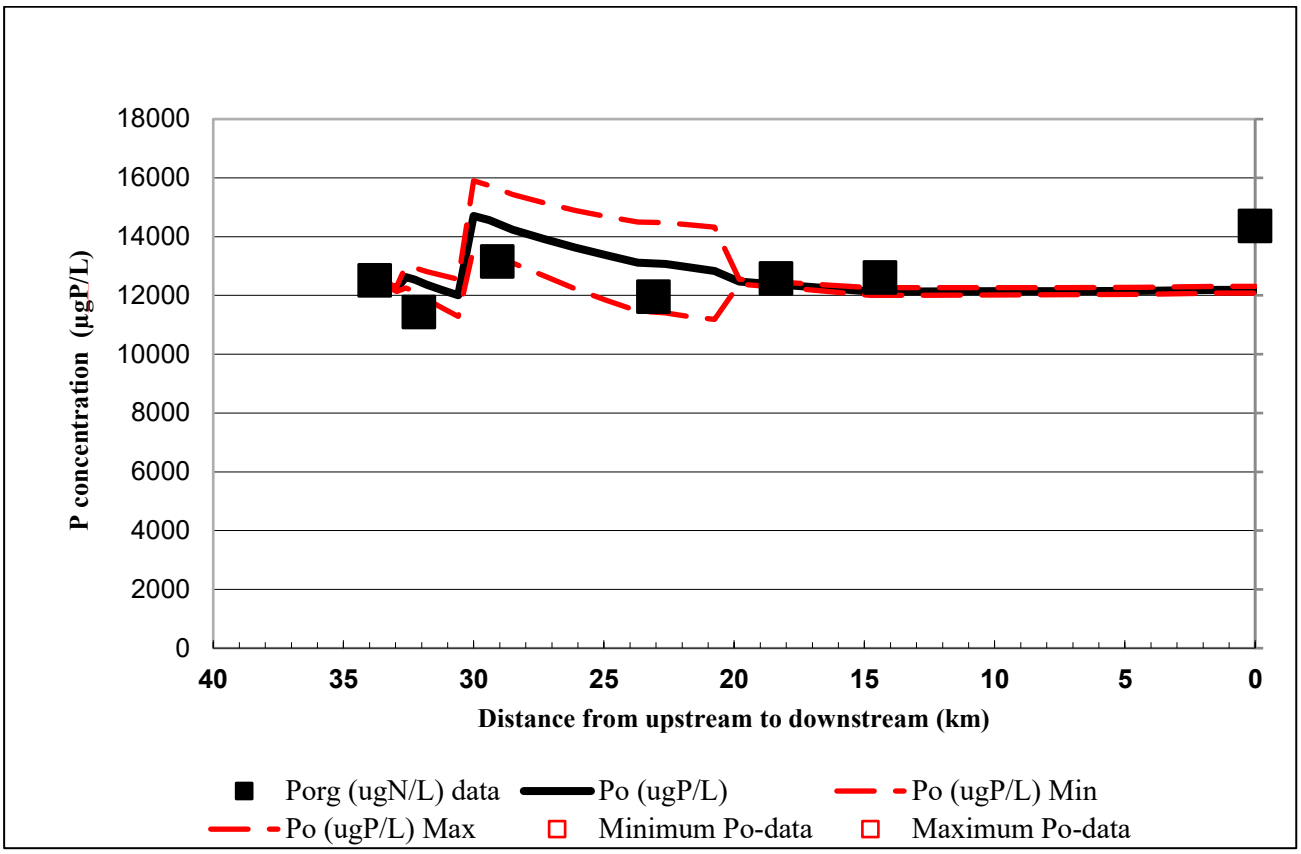

Figure 4-17 Phosphate concentration profile in the Rákos Stream, Validation period (June 2021)

Overall, both calibration and validation results demonstrated that the QUAL2K model is capable of reproducing the spatial patterns of key water quality parameters in the Rákos Stream with acceptable accuracy. During calibration, the model showed strong agreement with observed values for ammonium, phosphate, and dissolved oxygen, confirming the effectiveness of the parameter adjustment process. Validation against an independent dataset further corroborated these findings, with most observed values falling within the model's uncertainty bounds. Although some discrepancies were noted—such as the underestimation of ammonium and phosphate peaks—the general consistency across both phases provides confidence in the model's robustness and predictive reliability under varying hydrological conditions.

4.7.6 Analysis Load Contribution in *Rákos* Stream

Figure 4-18 presents the proportional contribution of various land use types to the total ammonium (NH_4^+) load within the Rákos Stream catchment. The results indicate that agricultural areas are the dominant contributor, accounting for approximately 60% of the total NH_4^+ load. This substantial

contribution is primarily attributed to surface runoff from croplands, which likely contain residual nitrogen from fertilizers, manure, and other nutrient-rich sources commonly used in farming practices. Forest and semi-natural areas contribute around 35% of the NH_4^+ load. While these areas are typically associated with lower pollution risk, the notable contribution observed here may result from natural processes such as nitrogen mineralization, soil leaching, and subsurface flow. In addition, hydrological pathways from upstream semi-natural zones may transport background nitrogen levels into the stream network.

Artificial surfaces, including urban areas with impervious cover, represent the remaining 5% of the NH_4^+ load. Although this share is comparatively small, it may reflect contributions from urban stormwater runoff, particularly in areas where combined sewer overflows or inadequate stormwater infrastructure exist.

From a modeling standpoint, these findings emphasize the need to focus nutrient management efforts on agricultural landscapes. Measures such as vegetated buffer strips, optimized fertilizer application, and improved manure storage can substantially reduce ammonium inputs to surface waters. Simultaneously, maintaining the ecological integrity of semi-natural areas and implementing urban runoff mitigation strategies remain important components of a comprehensive watershed management plan.

The load estimations were derived using a calibrated QUAL2K model integrated with high-resolution land use data. The model accounted for key hydrological features within the catchment, including tributary inflows, weirs, and regulated withdrawals. Calibration against field observations ensured that simulated NH_4^+ concentrations closely matched measured values, thereby strengthening confidence in the model's source attribution results.

In summary, the predominance of agricultural land use in contributing to NH_4^+ pollution highlights the critical importance of targeted nutrient control strategies in these areas. Effective mitigation across all land use types is essential to protect the ecological status of the Rákos Stream and reduce downstream nutrient export to the Danube River.

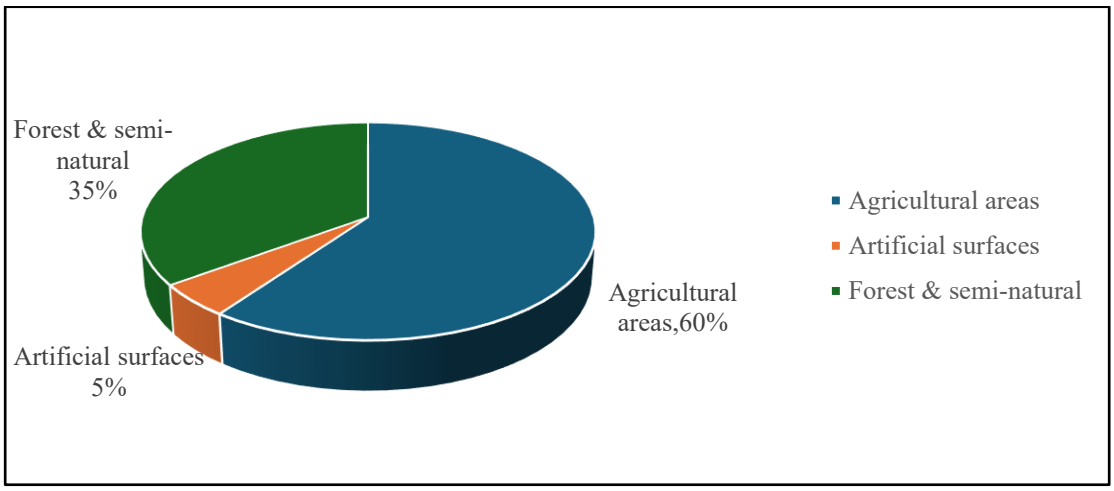

Figure 4-18 Analysis of NH_4^+ Load Contribution in Rákos Stream

The pie chart (Figure 4-19) provides insight into the relative contribution of different land use types to phosphate (PO_4^{3-}) pollution in the *Rákos* stream watershed. According to the data, agricultural areas remain the leading source of phosphorus, accounting for 46% of the total PO_4 load. This is consistent with well-established findings that agricultural lands, due to fertilizer application and soil erosion, are major contributors to phosphate runoff.

Notably, artificial surfaces contribute a significant 30% of the phosphate load. This elevated share reflects the impact of urban runoff, which often contains detergents, leaking sewage, and other phosphorus-rich contaminants from residential and industrial zones. The impermeable nature of artificial surfaces also amplifies direct runoff during rainfall events, leading to higher pollutant discharge.

Forest and semi-natural areas are responsible for the remaining 24%. While generally lower in pollution, these areas may still contribute phosphorus through natural processes like organic matter decomposition or via transport from upstream soils and sediments.

From a modeling perspective, this phosphate distribution illustrates the dual importance of rural and urban land uses in shaping nutrient loads. While agricultural management remains a priority, these results also highlight the need for urban stormwater control measures, such as green infrastructure, retention ponds, and separation of stormwater and wastewater networks.

The model that generated these insights was carefully constructed with detailed hydrological features—including stream geometry, flow direction, barriers, and intakes—and calibrated using observed data at key sampling points. This ensured reliable representation of PO_4^3 behavior under current land use conditions.

In conclusion, the phosphate load distribution in *Rákos* stream suggests that both agricultural practices and urban runoff management must be addressed in future water quality strategies to reduce eutrophication risk and protect downstream water bodies, including the Danube River.

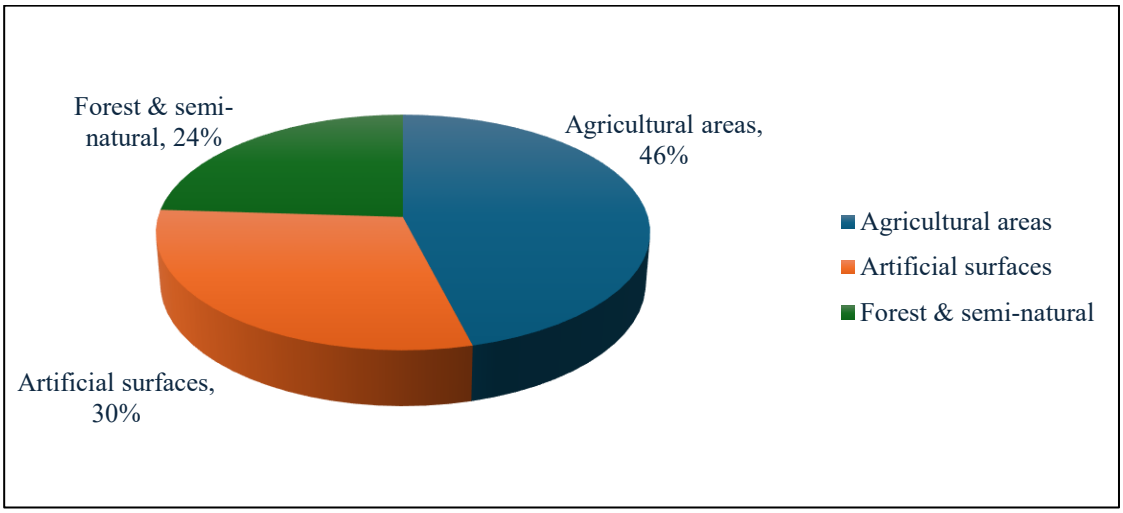

Figure 4-19: Analysis of PO_4^{3-} Load Contribution in Rákos Stream

4.7.7 NRMSE Results

The model performance was evaluated using the Normalized Root Mean Square Error (NRMSE) for both calibration and validation periods. During calibration (Table 4-8), the model demonstrated high accuracy in simulating ammonium (NH_4^+; NRMSE = 0.06) and dissolved oxygen (DO; NRMSE = 0.10), while phosphate (PO_4^{3-}; NRMSE = 0.11) was also reproduced with good reliability. Streamflow showed a relatively higher error (NRMSE = 0.38), which remains within an acceptable range given the uncertainties in hydrological inputs and boundary conditions typical of small urban catchments.

Table 4-8 Calibration errors (NRMSE) between observed and simulated values

Parameter	NRMSE
Flow	0.38
DO	0.10
NH_4^+	0.06
PO_4^{3-}	0.11

For the validation period (Table 4-9), the model maintained acceptable predictive performance. Phosphate was captured with the highest accuracy (NRMSE = 0.08), followed by DO (NRMSE = 0.12). Ammonium showed a higher deviation (NRMSE = 0.27) compared to the calibration phase, reflecting the influence of temporal variability and unmodeled processes during independent testing.

Despite this, the overall consistency between calibration and validation results demonstrates that the model is robust and reliable for simulating key water quality parameters in the Rákos Stream.

Table 4-9 Validation errors (NRMSE) between observed and simulated values

Parameter	NRMSE
DO	0.12
NH_4^+	0.27
PO_4^{3-}	0.08

5 CONCLUSION AND RECOMMENDATIONS

This study demonstrates a clear relationship between land use and water quality in the Rákos Stream. Urban and agricultural sites, particularly Points 8 and 3, consistently exhibited elevated nutrient concentrations, higher electrical conductivity, and increased chlorophyll-a, accompanied by reduced dissolved oxygen levels. In contrast, forested and less disturbed reaches, such as Points 4 and 5, showed more stable nutrient dynamics, lower conductivity, and balanced dissolved oxygen and pH values, highlighting the buffering capacity of natural landscapes. These stabilizing effects can be attributed to natural processes such as sedimentation, nutrient uptake, and microbial activity, which contribute to pollutant attenuation.

Seasonal patterns were also evident, with higher nutrient concentrations, chlorophyll-a, and pH typically observed during the summer months. These seasonal peaks were closely linked to warmer temperatures, enhanced biological activity, and greater runoff contributions from urban and agricultural areas.

The QUAL2K model performed well in simulating pollutant concentrations under both high-flow and low-flow conditions, confirming its robustness across contrasting hydrological regimes. Normalized Root Mean Square Error (NRMSE) values indicated strong agreement between observed and simulated data, particularly for ammonium (NH_4^+) and dissolved oxygen (DO), confirming the model's reliability in representing spatial and temporal water quality dynamics. Importantly, the multiple methodological approaches employed—including monitoring, spatial interpolation, statistical analysis, and process-based modelling—produced consistent and mutually reinforcing results. This convergence of evidence strengthens confidence in the study's conclusions.

Based on these outcomes, targeted management actions are recommended. Nutrient reduction measures should be prioritized in high-pressure areas, particularly Points 8 and 3, with special attention to the summer season when pollutant loads are highest. The conservation and enhancement of forested and semi-natural sections should be a management priority, given their demonstrated role in maintaining ecological balance. In addition, the ecological and hydraulic functions of existing structures should be explicitly considered in future planning, as they contribute to both aeration and pollutant attenuation.

For future research, the application of spatially explicit or coupled hydraulic–water quality models, such as HEC-RAS integrated with QUAL2K, could provide a more detailed evaluation of restoration options under varying flow and land use scenarios. Furthermore, the establishment of long-term, continuous monitoring programs for both water quality and meteorological conditions is essential. Such measures would generate valuable data to inform adaptive management and support ongoing restoration efforts in the Rákos Stream and similar mixed-use catchments.

6 NEW SCIENTIFIC RESULTS

1. Quantified, for the first time, the contribution of specific land use types to pollutant loads in the Rákos Stream catchment using a calibrated QUAL2K model, providing a scientifically grounded basis for targeted and evidence-based watershed management.
2. Identified a key in-stream attenuation reach (km 29–23), where hydraulic structures (weirs, sedimentation basins, step-pools, and vegetated banks) coincided with lower ammonium and phosphate levels and higher dissolved oxygen concentrations. Field data combined with model simulations confirm that hydraulic regulation and channel morphology can mitigate nutrient loads and enhance re-aeration under local stream conditions.
3. Developed an integrated methodological framework that combines in-situ water quality monitoring, GIS-based land use classification, and process-based QUAL2K modeling, offering a transferable approach for similar catchments in temperate urbanizing regions.
4. Quantified seasonal variations in nutrient concentrations and dissolved oxygen (2019–2021) and demonstrated statistically significant land use–driven shifts (e.g., heterogeneous agriculture with NH_4^+ and NO_2^-).
5. Confirmed that EC and nutrient levels are reliable metrics for identifying pollution hotspots and guiding targeted management.

7 SUMMARY

This study investigated the impacts of land use and land cover (LULC) on surface water quality in the Rákos Stream catchment, Hungary—an urbanizing watershed increasingly affected by anthropogenic pressures. The research specifically examined how different land use types influence pollutant generation, transport, and attenuation across spatial and temporal scales.

A multi-method approach was employed, combining biweekly water quality monitoring (2019–2021) at eight sampling stations with spatial analysis using CORINE land cover data and dynamic simulation with the QUAL2K water quality model. Key parameters monitored included ammonium (NH_4^+), nitrate (NO_3^-), phosphate (PO_4^{3-}), dissolved oxygen (DO), electrical conductivity (EC), and chlorophyll-a (Chl-a). GIS tools were applied to characterize land use distribution, while statistical analyses (e.g., Pearson correlation and ANOVA) were used to explore linkages between land cover patterns and stream water quality.

The QUAL2K model was successfully calibrated and validated using field observations and demonstrated strong agreement between observed and simulated values. Modelling results revealed that agricultural areas contributed disproportionately to ammonium and phosphate loads, while urban surfaces were more closely associated with elevated nitrate, nitrite, and EC concentrations. By contrast, forested and semi-natural areas exhibited a clear buffering capacity, supporting dilution and nutrient retention through natural processes.

A central stretch of the stream (km 29–23), containing sedimentation ponds, weirs, and impoundments, was identified as a critical attenuation zone where pollutant concentrations declined markedly. These findings underscore the complementary roles of both natural features and engineered structures in improving stream health.

Seasonal analyses further indicated that pollutant concentrations were generally higher during wetter months, highlighting the influence of runoff-driven inputs and land use practices. This seasonal behavior reinforces the need for temporally adaptive management strategies.

Overall, the study demonstrates the importance of integrated catchment management that accounts for spatial heterogeneity, hydrological behavior, and land use dynamics. The combined use of field monitoring, GIS-based assessment, and process-based modelling provides a transferable framework

for peri-urban and mixed-use catchments, supporting long-term ecological resilience and alignment with European water quality directives.

8 REFERENCES

Abdeveis, S., Sedghi, H., Hassonizadeh, H., & Babazadeh, H. (2020). Application of water quality index and water quality model QUAL2K for evaluation of pollutants in Dez River, Iran. Water Resources, 47(5), 892-903. https://doi.org/10.1134/S0097807820050188.

Aboelnour, M. A., Engel, B. A., Frisbee, M. D., Gitau, M. W., & Flanagan, D. C. (2021). Impacts of watershed physical properties and land use on baseflow at regional scales. *Journal of Hydrology: Regional Studies*, *35*(September 2020), 100810. https://doi.org/10.1016/j.ejrh.2021.100810.

Adami, M., Rudorff, B. F. T., Freitas, R. M., Aguiar, D. A., Sugawara, L. M., & Mello, M. P. (2012). Remote sensing time series to evaluate direct land use change of recent expanded sugarcane crop in Brazil. *Sustainability*, *4*(4), 574–585. https://doi.org/10.3390/su4040574.

Amlor, M. Q., & Alidza, M. Q. (2016). Indigenous Education in Environmental Management and Conservation in Ghana: The Role of Folklore. *Journal of Environment and Ecology*, *7*(1), 37. https://doi.org/10.5296/jee.v7i1.9705.

Angyal, Z., Sárközi, E., Gombás, Á., & Kardos, L. (2016). Effects of land use on chemical water quality of three small streams in Budapest. *Open Geosciences*, *8*(1), 133–142. https://doi.org/10.1515/geo-2016-0012.

Arslan, O. (2009). A GIS-based spatial-multivariate statistical analysis of water quality data in the Porsuk river, Turkey. *Water Quality Research Journal of Canada*, *44*(3), 279–293. https://doi.org/10.2166/wqrj.2009.029.

Azevedo-Santos, V. M., Daga, V. S., Tonella, L. H., Ruaro, R., Arcifa, M. S., Fearnside, P. M., & Giarrizzo, T. (2023). Brazil's urban ecosystems threatened by law. *Land Use Policy*, *131*(June), 106721. https://doi.org/10.1016/j.landusepol.2023.106721.

Bottino, F., Ferraz, I. C., Mendiondo, E. M., & Calijuri, M. do C. (2010). Calibration of QUAL2K model in brazilian micro watershed: effects of the land use on water quality. *Acta Limnologica Brasiliensia*, *22*(4), 474–485. https://doi.org/10.4322/actalb.2011.011.

Burkhard, B., Kroll, F., Nedkov, S., & Müller, F. (2012). Mapping ecosystem service supply, demand and budgets. *Ecological Indicators*, *21*, 17–29. https://doi.org/10.1016/j.ecolind.2011.06.019.

Chang, C. L., Kuan, W. H., Lui, P. S., & Hu, C. Y. (2008). Relationship between landscape characteristics and surface water quality. *Environmental Monitoring and Assessment*, *147*(1–3), 57–64. https://doi.org/10.1007/s10661-007-0097-1.

Chapra, S., Pelletier, G., & Tao, H. (2013). *Steve Chapra, Greg Pelletier and Hua Tao*. 1–91.

Chhabra, S., Kunimoto, D. Y., Kazi, L., Regillo, C. D., Ho, A. C., Belmont, J., Maguire, J., Vander, J., & Brown, G. C. (2006). Endophthalmitis After Open Globe Injury: Microbiologic Spectrum and Susceptibilities of Isolates. *American Journal of Ophthalmology*, *142*(5), 852–854. https://doi.org/10.1016/j.ajo.2006.05.024.

Cuo, L., Zhang, Y., Gao, Y., Hao, Z., & Cairang, L. (2013). The impacts of climate change and land cover/use transition on the hydrology in the upper Yellow River Basin, China. *Journal of Hydrology*, *502*, 37–52. https://doi.org/10.1016/j.jhydrol.2013.08.003.

de Oliveira, K. L., Ramos, R. L., Oliveira, S. C., & Christofaro, C. (2021). Spatial variability of surface water quality in a large Brazilian semiarid reservoir and its main tributaries. *Environmental Monitoring and Assessment*, *193*(7). https://doi.org/10.1007/s10661-021-09194-9.

Donohue, I., McGarrigle, M. L., & Mills, P. (2006). Linking catchment characteristics and water chemistry with the ecological status of Irish rivers. *Water Research*, *40*(1), 91–98. https://doi.org/10.1016/j.watres.2005.10.027.

Faruq, O., Malak, M. A., Hossain, N. J., Sami, M. S., & Sajib, A. M. (2025). Investigating the relationship between land use and water quality in urban water bodies. *Cleaner Water*, *3*(February), 100070. https://doi.org/10.1016/j.clwat.2025.100070.

Feng, L. H., & Huang, C. F. (2008). A risk assessment model of water shortage based on information diffusion technology and its application in analyzing carrying capacity of water resources. *Water Resources Management*, *22*(5), 621–633. https://doi.org/10.1007/s11269-007-9182-z.

Ferreira, M. D. P., & Féres, J. G. (2020). Farm size and Land use efficiency in the Brazilian Amazon. *Land Use Policy*, *99*(January), 104901. https://doi.org/10.1016/j.landusepol.2020.104901.

Foley, J. A., DeFries, R., Asner, G. P., Barford, C., Bonan, G., Carpenter, S. R., Chapin, F. S., Coe, M. T., Daily, G. C., Gibbs, H. K., Helkowski, J. H., Holloway, T., Howard, E. A., Kucharik, C. J., Monfreda, C., Patz, J. A., Prentice, I. C., Ramankutty, N., & Snyder, P. K. (2005). Global consequences of land use. *Science*, *309*(5734), 570–574.

https://doi.org/10.1126/science.1111772.

Frankland, P. (1894). *‘ The existing literature in connection with the Bacteriology of Water is so extensive, that we venture to think an urgent necessity has arisen for a work in which this subject is specially discussed.’*

Gashaw, T., Tulu, T., Argaw, M., Worqlul, A. W., Tolessa, T., & Kindu, M. (2018). Estimating the impacts of land use/land cover changes on Ecosystem Service Values: The case of the Andassa watershed in the Upper Blue Nile basin of Ethiopia. *Ecosystem Services*, *31*, 219–228. https://doi.org/10.1016/j.ecoser.2018.05.001

Halász, G., Szlepák, E., Szilágyi, E., Zagyva, A., & Fekete, I. (2007). Application of EU Water Framework Directive for monitoring of small water catchment areas in Hungary, II. Preliminary study for establishment of surveillance monitoring system for moderately loaded (rural) and heavily loaded (urban) catchment areas. *Microchemical Journal*, *85*(1 SPEC. ISS.), 72–79. https://doi.org/10.1016/j.microc.2006.06.008

Hamilton, L. S., & King, P. N. (1984). Watersheds and rural development planning. *The Environmentalist*, *4*(7 Supplement), 80–86. https://doi.org/10.1007/BF01907298

Harris, J. (2007). The role of soil microbiology in restoration. *Ecosystems and Human Well-Being: Biodiversity Synthesis, Published by World Resources Institute, Washington, DC*, *September*, 91. http://chapter.ser.org/europe/files/2012/08/Harris.pdf.

Horvat, M., Horvat, Z., Majer, F., & Koch, D. (2024). Hydrological Modeling of Stream Drainage Basins: A Case Study on the Magyaregregy Experimental Catchment in Hungary. *Water*, 16(24), 3629.

Hossain, S. (2017). Impact of Land Use Change on Stream Waterquality: a Review of Modelling Approaches. *Journal of Research in Engineering and Applied Sciences*, *02*(01), 1–6. https://doi.org/10.46565/jreas.2017.v02i01.001

Hughes, A. O., & Quinn, J. M. (2019). The effect of forestry management activities on stream water quality within a headwater plantation Pinus radiata forest. *Forest Ecology and Management*, *439*(March), 41–54. https://doi.org/10.1016/j.foreco.2019.02.035

Ishtiaque, A., Shrestha, M., & Chhetri, N. (2017). Rapid urban growth in the kathmandu valley, nepal: Monitoring land use land cover dynamics of a himalayan city with landsat imageries.

Environments - MDPI, *4*(4), 1–16. https://doi.org/10.3390/environments4040072

Johnson, G. A., Davis, J. G., Qian, Y. L., & Doesken, K. C. (2006). Topdressing Turf with Composted Manure Improves Soil Quality and Protects Water Quality. *Soil Science Society of America Journal*, *70*(6), 2114–2121. https://doi.org/10.2136/sssaj2005.0287

Kim, J.-I., Choi, J.-W., & An, K.-G. (2014). Spatial and Temporal Variations of Water Quality in an Urban Miho Stream and Some Influences of the Tributaries on the Water Quality. *Journal of Environmental Science International*, *23*(3), 433–445. https://doi.org/10.5322/jesi.2014.23.3.433

Kindu, M., Schneider, T., Teketay, D., & Knoke, T. (2016). Changes of ecosystem service values in response to land use/land cover dynamics in Munessa-Shashemene landscape of the Ethiopian highlands. *Science of the Total Environment*, *547*, 137–147. https://doi.org/10.1016/j.scitotenv.2015.12.127

Kundu, S., Khare, D., & Mondal, A. (2017). Past, present and future land use changes and their impact on water balance. *Journal of Environmental Management*, *197*, 582–596. https://doi.org/10.1016/j.jenvman.2017.04.018

Lagakos, D. (2020). Does Internal Migration Offer Opportunities? *The Journal of Economic Perspectives*, *34*(3), 174–192. https://www.jstor.org/stable/26923546

Lewis, W. M., Wurtsbaugh, W. A., & Paerl, H. W. (2011). Rationale for control of anthropogenic nitrogen and phosphorus to reduce eutrophication of inland waters. *Environmental Science and Technology*, *45*(24), 10300–10305. https://doi.org/10.1021/es202401p

Li, P., & Wu, J. (2019). Drinking Water Quality and Public Health. *Exposure and Health*, *11*(2), 73–79. https://doi.org/10.1007/s12403-019-00299-8

Li, Y. L., Liu, K., Li, L., & Xu, Z. X. (2012). Relationship of land use/cover on water quality in the Liao River basin, China. *Procedia Environmental Sciences*, *13*(2011), 1484–1493. https://doi.org/10.1016/j.proenv.2012.01.140

Liang, Z., He, Z., Zhou, X., Powell, C. A., Yang, Y., He, L. M., & Stoffella, P. J. (2013). Impact of mixed land-use practices on the microbial water quality in a subtropical coastal watershed. *Science of the Total Environment*, *449*, 426–433. https://doi.org/10.1016/j.scitotenv.2013.01.087

Liu, J., Ning, J., Kuang, W., Xu, X., Zhang, S., Yan, C., Li, R., Wu, S., Hu, Y., Du, G., Chi, W., Pan, T., & Ning, J. (2018). Spatio-temporal patterns and characteristics of land-use change in China during 2010-2015. *Dili Xuebao/Acta Geographica Sinica*, *73*(5), 789–802. https://doi.org/10.11821/dlxb201805001

Locke, K. A. (2024a). Impacts of land use/land cover on water quality: A contemporary review for researchers and policymakers. *Water Quality Research Journal*, *59*(2), 89–106. https://doi.org/10.2166/wqrj.2024.002

Locke, K. A. (2024b). Modelling relationships between land use and water quality using statistical methods: A critical and applied review. *Journal of Environmental Management*, *362*(January), 121290. https://doi.org/10.1016/j.jenvman.2024.121290

Locke, K. A., & Winter, K. (2024a). Estimating thresholds of natural vegetation for the protection of water quality in South African catchments. *Science of the Total Environment*, *945*(June), 173924. https://doi.org/10.1016/j.scitotenv.2024.173924

Locke, K. A., & Winter, K. (2024b). Estimating thresholds of natural vegetation for the protection of water quality in South African catchments. *Science of the Total Environment*, *945*. https://doi.org/10.1016/j.scitotenv.2024.173924

Malmqvist, B., & Rundle, S. (2002). Threats to the running water ecosystems of the world. *Environmental Conservation*, *29*(2), 134–153. https://doi.org/10.1017/S0376892902000097

Mapili, M. (2005). *A GIS Model for the Identification of a Variable Width Buffer Zone in the Lower Fraser River Watersheds Based on Land Use-Water Quality Interactions*. 1–24.

Masood, A., Aslam, M., Pham, Q. B., Khan, W., & Masood, S. (2022). Integrating water quality index, GIS and multivariate statistical techniques towards a better understanding of drinking water quality. *Environmental Science and Pollution Research*, *29*(18), 26860–26876. https://doi.org/10.1007/s11356-021-17594-0

Mello, K. de, Valente, R. A., Randhir, T. O., dos Santos, A. C. A., & Vettorazzi, C. A. (2018a). Effects of land use and land cover on water quality of low-order streams in Southeastern Brazil: Watershed versus riparian zone. *Catena*, *167*(December 2017), 130–138. https://doi.org/10.1016/j.catena.2018.04.027

Mello, K. de, Valente, R. A., Randhir, T. O., dos Santos, A. C. A., & Vettorazzi, C. A. (2018b). Effects

of land use and land cover on water quality of low-order streams in Southeastern Brazil: Watershed versus riparian zone. *Catena*, *167*(April), 130–138. https://doi.org/10.1016/j.catena.2018.04.027.

Metzger, M. J., Rounsevell, M. D. A., Acosta-Michlik, L., Leemans, R., & Schröter, D. (2006). The vulnerability of ecosystem services to land use change. *Agriculture, Ecosystems and Environment*, *114*(1), 69–85. https://doi.org/10.1016/j.agee.2005.11.025.

Mo, W., Yang, N., Zhao, Y., & Xu, Z. (2023). Impacts of land use patterns on river water quality: the case of Dongjiang Lake Basin, China. *Ecological Informatics*, *75*. https://doi.org/10.1016/j.ecoinf.2023.102083.

Njeban, H. S. (2018). Comparison and Evaluation of GIS-Based Spatial Interpolation Methods for Estimation Groundwater Level in AL-Salman District—Southwest Iraq. *Journal of Geographic Information System*, *10*(04), 362–380. https://doi.org/10.4236/jgis.2018.104019.

Noor, S. S. M., & Saad, N. A. (2024). A Review on QUAL2K Water Quality Model: Comparative Analysis with Other Models, Recent Advances and Future Directions. In E3S Web of Conferences (Vol. 599, p. 02008). EDP Sciences.

Obilonu, A. N., Chijioke, C., Igwegbe, W. E., Ibearugbulem, O. I., & Abubakar, Y. F. (2013). Water Quality Challenges and Impact. *International Letters of Natural Sciences*, *4*, 44–53. https://doi.org/10.56431/p-2h3s76

Oliveira, T. E. de, Freitas, D. S. de, Gianezini, M., Ruviaro, C. F., Zago, D., Mércio, T. Z., Dias, E. A., Lampert, V. do N., & Barcellos, J. O. J. (2017). Agricultural land use change in the Brazilian Pampa Biome: The reduction of natural grasslands. *Land Use Policy*, *63*, 394–400. https://doi.org/10.1016/j.landusepol.2017.02.010

Plessis, A. du, Harmse, T., & Ahmed, F. (2014). Quantifying and predicting the water quality associated with land cover change: A case study of the blesbok spruit catchment, South Africa. *Electronic Journal of Theoretical Physics*, *11*(31), 2946–2968. https://doi.org/10.3390/w6102946

Puri, P. J., Yenkie, M. K. N., Sangal, S. P., Gandhare, N. V., Sarote, G. B., & Dhanorkar, D. B. (2011). Surface water (Lakes) quality assessment in nagpur city (India) based on water quality index (WQI). *Rasayan Journal of Chemistry*, *4*(1), 43–48.

Ribbe, J., Wolff, J. O., Staneva, J., & Gräwe, U. (2008). Assessing water renewal time scales for marine environments from three-dimensional modelling: A case study for Hervey Bay, Australia. *Environmental Modelling and Software*, *23*(10–11), 1217–1228. https://doi.org/10.1016/j.envsoft.2008.02.007

Romano, N., Nasta, P., Bogena, H., De Vita, P., Stellato, L., & Vereecken, H. (2018). Monitoring Hydrological Processes for Land and Water Resources Management in a Mediterranean Ecosystem: The Alento River Catchment Observatory. *Vadose Zone Journal*, *17*(1), 1–12. https://doi.org/10.2136/vzj2018.03.0042.

Saeed, O., Székács, A., Jordán, G., Mörtl, M., Abukhadra, M. R., El-Sherbeeny, A. M., ... & Eid, M. H. (2024). Assessing surface water quality in Hungary's Danube basin using geochemical modeling, multivariate analysis, irrigation indices, and Monte Carlo simulation. *Scientific Reports,* 14(1), 18639.

Samaneh Abdeveis, Sedghi, H., Hassonizadeh, H., & Babazadeh, H. (2020). Application of Water Quality Index and Water Quality Model QUAL2K for Evaluation of Pollutants in Dez River, Iran. *Water Resources*, *47*(5), 892–903. https://doi.org/10.1134/S0097807820050188

Santy, S., Mujumdar, P., & Bala, G. (2020). Potential Impacts of Climate and Land Use Change on the Water Quality of Ganga River around the Industrialized Kanpur Region. *Scientific Reports*, *10*(1), 1–13. https://doi.org/10.1038/s41598-020-66171-x

Schauer, L. S., Jawitz, J. W., Cohen, M. J., & Musolff, A. (2025). Spatial and Temporal Variability of River Water Quality. *Hydrological Processes*, *39*(5). https://doi.org/10.1002/hyp.70154

Sekulić, A., Kilibarda, M., Heuvelink, G. B. M., Nikolić, M., & Bajat, B. (2020). Random forest spatial interpolation. *Remote Sensing*, *12*(10), 1–29. https://doi.org/10.3390/rs12101687

Shen, Z., Hou, X., Li, W., Aini, G., Chen, L., & Gong, Y. (2015). Impact of landscape pattern at multiple spatial scales on water quality: A case study in a typical urbanised watershed in China. *Ecological Indicators*, *48*, 417–427. https://doi.org/10.1016/j.ecolind.2014.08.019

Shi, P., Zhang, Y., Li, Z., Li, P., & Xu, G. (2017). Influence of land use and land cover patterns on seasonal water quality at multi-spatial scales. *Catena*, *151*, 182–190. https://doi.org/10.1016/j.catena.2016.12.017

Shrestha, M., & Acharya, S. C. (2021). Assessment of historical and future land-use–land-cover

changes and their impact on valuation of ecosystem services in Kathmandu Valley, Nepal. *Land Degradation and Development*, *32*(13), 3731–3742. https://doi.org/10.1002/ldr.3837

Simedo, M. B. L., Martins, A. L. M., Pissarra, T. C. T., Lopes, M. C., Costa, R. C. A., Valle-Junior, R. F., Campanelli, L. C., Rojas, N. E. T., & Finoto, E. L. (2018). Effect of watershed land use on water quality: A case study in córrego da olaria basin, são paulo state, Brazil. *Brazilian Journal of Biology*, *78*(4), 625–635. https://doi.org/10.1590/1519-6984.168423

Tang, Q., Oki, T., Kanae, S., & Hu, H. (2008). Hydrological cycles change in the Yellow River basin during the last half of the twentieth century. *Journal of Climate*, *21*(8), 1790–1806. https://doi.org/10.1175/2007JCLI1854.1

Taniwaki, R. H., Cassiano, C. C., Filoso, S., Ferraz, S. F. de B., Camargo, P. B. de, & Martinelli, L. A. (2017). Impacts of converting low-intensity pastureland to high-intensity bioenergy cropland on the water quality of tropical streams in Brazil. *Science of the Total Environment*, *584–585*, 339–347. https://doi.org/10.1016/j.scitotenv.2016.12.150

Tanjung, R. H. R., Yonas, M. N., Suwito, Maury, H. K., Sarungu, Y., & Hamuna, B. (2022). Analysis of Surface Water Quality of Four Rivers in Jayapura Regency, Indonesia: CCME-WQI Approach. *Journal of Ecological Engineering*, *23*(1), 73–82. https://doi.org/10.12911/22998993/143998

Uriarte, M., Yackulic, C. B., Lim, Y., & Arce-Nazario, J. A. (2011). Influence of land use on water quality in a tropical landscape: A multi-scale analysis. *Landscape Ecology*, *26*(8), 1151–1164. https://doi.org/10.1007/s10980-011-9642-y

Vörösmarty, C. J., McIntyre, P. B., Gessner, M. O., Dudgeon, D., Prusevich, A., Green, P., Glidden, S., Bunn, S. E., Sullivan, C. A., Liermann, C. R., & Davies, P. M. (2010). Global threats to human water security and river biodiversity. *Nature*, *467*(7315), 555–561. https://doi.org/10.1038/nature09440

Welde, K., & Gebremariam, B. (2017). Effect of land use land cover dynamics on hydrological response of watershed: Case study of Tekeze Dam watershed, northern Ethiopia. *International Soil and Water Conservation Research*, *5*(1), 1–16. https://doi.org/10.1016/j.iswcr.2017.03.002

Wilk, R. (2006). Bottled water: The pure commodity in the age of branding. *Journal of Consumer Culture*, *6*(3), 303–325. https://doi.org/10.1177/1469540506068681

Woldesenbet, T. A., Elagib, N. A., Ribbe, L., & Heinrich, J. (2017). Hydrological responses to land use/cover changes in the source region of the Upper Blue Nile Basin, Ethiopia. *Science of the Total Environment*, *575*, 724–741. https://doi.org/10.1016/j.scitotenv.2016.09.124

Wu, Z., Lai, X., & Li, K. (2021). Water quality assessment of rivers in Lake Chaohu Basin (China) using water quality index. *Ecological Indicators*, *121*, 107021. https://doi.org/10.1016/j.ecolind.2020.107021

Xiao, W., Fu, Y., Wang, T., & Lv, X. (2018). Effects of land use transitions due to underground coal mining on ecosystem services in high groundwater table areas: A case study in the Yanzhou coalfield. *Land Use Policy*, *71*(December 2017), 213–221. https://doi.org/10.1016/j.landusepol.2017.11.059

Xu, Q., Wang, P., Shu, W., Ding, M., & Zhang, H. (2021). Influence of landscape structures on river water quality at multiple spatial scales: A case study of the Yuan river watershed, China. *Ecological Indicators*, *121*(November 2020), 107226. https://doi.org/10.1016/j.ecolind.2020.107226

Yavuz, H., & Erdoğan, S. (2012). Spatial Analysis of Monthly and Annual Precipitation Trends in Turkey. *Water Resources Management*, *26*(3), 609–621. https://doi.org/10.1007/s11269-011-9935-6

Ye, L., Cai, Q. hua, Liu, R. qiu, & Cao, M. (2009). The influence of topography and land use on water quality of Xiangxi River in three Gorges Reservoir region. *Environmental Geology*, *58*(5), 937–942. https://doi.org/10.1007/s00254-008-1573-9

Yong, S. T. Y., & Chen, W. (2002). Modeling the relationship between land use and surface water quality. *Journal of Environmental Management*, *66*(4), 377–393. https://doi.org/10.1006/jema.2002.0593

Zang, C. F., Liu, J., Van Der Velde, M., & Kraxner, F. (2012). Assessment of spatial and temporal patterns of green and blue water flows under natural conditions in inland river basins in Northwest China. *Hydrology and Earth System Sciences*, *16*(8), 2859–2870. https://doi.org/10.5194/hess-16-2859-2012

Zhang, H., Wang, B., Liu, D. L., Zhang, M., Leslie, L. M., & Yu, Q. (2020). Using an improved SWAT model to simulate hydrological responses to land use change: A case study of a catchment

in tropical Australia. *Journal of Hydrology*, *585*(March), 124822. https://doi.org/10.1016/j.jhydrol.2020.124822

Zhang, J., Li, S., & Jiang, C. (2020). Effects of land use on water quality in a River Basin (Daning) of the Three Gorges Reservoir Area, China: Watershed versus riparian zone. *Ecological Indicators*, *113*(November 2019), 106226. https://doi.org/10.1016/j.ecolind.2020.106226

Zheng, F., & Hu, Y. (2018). Assessing temporal-spatial land use simulation effects with CLUE-S and Markov-CA models in Beijing. *Environmental Science and Pollution Research*, *25*(32), 32231–32245. https://doi.org/10.1007/s11356-018-3189-2